



TECHNICAL UNIVERSITY OF CRETE

SCHOOL OF PRODUCTION ENGINEERING & MANAGEMENT

Model-assisted Control for Energy Efficiency in Buildings

By

Georgios D. Kontes

A dissertation submitted in partial fulfilment of the
requirements for the degree of

Doctor of Philosophy (PhD)

Supervisors:

Dr. Dimitrios V. Rovas, Lecturer, University College London

Dr. Ioannis K. Nikolos, Associate Professor, Technical University of Crete

Chania, September 1st, 2017

THIS PAGE INTENTIONALLY LEFT BLANK



TECHNICAL UNIVERSITY OF CRETE

SCHOOL OF PRODUCTION ENGINEERING & MANAGEMENT

Model-assisted Control for Energy Efficiency in Buildings

By

Georgios D. Kontes

Supervised and approved by:

Approved by:

Dr. Ioannis K. Nikolos

Associate Professor
Technical University of Crete
School of Production Engineering
& Management

Dr. Markos Papageorgiou

Professor
Technical University of Crete
School of Production Engineering
& Management

Dr. Michail G. Lagoudakis

Associate Professor
Technical University of Crete
School of Electrical & Computer
Engineering

Dr. Georgios S. Stavrakakis

Professor
Technical University of Crete
School of Electrical & Computer
Engineering

Dr. Fotios Kanellos

Assistant Professor
Technical University of Crete
School of Production Engineering
& Management

Dr. Dimitrios Rovas

Lecturer
University College London
Faculty of the Built Environment
Bartlett School of Environment,
Energy & Resources

Dr. Georgios N. Yannakakis

Associate Professor
University of Malta
Institute of Digital Games

THIS PAGE INTENTIONALLY LEFT BLANK

To my family

Natalia, Dimitris-Chrysanthos and Vasilis-Nektarios

And to my sister Vasiliki

The bravest person I know

THIS PAGE INTENTIONALLY LEFT BLANK

Abstract

Effective utilization of energy in buildings is receiving significant attention. This interest is justified on the observation that buildings account for a significant portion of end-energy use. In Europe 40% of the total energy consumed is used for the operation of buildings with a significant part of that energy used for conditioning occupied spaces. Thus the value of effective energy utilization during the building operational phase is undisputed both in terms of achieving good occupant comfort and in reducing energy consumption.

In energy management of buildings, Building Management Systems (BMS) (or Building Automation and Control Systems (BACS)) play an essential role in managing buildings by providing some monitoring and control capability for multiple sub-systems including the Heating Ventilation and Air Conditioning (HVAC) system. Very often, the installation and commissioning of a BMS system is viewed largely as a quality control process, and more specifically the target is proper installation and ensuring a minimum-level of functionality, rather than good operational performance. This has enabled the utilization of flexible and scalable BMS solutions. Here, the BMS is divided into two parts: Local and Remote. The local part is responsible for managing local control loops (usually PID), data collection and transfer, and very simple analytics; and the remote layer is responsible for providing more advanced services. The availability of such a cloud-based platform enables the development and utilization of advanced building energy management services, which cannot be deployed in local hardware due to their computational requirements and allow for semi-automatic intelligent control.

One of the most recent and widely-applied methodologies for designing intelligent building control strategies is Model Predictive Control (MPC). Here, a model of the building is available and using available weather and occupancy forecasts an optimization process determines a set of control actions to be applied to the building for a pre-defined period of time (e.g. 24 hours). The different control strategies are evaluated in the optimizer on the basis of a cost function and a set of (visual, thermal, etc.) comfort constraints. Then, the first control command is applied to the building and the whole process repeats. This approach has certain limitations, mainly regarding the inability to incorporate in a structured manner more elaborate thermal comfort indices, such as the Fanger index, and the requirement for linear or bi-linear building models, in order to define a convex optimization task.

The methodology developed in this thesis tries to address these limitations while maintaining the benefits of the MPC paradigm. We have developed a framework to deliver optimized and integrated operation of all energy-influencing components of a building that include generation, distribution and emission elements. First, a set of parametric control functions (controllers) are identified for each emission/distribution/generation system, following guidelines available in international standards. Next, given (weather, occupancy, etc.) forecasts for a predefined time window, say three days, a surrogate-based stochastic optimization algorithm is used to create candidate controller parameters to be applied to the building, and a detailed thermal simulation model (designed using detailed thermal simulation software like e.g. EnergyPlus or TRNSYS) is used to evaluate these candidate solutions. The evaluation is performed on the basis of a defined cost function and a set of (visual, thermal, air-quality, etc.) comfort constraints. The final, improved controllers are communicated to the building-side and are applied to the building.

In order to verify the efficiency of the proposed methodology, a hierarchy of experiments has been designed, facilitating simulation-based studies and real building experiments in two study buildings located in Greece and Germany. The simulation-based studies are used to

evaluate the potential of the proposed approach in a controlled and disturbance-free environment, while the goal of the real building experiments is to study the behavior of the control design process under real-world conditions, influenced by user- and weather-induced disturbances.

In all our experiments the proposed methodology was able to outperform the baseline control strategy of the buildings (usually hard-coded in a set of pre-defined rules) in terms of total energy consumed, while preserving comfortable interiors. This is because a static, rule-based controller is unable to properly account for all the predicted and un-predicted disturbances (e.g. weather conditions, occupancy, setpoint tracking errors, etc.), whereas the model-based control design approach, utilizing the thermal simulation model of the building and the automated control design setup, was able to make informative decisions and control the building in an efficient manner.

An important aspect investigated through the experiments is the topic of (thermal) comfort-based control, since it was clear from the results that a discussion on energy efficiency seems untimely when discussed without any reference to comfort as there is a clear trade-off between comfort and energy. Having methods that allow the automated selection of building operation to desired levels of comfort is both desirable and can have significant implications. On the other hand, in existing state of the art, comfort is often synonymous with the temperature in the building zones being maintained within certain (prescribed) limits. As we investigate in the thesis this assumption while true in certain cases, in many cases is not sufficient to ensure true comfort for the building occupants, with detrimental effects to health and productivity (when office buildings are considered). In the proposed approach, we define comfort based on ISO 7730, which supports the definition and use of the Fanger index which captures, among other parameters, the influence of air and radiant temperatures along with humidity.

Keywords: Energy Efficient Buildings, Model-assisted Control, Surrogate-based Stochastic Optimization, Bayesian Optimization, Design of Experiments, Thermal Comfort

Περίληψη

(Extended Abstract in Greek)

Τα τελευταία χρόνια, η βελτιστοποίηση της ενεργειακής απόδοσης κτηρίων έχει λάβει σημαντική προσοχή. Αυτό το ενδιαφέρον είναι δικαιολογημένο, μιας και τα κτήρια είναι υπεύθυνα για ένα μεγάλο ποσοστό της τελικής κατανάλωσης ενέργειας. Συγκεκριμένα, στην Ευρώπη το 40% της ολικής κατανάλωσης ενέργειας χρησιμοποιείται για τη λειτουργία των κτηρίων, ενώ ένα μεγάλο ποσοστό από αυτή την ενέργεια χρησιμοποιείται για την επίτευξη θερμικής άνεσης στους εσωτερικούς χώρους. Επομένως η βελτιστοποίηση της ενεργειακής απόδοσης κτηρίων κατά τη διάρκεια της χρήσης τους έχει πολλαπλά οφέλη και προς την κατεύθυνση της μείωσης της συνολικής κατανάλωσης ενέργειας και προς την κατεύθυνση της βελτίωσης της θερμικής άνεσης των χρηστών.

Στην ενεργειακή διαχείριση των κτηρίων, κεντρικό ρόλο παίζουν τα Συστήματα Διαχείρισης Κτηρίων (Building Management System (BMS)) ή Συστήματα Αυτοματισμού και Ελέγχου Κτηρίων (Building Automation and Control Systems (BACS)). Τα συστήματα αυτά προσφέρουν λειτουργίες παρακολούθησης της απόδοσης του κτηρίου, καθώς και λειτουργίες ελέγχου όλων των συστημάτων Θέρμανσης, Ψύξης και Κλιματισμού (Heating Ventilation and Air Conditioning (HVAC)). Πολυ συχνά η εγκατάσταση και η παράδοση των BMS στοχεύει στην σωστή εγκατάσταση του εξοπλισμού και στην επίτευξη κάποιας βασικής λειτουργικότητας στον μικρότερο δυνατό χρόνο και όχι στην βελτιστοποίηση της ολικής λειτουργίας του συστήματος. Για το τελευταίο, έχουν αναπτυχθεί επεκτάσιμα και ευέλικτα συστήματα BMS. Εδώ το BMS χωρίζεται σε δύο διακριτά μέρη: στην τοπική εγκατάσταση και στην απομακρυσμένη εγκατάσταση. Η τοπική εγκατάσταση περιλαμβάνει την διαχείριση των τοπικών βρόχων ελέγχου (για παράδειγμα PID ελεγκτές), καθώς και τη συλλογή δεδομένων και την αποστολή τους στο απομακρυσμένο σύστημα. Το απομακρυσμένο σύστημα με τη σειρά του είναι υπεύθυνο για την εκτέλεση πιο πολύπλοκων υπηρεσιών, συνήθως σε ένα περιβάλλον υπολογιστικού νέφους (cloud-based). Η διαθεσιμότητα μιας τέτοιας υπολογιστικής πλατφόρμας επιτρέπει την υλοποίηση και χρήση εξελιγμένων και πολύπλοκων υπηρεσιών ενεργειακής διαχείρισης κτηρίων, που δεν θα μπορούσαν να αναπτυχθούν στον εξοπλισμό που είναι διαθέσιμος στην τοπική εγκατάσταση, λόγω της υπολογιστικής τους πολυπλοκότητας.

Αυτό το περιβάλλον ευνοεί και την ανάπτυξη εξελιγμένων αλγορίθμων/μεθοδολογιών ενεργειακής διαχείρισης κτηρίων. Μια από τις πιο διαδεδομένες μεθοδολογίες τέτοιου τύπου είναι ο Προβλεπτικός Έλεγχος με χρήση Μοντέλων (Model Predictive Control (MPC)). Εδώ ένα μοντέλο του κτηρίου, καθώς και προβλέψεις για τις μελλοντικές και καιρικές συνθήκες και την πληρότητα του κτηρίου, είναι διαθέσιμα. Χρησιμοποιώντας αυτές τις διαθέσιμες πληροφορίες, μπορεί να οριστεί ένα πρόβλημα βελτιστοποίησης ώστε να σχεδιάσουμε βελτιστοποιημένες αποφάσεις ελέγχου για όλα τα συστήματα του κτηρίου και για ορισμένο χρονικό διάστημα στο μέλλον (π.χ. για τις επόμενες 24 ώρες). Οι διαφορετικές αυτές στρατηγικές ελέγχου αξιολογούνται με βάση το μοντέλο ως προς μια ορισμένη συνάρτηση κόστους (π.χ. η συνολική κατανάλωση ενέργειας του κτηρίου) και ένα σύνολο περιορισμών στην (θερμική, οπτική, ακουστική, κ.λ.π.) άνεση των χρηστών του κτηρίου. Στη συνέχεια, μόνο η πρώτη απόφαση ελέγχου εφαρμόζεται στα συστήματα του κτηρίου και η όλη διαδικασία επαναλαμβάνεται.

Η κλασική εκδοχή αυτής της μεθοδολογίας στο πεδίο της ενεργειακής διαχείρισης κτηρίων έχει συγκεκριμένα μειονεκτήματα, κυρίως ως προς την ικανότητα να συμπεριλάβει με γενικό τρόπο πιο πολύπλοκους δείκτες θερμικής άνεσης, όπως είναι ο δείκτης Fanger,

καθώς και η απαίτηση για γραμμικά ή διγραμμικά μοντέλα κτηρίων, ώστε το τελικό πρόβλημα βελτιστοποίησης να είναι κυρτό (convex).

Η μεθοδολογία που αναπτύχθηκε στην παρούσα εργασία έχει σαν στόχο να αντιμετωπίσει αυτά τα μειονεκτήματα, διατηρώντας παράλληλα και τα πλεονεκτήματα του MPC. Η συγκεκριμένη μεθοδολογία έχει τη δυνατότητα να σχεδιάζει βελτιστοποιημένες αποφάσεις ελέγχου για όλα τα συστήματα του κτηρίου ταυτόχρονα. Αρχικά, σχεδιάζεται ένα σετ από παραμετρικούς ελεγκτές για όλα τα συστήματα του κτηρίου, ακολουθώντας τα σχετικά πρότυπα στη βιβλιογραφία. Στη συνέχεια – και με δεδομένες τις προβλέψεις για τις καιρικές συνθήκες και την πληρότητα του κτηρίου – ένας στοχαστικός αλγόριθμος βασισμένος σε μετα-μοντέλα χρησιμοποιείται για να σχεδιαστούν υποψήφιος στρατηγικές ελέγχου για το κτήριο. Οι στρατηγικές αυτές αξιολογούνται χρησιμοποιώντας ένα λεπτομερές μοντέλο προσομοίωσης του κτηρίου (που έχει δημιουργηθεί χρησιμοποιώντας λογισμικά θερμικής προσομοίωσης κτηρίων όπως για παράδειγμα το EnergyPlus και το TRNSYS). Τέλος, η τελική (βελτιστοποιημένη) στρατηγική ελέγχου αποστέλλεται στο κτήριο ώστε να εφαρμοστεί στα συστήματα του κτηρίου.

Για την επαλήθευση της αποτελεσματικότητας της προτεινόμενης μεθοδολογίας, μια σειρά πειραμάτων σχεδιάστηκε και εκτελέστηκε τόσο σε επίπεδο προσομοίωσης όσο και σε πραγματικές συνθήκες, χρησιμοποιώντας δύο κτήρια, ένα στην Κρήτη και ένα στη Γερμανία. Τα πειράματα σε περιβάλλον προσομοίωσης χρησιμεύουν ώστε να διαπιστωθεί η αποτελεσματικότητα της μεθόδου σε ελεγχόμενο περιβάλλον, χωρίς τυχαίες μεταβολές, ενώ τα πειράματα σε πραγματικές συνθήκες καταδεικνύουν την αποτελεσματικότητα και τη σταθερότητα της προτεινόμενης μεθόδου σε πραγματικές συνθήκες, όπου επιδρούν στοχαστικές διαταραχές στο σύστημα τόσο από τις καιρικές συνθήκες όσο και από τις ενέργειες των χρηστών.

Σε όλα τα πειράματα η προτεινόμενη μεθοδολογία κατάφερε να αποδώσει σημαντικά καλύτερα συγκριτικά με την υπάρχουσα στρατηγική ελέγχου των κτηρίων, η οποία χρησιμοποιείται σαν σημείο αναφοράς. Αυτό συμβαίνει γιατί οι στατικές και βασισμένες σε ένα σύνολο προκαθορισμένων κανόνων υπάρχουσες στρατηγικές ελέγχου δεν είναι σε θέση να αντιμετωπίσουν όλες τις προβλεπόμενες και μη διαταραχές που επιδρούν στο σύστημα. Σε αντίθεση, η προτεινόμενη μεθοδολογία με τη χρήση του αναλυτικού μοντέλου θερμικής προσομοίωσης, καθώς και της μεθόδου βελτιστοποίησης είναι σε θέση να σχεδιάζει πιο αποδοτικές στρατηγικές ελέγχου, προσαρμοσμένες στις αναμενόμενες μελλοντικές συνθήκες.

Μια σημαντική παράμετρος που διερευνήθηκε μέσω των πειραμάτων είναι το θέμα του ελέγχου βασισμένου στην θερμική άνεση των χρηστών, μιας και είναι ξεκάθαρο από τα αποτελέσματα πως μια στείρα συζήτηση για εξοικονόμηση ενέργειας είναι άστοχη χωρίς σαφή αναφορά στην θερμική άνεση των χρηστών, καθώς υπάρχει ένα σαφές αντιστάθμισμα μεταξύ των δύο (είναι ανταγωνιστικά κριτήρια). Η ανάπτυξη μεθόδων που επιτρέπουν την αυτόματη ρύθμιση της θερμικής άνεσης στους εσωτερικούς χώρους κτηρίων είναι ένα από τα κύρια στοιχεία των εξελιγμένων BMS. Από την άλλη πλευρά, πολύ συχνά η θερμική άνεση ορίζεται σαν μια προκαθορισμένη περιοχή τιμών της θερμοκρασίας του αέρα σε κάθε ζώνη του κτηρίου. Όπως καταδεικνύουν τα αποτελέσματα της παρούσας εργασίας, αν και αυτή η υπόθεση είναι αληθής σε συγκεκριμένα κτήρια και HVAC συστήματα, στη γενική περίπτωση δεν αρκεί για να εξασφαλίσει πραγματική θερμική άνεση για τους χρήστες του κτηρίου, με επιζήμιες επιπτώσεις στην υγεία και την αποδοτικότητα των χρηστών. Στην παρούσα εργασία χρησιμοποιούμε τον δείκτη Fanger, ο οποίος είναι ένας ορισμός θερμικής άνεσης που περιέχεται στο πρότυπο (ISO) 7730. Ο δείκτης αυτός συνυπολογίζει – ανάμεσα και σε άλλες παραμέτρους – τις επιπτώσεις της θερμοκρασίας αέρα και της θερμοκρασίας λόγω ακτινοβολίας, καθώς και της υγρασίας στους χώρους του κτηρίου.

Acknowledgements

Even though our lives are continuous flows of many small and larger events that define us, some of these moments represent important landmarks and tend to be remembered more vividly over the years.

At this point I am convinced that writing down the last words of a PhD thesis is one of these moments. It is a moment that you realize that an effort which started really early in life (from the first school years) has concluded here. This point in time marks the end of a very hard road, full of joy, disappointments, successes, failures, huge effort, commitment, adaptation, learning, evolution and the birth of a new road, full of uncertainty. It is a point where you are no longer considered a student so you can count on your advisor to show you the way and guide you through the rough patches, but you take your (research) life into your own hands and get out in the world. As with any other form of adulthood, it is a frightening moment.

Looking back in time, I can detect two major influences that shaped my (academic, research and everyday) personality. Thus, I have to express my deep gratitude to my BSc thesis advisor, Associate Prof. Michail Lagoudakis (TU Crete) and to my MSc thesis advisor Prof. Nikos Vlassis (now in Netflix, Los Gatos, California), for dripping in me the passion for defining and trying to address difficult engineering research problems, as well as the love for the Academic life. I can clearly see now that they set me on the path I am still following today.

During my PhD years, I was fortunate enough to have two advisors: Associate Prof. Ioannis Nikolos (TU Crete) and Assistant Prof. Dimitrios Rovas (formerly TU Crete and now University College London). Even though Prof. Nikolos took me over in the last turn of my PhD, I cannot thank him enough for being next to me all these years, always willing to sacrifice a lot of his time for providing advices and support.

With Prof. Rovas we walked together for the greater part of this thesis. Even though this road was bumpy from time to time, I cannot thank him enough for providing me the ideal environment to grow and for forming a group with the best people I could ever work with. He always believed in me (much more than I believed into myself) and I can never forget the opportunity he gave me to work in his group, judging me only from my CV. Prof. Rovas taught me that sometimes we succeed, sometimes we fail, but we always set the bar really high and we are not afraid to compare with the best in the field. In addition, he taught me *by example* the academic principles and how never to stray away from them, no matter how high the (temporary) benefit.

I will also like to thank Associate Prof. Lagoudakis and Prof. Papageorgiou for their timely and valuable feedback throughout this thesis, as co-supervisors of my PhD. In addition, I would like to thank all the members of my thesis committee for their helpful comments towards improving this thesis.

Of course I cannot thank enough my friends in our old lab: Georgios Giannakis (who became one of my closest friends and is also the Godfather of my son Dimitris), Kyriakos Katsigarakis and Georgios Lilis. Their skillset, professionalism and goodness of their hearts are definitely unmet! I really miss our Metaxa 5* tradition after successful experiments and our Christmas outings!

The final part of my PhD was conducted while I had already moved to Germany to work for Fraunhofer IBP. Here, I have to thank Prof. Rovas and Alexandra, Dimitris and Soula Kalapothou and Gianna Arroni for “adopting” me upon my arrival and helping me to ease the transition to my new country, especially with my family away.

In addition, I have to thank all the colleagues of the 3rd floor of EnCN building for our great discussions during lunch and our even greater barbeques! Of course, I cannot forget all the colleagues in the Technical Building System Solutions Group for the excellent collaboration and all the fun moments: Max (I am really proud for our work together), Mounika, Andre. Niroz, mini-Marcus (who still visits and we gossip over coffee or beer), Georg Schneider (who taught me what German meeting times actually mean), Georg Pessler (who taught me how to drink beer properly), Lars (who has now access to the best coffee machine known to mankind!), Haonan and many others. I also owe a great thank you to my manager, Mrs. Simone Steiger, for her continuous support, her understanding and her open door to all discussions.

At this point, I would like to thank my old friends Giorgos Kardaras and Petros Xanthopoulos, who have been next to me from our first days at the University and stayed by my side even on my darkest moments, despite the huge kilometric distance between us.

Finally, I would like to thank my family in Papadianika (mother, father, sister, uncle Chrysanthos, uncles and grandparents – basically everyone!) for their continuous support and their faith in me. Without their presence and support I would be completely lost.

But above all, my deepest thank you goes to my family: Natalia, Dimitris-Chrysanthos and Vasilis-Nektarios. I entered my PhD adventure as a typical student and at the end of the line I come out of it with a beautiful wife and two amazing kids! I owe a big thank you to Natalia for her love and support all these years!

Κ. Π. Καβάφης – Το Πρώτο Σκαλί

Εις τον Θεόκριτο παραπονιούνταν
μια μέρα ο νέος ποιητής Ευμένης·
«Τώρα δυο χρόνια πέρασαν που γράφω
κ' ένα ειδύλλιο έκαμα μονάχα.
Το μόνον άρτιόν μου έργον είναι.
Αλλοίμονον, είν' υψηλή το βλέπω,
πολύ υψηλή της Ποίησης η σκάλα·
κι απ' το σκαλί το πρώτο εδώ που είμαι
ποτέ δεν θ' ανεβώ ο δυστυχισμένος.»
Είπ' ο Θεόκριτος· «Αυτά τα λόγια
ανάρμοστα και βλασφημίες είναι.
Κι αν είσαι στο σκαλί το πρώτο, πρέπει
νάσαι υπερήφανος κ' ευτυχισμένος.
Εδώ που έφθασες, λίγο δεν είναι·
τόσο που έκαμες, μεγάλη δόξα.
Κι αυτό ακόμη το σκαλί το πρώτο
πολύ από τον κοινό τον κόσμο απέχει.
Εις το σκαλί για να πατήσεις τούτο
πρέπει με το δικαίωμά σου νάσαι
πολίτης εις των ιδεών την πόλι.
Και δύσκολο στην πόλι εκείνην είναι
και σπάνιο να σε πολιτογραφήσουν.
Στην αγορά της βρίσκεις Νομοθέτας
που δεν γελά κανέναν τυχοδιώκτης.
Εδώ που έφθασες, λίγο δεν είναι·
τόσο που έκαμες, μεγάλη δόξα.»

THIS PAGE INTENTIONALLY LEFT BLANK

Contents

1	Introduction	1
1.1	Overview	1
1.2	Model-assisted Control Design	4
1.2.1	Occupant Thermal Comfort	6
1.2.2	State-of-The-Art Analysis and Limitations	10
1.2.3	The Proposed Methodology	13
1.3	Novelty and Contributions of the Thesis	20
1.4	Publications	21
1.5	Funding	23
2	Surrogate-based Stochastic Optimization	25
2.1	Formal Definition of the Optimization Problem	25
2.2	Cognitive Adaptive Optimization with Constraints (CAO-C)	28
2.2.1	Support Vector Machines as Meta-Models	28
2.2.2	Optimization over the Support Vector Machines Meta-Models	31
2.2.3	Comparison to Previous CAO Versions	34
2.3	Bayesian Optimization	34
2.3.1	Gaussian Processes as Meta-Models	34
2.3.2	Optimization over the GP Meta-Models	36
3	Experiments	39
3.1	Description of the Test Buildings	39
3.1.1	TUC Building	39
3.1.2	ZUB Building	43
3.2	Thermal Comfort Study	46
3.2.1	The Experimental Setup	47
3.2.2	Conclusions	55
3.3	Experiments on TUC Building	57
3.3.1	Real Heating Experiment with Radiators	58
3.3.2	Real Heating Experiment with AC Units	64
3.3.3	Simulation-based Evaluations with AC Units	70
3.4	Experiments on ZUB Building	73
3.4.1	Simulation-based Experiments on ZUB Building	73
3.4.2	Real Experiments in ZUB Building	87
4	Conclusions and Future Work	95

THIS PAGE INTENTIONALLY LEFT BLANK

List of Figures

1-1	Functional layers of Building Management Systems	2
1-2	Controllable Layers of a Building (Comite Europeen de Normalization (CEN), 2010)	3
1-3	Building Automation and Control System schematic according to EN15232	4
1-4	Desired functionality of an Intelligent Building Automation and Control System	5
1-5	CARTIF office building in Spain (Rovas et al., 2014a)	6
1-6	Acceptable range of operative temperature and humidity ratio based on ASHRAE Standard 55 (ASHRAE, 2010). The chart was designed using the web-based CBE Thermal Comfort Tool (Schiavon et al., 2014).	9
1-7	MPC scheme for building climate control (adapted from (Oldewurtel et al., 2012))	10
1-8	Moving Horizon Definition of the Optimization Problem	10
1-9	Model-assisted adaptive BACS design using detailed thermal simulation models	14
1-10	An example of a supply water temperature curve (Figure from GEOTABS project (Arteconi et al., 2014))	15
1-11	Simulation model view in this work	15
1-12	5R1C Representation of a zone (ISO, 2008)	17
1-13	Comparison of different model types	18
1-14	The Controller Actors in BCVTB	19
1-15	Coupling between the simulation model and the controller actors	19
1-16	The Actors of the Model/Controllers and the Control Design in BCVTB	20
2-1	Flow-diagram of the Optimization Algorithm	27
2-2	The ε -sensitive tube	29
2-3	SVM regression with different values of the hyper-parameters C , ν and γ	30
2-4	A simple GP with three observed points (Brochu et al., 2010).	35
3-1	The TUC building	40
3-2	Central heating system branches and the corresponding flow valves (T1-T8)	41
3-3	Simplified TUC simulation model for control	43
3-4	ZUB building and simplified Tower model views	43
3-5	Schema of the radiant distribution in ZUB building	44
3-6	Supply water temperature curve for ZUB building	44
3-7	South-East view of the Tower model with external shading groups	46
3-8	Summer results for office 08 using air temperature thermostat set at 24.5 °C	48
3-9	Summer results for office 04 using air temperature thermostat set at 24.5 °C	49
3-10	Summer results for office 08 using operative temperature thermostat set at 24.5 °C	49
3-11	Summer results for office 04 using operative temperature thermostat set at 24.5 °C	50
3-12	Summer results for office 08 using operative temperature thermostat set at 25.5 °C	50
3-13	Summer results for office 04 using operative temperature thermostat set at 25.5 °C	51
3-14	Winter results for office 08 using air temperature thermostat set at 22 °C	51
3-15	Winter results for office 04 using air temperature thermostat set at 22 °C	52
3-16	Winter results for office 08 using operative temperature thermostat set at 22 °C	52

3-17	Winter results for office 04 using operative temperature thermostat set at 22 °C . . .	53
3-18	Summer Experiments with different setpoints	53
3-19	Winter experiments with different setpoints	54
3-20	Results for office 107 of ZUB building	56
3-21	The Experimental Setup	57
3-22	Floor plan of the experimental building and test zones	58
3-23	Central heating system branches and corresponding flow control valves	59
3-24	Optimized operation for Office O4	62
3-25	Rule-based control for Office O4	62
3-26	Optimized operation for Office O5	63
3-27	Rule-based control for Office O5	63
3-28	22/02/2013 – 01/03/2013 real-building heating experiment results	64
3-29	Heating experiment results — hot water consumption	64
3-30	AC operation and comfort levels for Office 2	67
3-31	Weather and in-room conditions for Office 2	67
3-32	AC operation and comfort levels for Office 4	68
3-33	Door and windows opening schedules for Office 4	68
3-34	AC operation and comfort levels for Office 5	69
3-35	CAO controller performance for TUC building simulation study	71
3-36	Energy consumption – Comfort trade-off	72
3-37	Simulation study on the efficiency of BO vs RB controller for the whole cooling season for TUC	73
3-38	Weather data for the two simulation-based experiments on ZUB	75
3-39	Performance of ZUB under different levels of chance constraint relaxation, for the simulation-based evaluations on ZUB building	76
3-40	Performance of each office of ZUB under different levels of chance constraint relaxation for the January Experiment	77
3-41	Performance of each office of ZUB under different levels of chance constraint relaxation for the March Experiment	78
3-42	Hot water temperature under different levels of chance constraint relaxation, for the January Experiment	79
3-43	Indoor climate conditions for Office 207, under different levels of chance constraint relaxation, for the January Experiment	80
3-44	Indoor climate conditions for Office 107, under different levels of chance constraint relaxation, for the January Experiment	81
3-45	Indoor climate conditions for Office 007, under different levels of chance constraint relaxation, for the January Experiment	82
3-46	Hot water temperature under different levels of constraint relaxation, for the March Experiment	83
3-47	Indoor climate conditions for Office 207, under different levels of chance constraint relaxation, for the March Experiment	84
3-48	Indoor climate conditions for Office 107, under different levels of chance constraint relaxation, for the March Experiment	85
3-49	Indoor climate conditions for Office 007, under different levels of chance constraint relaxation, for the March Experiment	86
3-50	BaaS Platform – Core Components (Rovas et al., 2014b)	87
3-51	Baseline control of ZUB heating distribution system (12/11/2015 – 17/11/2015) . .	89
3-52	Knowledge-based control of ZUB heating distribution system (10/12/2015 – 15/12/2015)	90
3-53	Model-based control of ZUB heating distribution system (03/03/2016 – 08/03/2016)	91
3-54	Thermal Comfort sensation according to ISO 7730 comfort classes for ZUB building during winter — cumulative evaluation	91

3-55 Thermal Comfort sensation according to ISO 7730 comfort classes for ZUB building during winter — daily illustration. The solid lines indicate the Fanger PMV limits for comfort classes A, B and C and each dashed line represents the *measured* PMV values for one day of the experiment. 92

THIS PAGE INTENTIONALLY LEFT BLANK

List of Tables

1.1	Acceptable operative temperature and operative temperature band for thermal comfort in office buildings based on ISO 7730 (International Organization for Standardization, 2005)	8
3.1	TUC AC heating experiment results	69

THIS PAGE INTENTIONALLY LEFT BLANK

Chapter 1

Introduction

1.1 Overview

Effective utilization of energy in buildings is receiving significant attention. This interest is justified on the observation that buildings account for a significant portion of end-energy use: in Europe 40% of the total energy consumed is used for the operation of buildings (Pérez-Lombard et al., 2008) with a significant part of that energy used for conditioning occupied spaces. Energy retrofits, properly selected and executed, can yield appreciable reduction in energy demands. But the value of effective energy utilization during the building operational phase is undisputed both in terms of achieving good occupant comfort and in reducing energy consumption.

In energy management of buildings, Building Management Systems (BMS) (or Building Automation and Control Systems (BACS)) play an essential role in managing buildings by providing some monitoring and control capability for multiple sub-systems including HVAC, electrical systems, fire systems, security systems and others at minimal cost. Traditionally BMSs are offered to customers as products, comprising a software and a hardware component. Typically the purchase of a BMS product occurs at the same time as the purchase of other sub-systems (HVAC equipment, lighting, fire and security systems). Configuration and software installation happens during the installation and commissioning phases before handing the system to the building manager.

Functionality in most BACS is delivered in three hierarchical layers (see Figure 1-1):

- Field layer comprises primarily sensing (temperature, humidity, interior air quality, occupancy detectors, etc.) and actuation components (valves, light switches, etc.);
- Automation layer consists of controllers whose logical functions may range from the single input single output (SISO) closed-loop control at the base level, to plant-level control and supervisory control at the upper level. At the supervisory level, logic related to energy management and integrated system operation is implemented as a set of rules in Programmable Logic Controllers (PLCs);
- Management system layer provides capabilities for monitoring and centralized management of the building.

Very often, the installation and commissioning of the BMS system is viewed largely as a quality control process, and more specifically the target is proper installation and ensuring a minimum-level of functionality, rather than good operational performance. As such emphasis is placed on the lower field and automation layers. Energy-management and related functionalities – presumably key components in making a building smart or intelligent – are only seen as sub-products of installing the controller hardware and are typically addressed by installation of simple software that can provide

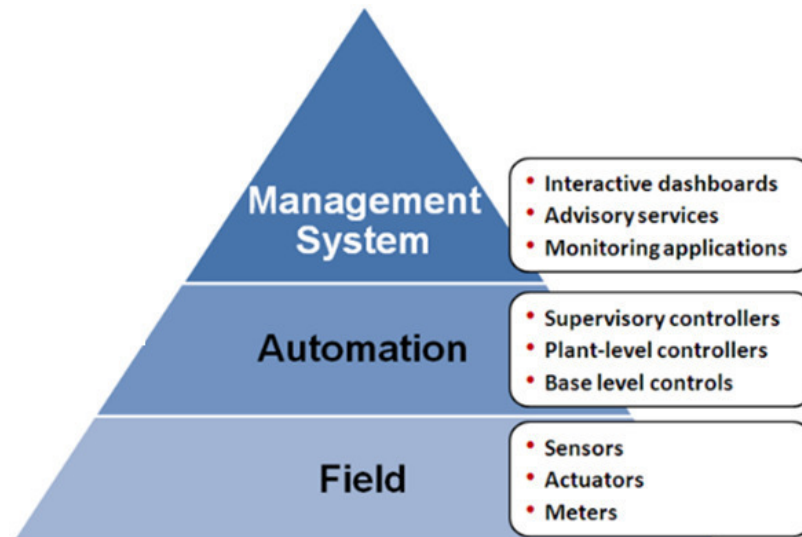


Figure 1-1: Functional layers of Building Management Systems

various advisory services for the people involved in daily operation, such as service technicians, engineers, or facility managers.

The above shortcomings have enabled the utilization of flexible and scalable BMS solutions, like e.g. the Johnson's Controls METASYS®. Here, the BMS is divided into two parts: Local and Remote. The local part is responsible for managing local control loops (usually PID), data collection and transfer, and very simple analytics; and the remote layer is responsible for providing more advanced services. The availability of such a cloud-based platform enables the development and utilization of advanced building energy management services, which cannot be deployed in local hardware due to their computational requirements.

On the other hand, even with a solution that offers high flexibility, a question that arises is which actuating elements of the building should be controlled and how, in order to achieve energy-efficient operation. In this direction, EN15232 (Comite Europeen de Normalization (CEN), 2010) which evolved in ISO 16484-7 provides a generic description of efficient BACS. According to the standard, a BACS has access to the following three layers (Figure 1-2)

- The Generation layer, which schedules the operation of all available energy providers/generators;
- The Distribution layer, which regulates the energy transferred from the generators to the building spaces;
- The Emission layer, which schedules the operation of all terminal units in all building spaces.

Depending on the specific sub-systems consisting each of these layers, the goal is to design an intelligent BACS that would take into account the properties of the installed HVAC and the interactions among the layers, to operate in an energy-efficient manner. Here, the EN15232 standard is an effort to identify and enumerate the functional components that influence the building performance, and thus identify functionalities that a BACS should address. The BACS is divided into two parts: the Building Automation and Control (BAC) functions and the Technical Building Management (TBM) functions. The BAC functions directly affect the energetic performance of the building, by adjusting the operation of selected emission, distribution and generation systems, while TBM functionalities have an indirect effect to this direction by identifying discrepancies, thus assisting towards efficient operation. This set of enumerated control and TBM functions provides all the necessary building blocks towards designing and deploying a BACS suitable for any building, facilitating any combination of commonly found HVAC and energy systems.

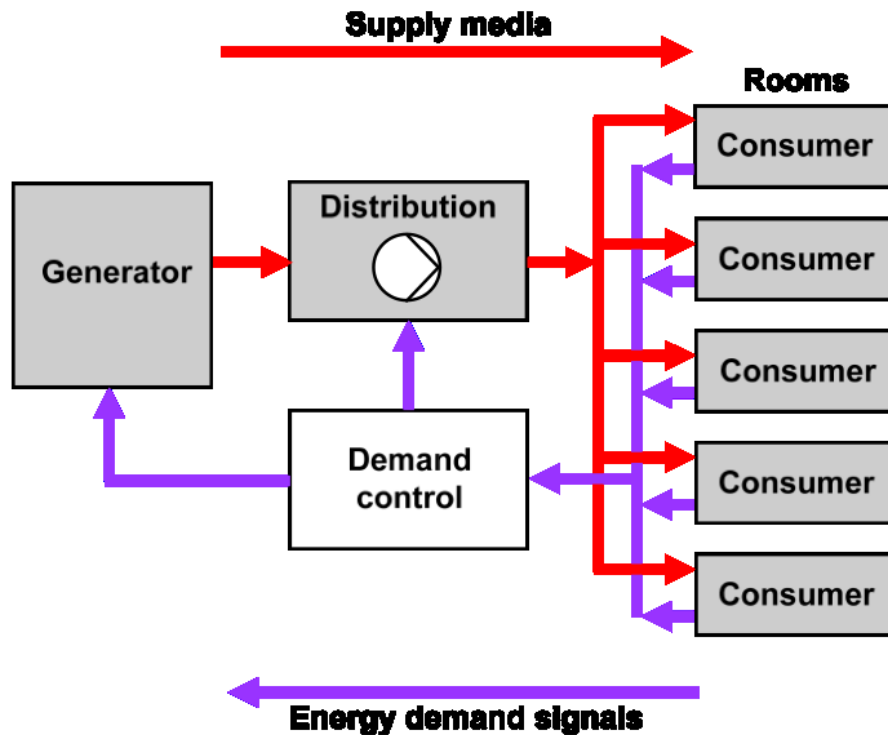


Figure 1-2: Controllable Layers of a Building (Comite Europeen de Normalization (CEN), 2010)

Shown in Figure 1-3 is a schematic of a high-performance BACS according to EN15232. In this figure E_1, \dots, E_M are controller functions (often physical control devices with embedded logic) for emission elements; similarly D_1, \dots, D_N are controller functions for distribution elements; and G_1, \dots, G_K are controller functionalities for generation elements. Here, according to the standard, the BMS is a basic entity in energy management and comprises of a set of standard control schemes (controllers), such as thermostats, on/off controllers, scheduled tasks, etc. The initial configuration (or tuning) of these controllers is performed by the BMS installation team based on expert knowledge, while the building maintenance staff periodically re-configures the parameters of few high-level controllers (e.g. thermostat setpoints and operational schedules), usually on seasonal basis. Thus, the building administrator is tasked to study historical data of the building performance and/or the occupant behavior and manually adapt the control logic (tuning controller parameters) following common rules.

It is very often the case that these decisions are not good enough: it is estimated (Roth et al., 2005) that up to 20% of the energy used for HVAC and lighting system operation is lost due to poor configuration, wrong operational assumptions during the design and commissioning phases, or system faults that go undetected. Even in the case of good configurations, it is very hard to encapsulate good strategies within a static set of simple rules. Also tuning of individual controller parameters might not (and probably will not) result in good performance of the overall control strategy. The situation can be particularly egregious for buildings with complex energy concepts or when renewable energy systems are installed, where, in the former case, the complexity of integration becomes formidable as all the systems have to operate harmoniously together, while in the latter case generation patterns strongly depend on weather conditions. It is conceivable that such a manual configuration process can be a laborious and error-prone non-trivial task. In addition, in locations characterized by high weather variability between days or weeks during specific periods (e.g. spring), more frequent adaptation of the control parameters is required.

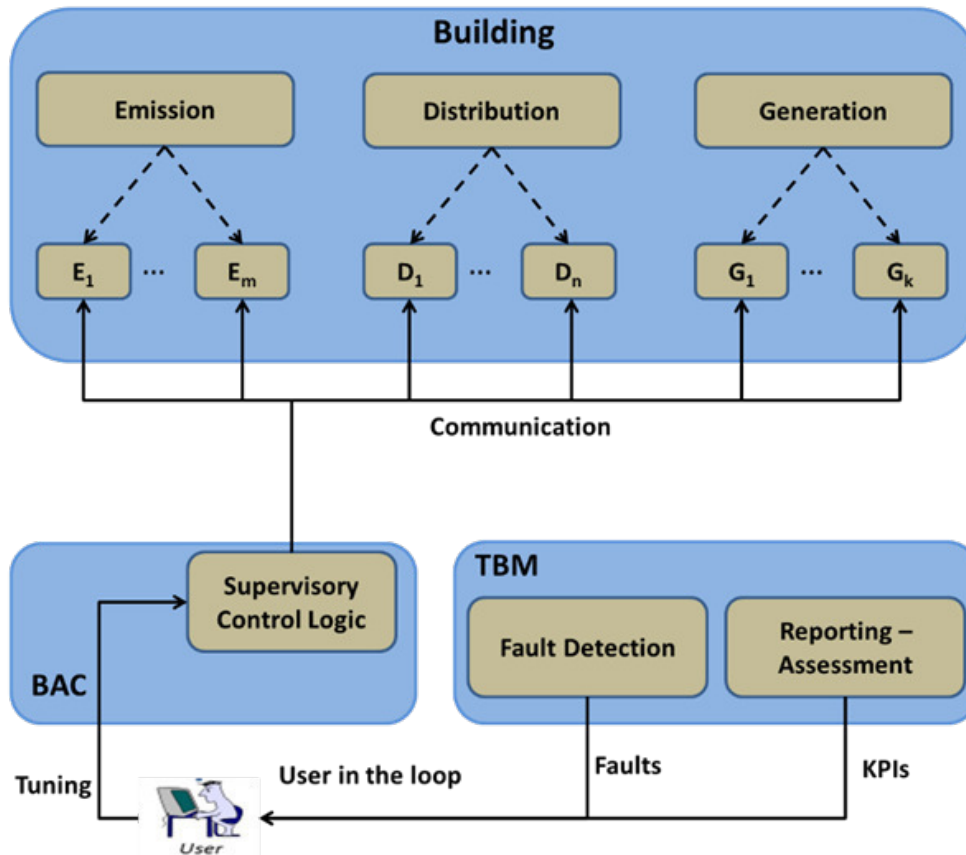


Figure 1-3: Building Automation and Control System schematic according to EN15232

1.2 Model-assisted Control Design

In current research efforts, this manual tuning process is replaced by a methodology called model-assisted control design and is developed following two axes:

- Predictions vs study of historical data: here instead of gathering and analyzing historical data from the building to improve the efficiency of BAC functions, (weather, occupancy, equipment gains, etc.) forecasts are utilized to determine the (near-) future state (e.g. comfort conditions, demand, etc.) of the building. This allows for a constant adaptation of the control logic to the (predicted) needs of the building and the microclimatic conditions of each site — a process that needs to be iterative.
- Automated control strategies: since using predicted data for BAC functions optimization implies frequent design intervals (e.g. once a day), it is practically infeasible to tune all these functions by hand. Thus, an optimization process is defined to design efficient controllers in an automated and laborious-free manner.

A schematic of the proposed enhancements, as described above, is shown in Figure 1-4. Here the user defines the control logic tuning problem (cost function and constraints) and the optimizer generates new sets of parameters. The new block is in charge of continuous monitoring and improvement of the control logic.

Even though this formulation seems trivial, the associated complexity can be formidable. In order to highlight this complexity, we will use as an example the building shown in Figure 1-5, which is a typical mid-sized office building, located in Valladolid, Spain (Rovas et al., 2014a). The building has two floors and 15 heated spaces according to the schematics (11 offices and laboratories and 4

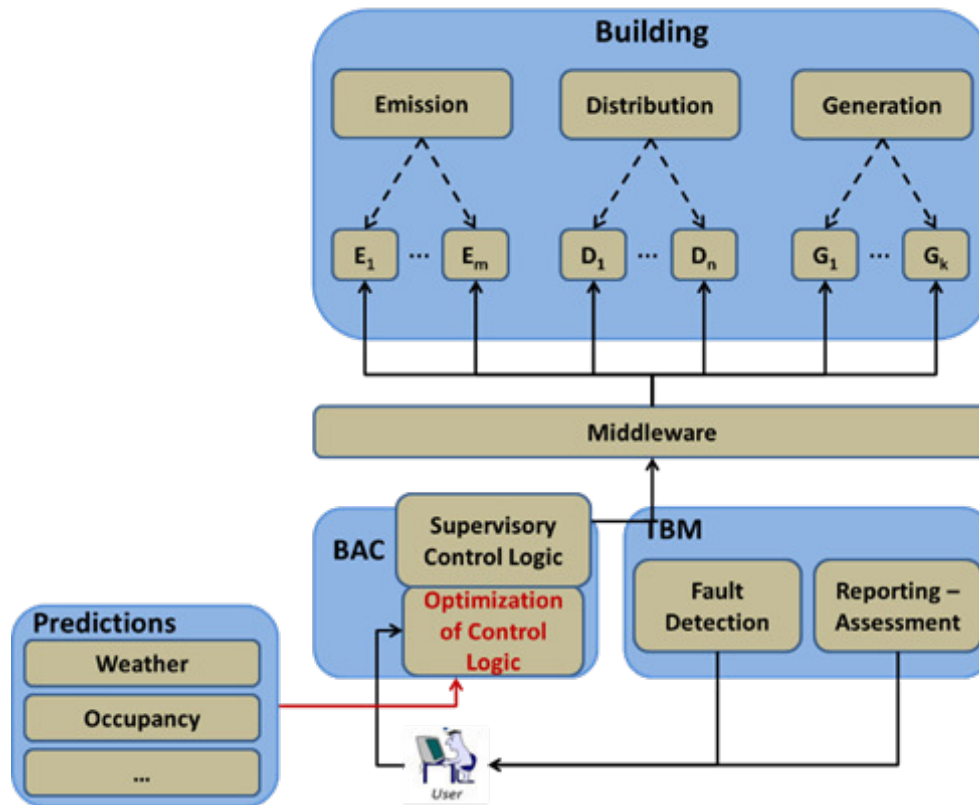


Figure 1-4: Desired functionality of an Intelligent Building Automation and Control System

common areas).

At the generation level, a gas boiler is available and is combined with a solar-thermal installation and a heat storage. The boiler operates within a pre-defined time schedule (from 2 a.m. to 12 p.m.). In addition, once the water in the tank reaches a pre-defined temperature, a valve bypasses the boiler and uses the water heated from the solar-thermal installation.

At the distribution level, a three-way valve controlled by a PID controller is installed, allowing the hot water entering from the generation side to be cooled at any temperature.

The emission system is underfloor heating with Thermally Activated Building Systems (TABS) and in each heated area, different number of heating circuits are included. There is a temperature sensor in each thermal zone and its measurements are provided as input to the PID controllers regulating the hot water flow in all circuits of the zone. In addition to this, there is a rotary switch in all offices and laboratories, so the users can change the heating setpoint of each room.

Now let's take this typical building example and try to examine the complexity of designing new control actions for all controllable elements for one day. If we assume for simplicity that the boiler schedule and the strategy of using hot water from the solar-thermal installation remain fixed, and we send new control actions to all controllable elements every one hour, then we define the following controllers:

- 10 setpoints (one per hour for the 10-hour availability of the boiler) *for each heating zone*, i.e. $10 \times 15 = 150$ decision variables; and
- 10 setpoints (one per hour for the 10-hour availability of the boiler) for the hot water temperature in the distribution circuit. i.e. another 10 decision variables.

This means that the optimization problem defined (and will be required to be solved every few

minutes or hours as we will see next) comprises of 160 decision variables, while if we select to also optimize the operation schedule of the boiler and the use of the hot water from the solar-thermal installation, the complexity of the problem increases significantly. To add to this, we are also dealing with several stochastic disturbances, since e.g. the weather forecasts are not always accurate, different people have different heating preferences, we have noisy sensor measurements, etc.

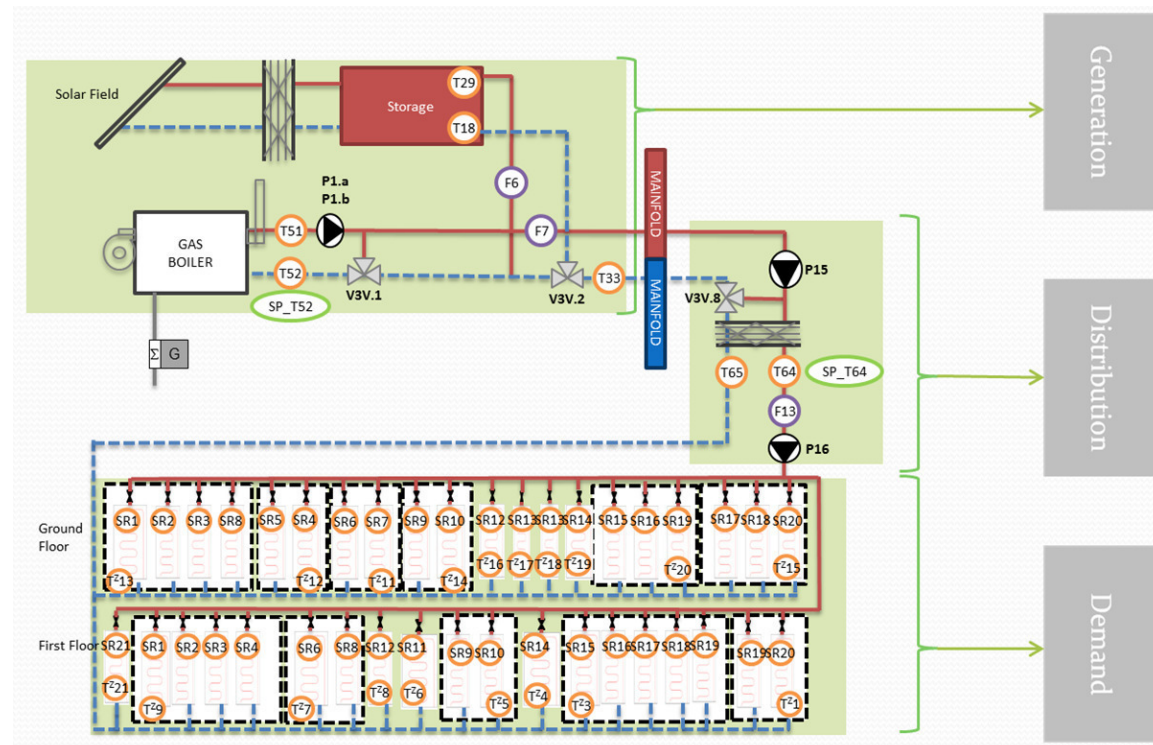


Figure 1-5: CARTIF office building in Spain (Rovas et al., 2014a)

1.2.1 Occupant Thermal Comfort

An important question in this automated setup is to determine the desired outcome of the process. Here, although in the majority of cases building owners expect to see “energy-saving operation,” it is important to emphasize that the goal for “energy-savings” is untimely if treated separated and isolated from parameters, like user thermal comfort; the final target of an intelligent BAC functions optimization mechanism should not only be the minimization of a performance index, such as the total energy consumption or the operational cost, but should also ensure smooth building operation, taking into account user comfort. For example, in a real building, a newly-installed BACS can consume more energy than the existing system, in order to improve user comfort levels.

A wide range of methodologies for indoor thermal comfort estimation exist: from simple dry-bulb temperature-tracking (Ma et al., 2012a; Oldewurtel et al., 2012) to more elaborate indices (Azer and Hsu, 1977; Fanger et al., 1970; Gagge, 1971). The most widely accepted models, as evidenced by their adoption in indoor climate thermal comfort standards are: i) Fanger’s Predictive Mean Vote (PMV) model (Fanger et al., 1970) used in ISO 7730 (International Organization for Standardization, 2005) and ASHRAE 55 (ASHRAE, 2010) standards; ii) the Adaptive Comfort Model of the ASHRAE Standard 55-2010 (ASHRAE, 2010); and iii) the Adaptive Comfort Model of the European Standard EN 15251 (CEN, 2007).

These methodologies can be put into two broad categories: i) human body heat balance approaches (Azer

and Hsu, 1977; Fanger et al., 1970; Gagge, 1971); and, ii) thermal adaptation approaches (ASHRAE, 2010; CEN, 2007). The first category applies to buildings with mechanical Heating, Ventilation and Air Conditioning (HVAC) systems where the building occupants are allowed to control the internal environment to desired levels of air temperature, while the second category applies to naturally ventilated buildings.

1.2.1.1 Fanger Predicted Mean Vote model

Fanger's Predicted Mean Vote (PMV) model is based on human body heat-balance considerations. Taking into account that thermal sensation is influenced by environmental (air temperature, radiant temperature, humidity and air velocity) and personal factors (activity and clothing), the PMV index predicts the thermal comfort on a seven-point sensation scale (-3 cold, -2 cool, -1 slightly cool, 0 neutral, +1 slightly warm, +2 warm and +3 hot). The Fanger Predicted Percentage of Dissatisfied (PPD) people index, derived by the PMV index, predicts the percentage of a large group of people likely to be thermally (dis-)satisfied with their environment.

Precise quantification of personal factors is a challenging task, due to the difficulty associated with making robust measurements. Instead, metabolic rate estimation methods and predefined clothing insulation values are used. Methods for metabolic rate estimation are divided into four levels in ascending order of accuracy (International Organization for Standardization, 1989). At Levels 1 (screening) and 2 (observation), look-up tables are used to estimate metabolic rates for various occupation and activity types. At Level 3 (analysis), the metabolic rate is estimated using an empirical correlation to the total heart rate. The total heart rate is the sum of the heart rate at rest and its increase under specified conditions. When the total heart rate is known a linear relationship can be established between the two parameters. At Level 4 (expertise), the metabolic rate is determined by measuring oxygen consumption and carbon dioxide production rates. Level 3 and 4 methods require measurements that might be hard to collect and the improvement in accuracy ($\pm 20\%$ error for Level 2 vs. $\pm 5\%$ error for Level 4) does not significantly impact the results of our study as a simple sensitivity analysis might show.

The role of clothing as an insulating material is captured by the thermal resistance, and typically measured in units of clo. In many applications constant values of 0.5 clo are used during the cooling season, and 1.0 clo during the heating season. To account for the fact that humans adjust their clothing based on prevailing conditions, three predictive clothing insulation models are proposed ASHRAE 55-2013 (Schiavon and Lee, 2013); in all these models, the clothing insulation varies as a function of outdoor air temperature measured early in the morning (at 6:00) and the indoor operative temperature.

Concerning environmental factors, air temperature, humidity and air velocity are relatively easy to measure, and low-cost sensors are readily available and installed in many buildings. Radiant temperature measurements are not frequently performed, except in experimental buildings (both buildings in our study are equipped with such sensors). In cases where sensed measurements of radiant temperature are missing, two methods are commonly used to estimate radiant temperature: the space averaged radiant temperature, calculated assuming that the occupant is at the center of a space; and the angle-factor radiant temperature, calculated based on angle factors between a person's location and the different surfaces of a space. As can be inferred from the discussion above evaluation of the PMV index is not easy, since many of the parameters have to be estimated or require sensing modalities that may not be available. For this reason, both ASHRAE 55 and ISO 7730 introduce simplified calculation methodologies to define acceptable limits for thermal comfort.

In ISO 7730 the simplification is based upon an operative temperature of 24.5°C in summer and 22.0°C in winter. These recommendations correspond to zero values of the PMV index, under standard assumptions on the metabolic rate (1.2 met, corresponding to sedentary activity), clothing

level (0.5 clo in summer and 1 clo in winter), relative humidity (60% in summer and 40% in winter), and air velocity (as in the Table 1.1). Three different comfort categories are introduced in ISO 7730 with varying ranges, corresponding to varying percentages of the PPD index: i) Category A is recommended for buildings occupied by people with special thermal comfort requirements (e.g. very young children, elderly); ii) Category B is suitable for most new buildings and renovations; and iii) Category C is suitable for existing, less energy efficient, buildings.

Table 1.1: Acceptable operative temperature and operative temperature band for thermal comfort in office buildings based on ISO 7730 ([International Organization for Standardization, 2005](#))

Category	Thermal Comfort Indices		Operative Temperature (°C)		Max Air Velocity (m/s)	
	PPD (%)	PMV	Summer	Winter	Summer	Winter
A	≤ 6	[-0.2,+0.2]	24.5 ± 1.0	22.0 ± 1.0	0.12	0.10
B	≤ 10	[-0.5,+0.5]	24.5 ± 1.5	22.0 ± 2.0	0.19	0.16
C	≤ 15	[-0.7,+0.7]	24.5 ± 2.5	22.0 ± 3.0	0.24	0.21

In ASHRAE 55 acceptable ranges of operative temperature (defined as the average of radiant and dry-bulb air temperature) and humidity ratio are defined. In Figure 1-6, comfort ranges (shaded polygons) are illustrated for heating season (clothing value = 1.0 clo) and cooling season (clothing value = 0.5 clo), for occupants under light activity (1.2 met). The limits for each season are defined for a value of PPD = 10% (corresponding to $-0.5 \leq \text{PMV} \leq 0.5$), where 10% of the users are expected to express discomfort with their environment. The discomfort levels approach a PPD = 10% level near the edges of the polygons and approximate a value of PPD = 5% (or PMV = 0) as we move towards the center of the shaded areas. We can move to the right of the diagram by heating a space, to the left by cooling it, upwards by humidifying a space and downwards by dehumidifying it.

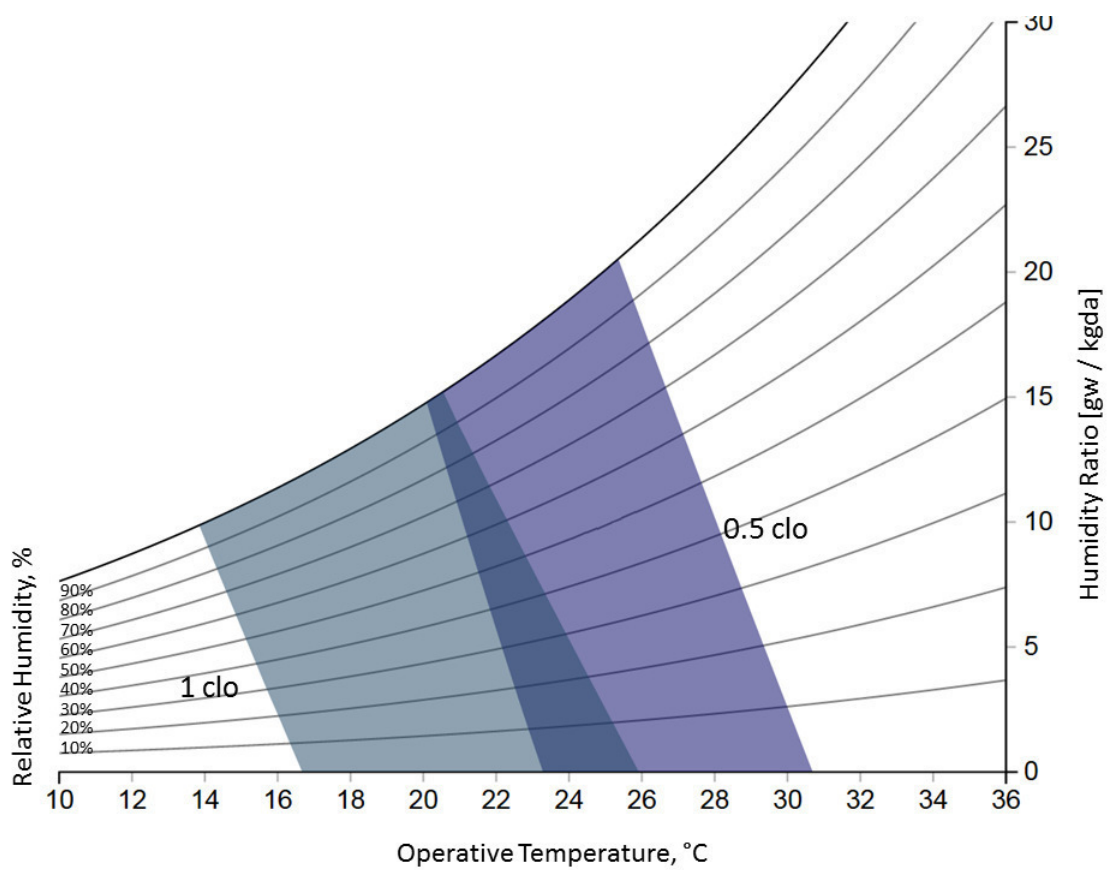


Figure 1-6: Acceptable range of operative temperature and humidity ratio based on ASHRAE Standard 55 (ASHRAE, 2010). The chart was designed using the web-based CBE Thermal Comfort Tool (Schiavon et al., 2014).

1.2.2 State-of-The-Art Analysis and Limitations

State-of-the-Art research in the field of generating automatically optimized control strategies for efficient building operation is based on the Model Predictive Control (MPC) paradigm. Here, as shown in Figure 1-7, we assume that a model of the process (of the real building in our case), as well as (weather, occupancy, etc.) forecasts for a predefined time window are available. This way a constrained optimization problem is formulated and solved for a predefined period in the future, generating a control signal (or control strategy) which is optimized for the system on the basis of a defined cost function and a set of (visual, thermal, air-quality, etc.) comfort constraints.

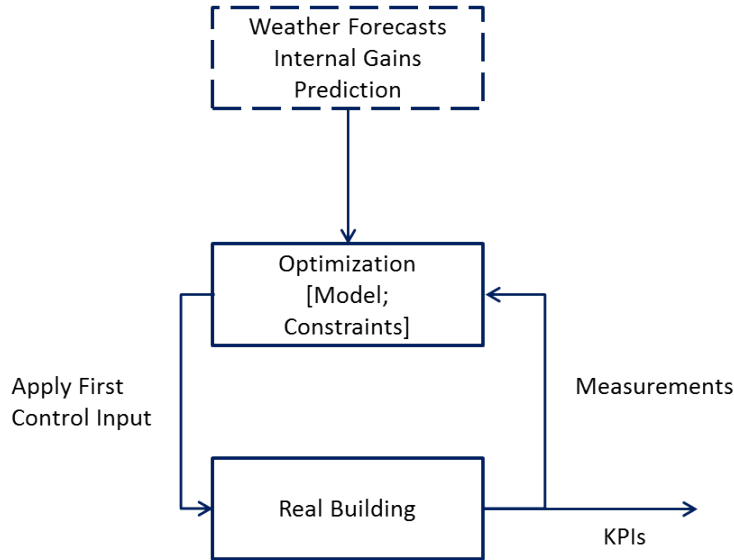


Figure 1-7: MPC scheme for building climate control (adapted from (Oldewurtel et al., 2012))

To account for modeling/prediction errors and unpredicted disturbances like user actions, this strategy is then applied to the building for a shorter period of time and the whole process re-initiates — see Figure 1-8 for a schematic.

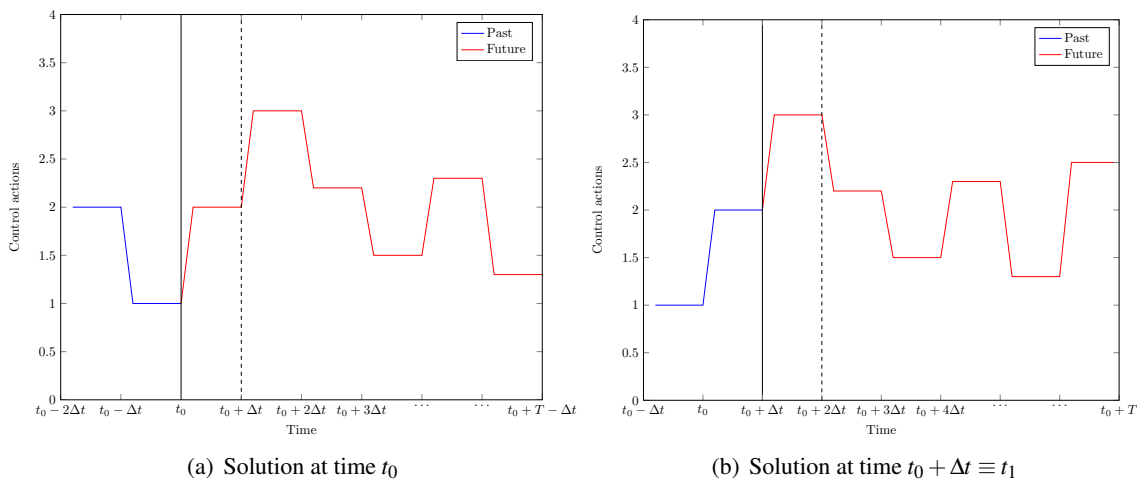


Figure 1-8: Moving Horizon Definition of the Optimization Problem

As the body of literature regarding MPC techniques in the control of HVAC systems has grown huge over time, in this thesis we do not provide an exhaustive literature review of all available research papers in the field; instead, we refer the interested reader to (Afram and Janabi-Sharifi,

2014) for an overview of the application of MPC setups in energy efficient building operation and in (Sturzenegger et al., 2016) for a comprehensive list of real-world model-based building control applications, while we reference selected publications in the remainder of the Section to highlight the limitations of existing approaches and determine the contributions of the approach presented here.

A first limitation of classical MPC approaches, which require physics-based models of special linear or quasi-linear structure – see (Cigler and Privara, 2010; Ma et al., 2011; Morosan et al., 2010; Nghiem and Pappas, 2011; Oldewurtel et al., 2012; Široký et al., 2011) for successful implementation – is the treatment of thermal comfort constraints. As we aspire to save energy by exploiting the inherent trade-off between energy consumption and thermal comfort, with the latter acting as a constraint defining a theoretical and practical upper bound on potential energy savings (Ghahramani et al., 2016; Oldewurtel et al., 2012; Pichler et al., 2011; Zavala, 2012). It is conceivable that different definitions for comfort yield different energy saving potential (Kontogianni et al., 2013; Morales-Valdés et al., 2014), while improper definitions – favoring higher energetic benefits – can lead to dissatisfied users and productivity loss (Akimoto et al., 2010; Fisk, 2000). Thus the ability to estimate (or predict) thermal comfort is critical for parsimonious and cost-efficient building operation.

Despite the active research effort towards better understanding and estimating thermal sensation, which is distilled in international standards, as analyzed in the previous Section, as well as the expressed need for proper comfort definitions on building control from both the research community (Cigler et al., 2012; Donaisky et al., 2007; Drgona et al., 2013; Freire et al., 2008; Katsigarakis et al., 2016; Kontes et al., 2014) and the industry (Mařík et al., 2011), current practice in BACS design and performance evaluation facilitates defining comfort as a region (or band) of air temperature upper and lower limits (Ma et al., 2012b) around a target set point (e.g. $22^{\circ}\text{C} \pm 2^{\circ}\text{C}$).

Changing the set point or increasing the dead band can lead to significant energy savings (Atam and Helsen, 2016; Ghahramani et al., 2016; Hoyt et al., 2015; Ma et al., 2012b; Moon and Han, 2011), but is also evident from field experiments in spaces with dry-bulb temperature control that users tend to act upon the controllable elements of a building — such as windows, blinds, lights and thermostats — in response to their feeling of thermal discomfort (IEA Annex 66, 2013), with potentially detrimental effects to energy performance (Azar and Menassa, 2015; D’Oca et al., 2014; Li et al., 2014). One of the main reasons for this, is that zone dry-bulb air temperature measurements when used in isolation might not always be suggestive of the actual thermal sensation of the occupants due to all other factors also affecting thermal comfort in building spaces, such as the effect of solar radiation or humidity (International Organization for Standardization, 2005). In view of this, the effect of solar radiation in thermal comfort has been studied extensively (Kang et al., 2010; Marino et al., 2015), while in (Feng et al., 2015; Gwerder et al., 2008, 2009; Lehmann et al., 2007) controllers able to compensate this effect in buildings with Thermally Activated Building Systems (TABS) were presented

Since the majority of MPC applications in buildings follows the temperature bound approach, the resulting optimization problem is solved using traditional optimal control or convex optimization techniques by linearisation of the model around feasible regions (Oldewurtel et al., 2012). As a consequence of strict requirements on the models, the arduous task of developing purpose-built models has to be addressed (Sturzenegger et al., 2014). For the model construction, one approach is to use first principle models (Oldewurtel et al., 2012), but for large buildings the problem can prove to be intractable (Privara et al., 2011). To overcome this problem, many data-driven approaches have been introduced, based on system identification methods (Cigler and Privara, 2010; Garnier et al., 2013; Kolokotsa et al., 2009; Privara et al., 2011; Vana et al., 2010), but the excitation process of the system has to be designed carefully, in order not to disturb the occupants of the building (Vana et al., 2010; Žáčková et al., 2014), thus leading to models with poor extrapolation properties. To

that direction, some approaches (Privara et al., 2011) use a thermal simulation model of the building for the identification process – which remains a difficult process necessitating expert knowledge. In addition, also in this case, the requirements of the models limit the potential to include more realistic thermal comfort indices, like the Fanger index, defined in relevant standards (International Organization for Standardization, 2005). Formulations that use approximation of the Fanger index by linear functions within a limited band of weather and indoor conditions (Cigler et al., 2012) or simplified building models (Klauco and Kvasnica, 2014) have been recently reported. Still what is more commonly observed is to define comfort as a region of the operative (Oldewurtel et al., 2012) or air temperature (Ma et al., 2012b) of each building zone.

In an effort to overcome the arduous task of defining models with special structure manually for every test building, selected publications utilize detailed thermal simulation models using thermal simulation software like EnergyPlus (Crawley et al., 2001) and TRNSYS (Klein et al., 1976). These models can be available from the design phase of the building or can be generated semi-automatically using available Building Information Models (Bazjanac et al., 2011; Lilis et al., 2015).

Here, a first approach is to utilize the simulation model as a surrogate model offline, and facilitating a large number of simulations to create a reduced model, used for the online optimization phase (Eisenhower et al., 2012; Privara et al., 2011). In this setup, the assumption is that the simulation model assimilates perfectly the real building, for all the different combinations of weather conditions and occupants actions, but from our experience with real-building setups, the simulation model is capable of providing accurate predictions for the indoor conditions in each room of a building for a short period of time (e.g. few days or weeks) and provided that the initial thermal conditions of the building are correctly estimated. Another source of inaccuracy is the incorporation of occupant's behavior (control actions and occupancy schedule) and of internal gains in a static manner, following a set of guidelines, but in practice, the behavior of the occupants in specific spaces can prove to be different compared to the one anticipated during the design phase. In the end, the effect of these two assumptions can largely affect the accuracy of the generated reduced model and we may end up with a model that provides accurate predictions for specific occupancy and weather conditions.

A second approach that addresses these problems, is to use the simulation model online, i.e. replacing the linear or bi-linear model used in classical MPC by a detailed thermal simulation model. Some early work here (Coffey et al., 2010; Henze et al., 2005) utilizes optimization approaches such as Genetic Algorithms, where each objective function and constraint evaluation is a single simulation call. It is conceivable that the computational burden of such approaches is enormous (and grows exponentially with the number of posed comfort constraints (Henze et al., 2005)), making this setup prohibitive for realistic, large-scale predictive control applications.

Newer approaches (Baldi et al., 2014; Giannakis et al., 2011; Karagevrekis et al., 2014; Kontes et al., 2012, 2014, 2013; Korkas et al., 2015; Pichler et al., 2011) utilize the available simulation model to construct a simple meta-model online, able to predict the behavior of the building only for the prediction horizon. This meta-model is used for the optimization of the control strategy, in an effort to reduce the number of simulation calls to the “expensive” simulation model. The problem with most of these approaches stems from the formulation of the optimization algorithm (Baldi et al., 2014; Kontes et al., 2014), since due to computational complexity constraints, the objective function to be optimized needs to contain one term for the energy consumption and one term for the *collective comfort constraint for the entire building*, properly weighted. In large-scale real-world setups, finding a proper weighting between the active constraints is not a trivial task. For example, in an office building with 30 offices, where thermal and visual comfort constraints need to be met, minimizing the energy consumption of the building while giving priority to thermal over visual comfort constraints requires: i) proper normalization between the energy consumption, the thermal comfort and visual comfort constraints values so no term is dominating the combined cost function (Luenberger and Ye, 2008); and ii) adjusting the relative importance of visual over thermal comfort

constraints. Hand-tuning a set of weights able to enforce this relative importance between the terms in a real, large-scale building application and being generic enough to capture all the real-world variations (e.g. varying daily consumption and constraints values, etc.) is a formidable task. In addition, in most cases average discomfort values for all offices are calculated, in contrast to normative guidelines (ASHRAE, 2010; CEN, 2007; International Organization for Standardization, 2005). We have to note here, that simulation model-free versions of these algorithms have been reported (Baldi et al., 2015; Michailidis et al., 2016), but they suffer from the same drawbacks described above, as well as the danger of “poor excitation,” as with any data-driven approach (Žáčková et al., 2014).

1.2.3 The Proposed Methodology

The methodology developed in this thesis tries to address the limitations of the approaches described in the previous version, while maintaining the benefits of the MPC paradigm. Therefore, we utilize detailed thermal simulation models for online model-based control, but in the heart of our methodology lies a constrained surrogate-based stochastic optimization algorithmic setup, able to treat every (thermal, visual, etc.) comfort constraint as separate constraint. Obviously the degree to which our methodology can achieve good performance depends on the quality of prediction of the disturbances. To reduce their adverse effects (in case of false predictions) we adopt parametric feedback controllers for all the controllable generation, distribution and emission elements of the building, instead of open-loop control strategies as in typical MPC approaches. Thus the building performance optimization task is transformed to a task of optimizing a set of control parameters — a process called Control Design (CD).

The overall methodology is shown in Figure 1-9. Here, an optimization algorithm facilitates several simulation calls with different sets of control parameters and the model, utilizing forecasts for the weather conditions and the occupancy, predicts the performance of each control parameters set in terms of total energy consumption and user comfort.

In the remainder of the Section, the requirements and the properties of each component of our methodology is presented, while in the following Chapter, the different versions of the proposed stochastic optimization approach are analyzed.

1.2.3.1 Controller Functions

The selection of proper parametric control functions is a key ingredient towards efficient building operation. These functions should be rich enough to be able to capture the complexity of the control task on one hand, but on the other hand the number of the control parameters should be kept as small as possible, to reduce the computational burden of the optimization algorithm. In this direction, the BAC functions defined in EN 15232 provide a comprehensive list and enables a generic BAC selection process suitable for many buildings, supporting common HVAC and energy systems. While the list describes (to a good level of detail) the function blocks, it does provide little by way of implementation on the logic behind each function.

Thus, it is clear that a first knowledge-based step/task is required towards applying the Control Design process on a study building. This step requires an expert to determine the *parametric* controller functions to be applied in each controllable element, along with all their properties (e.g. inputs, outputs, execution interval, etc.). These controllers can be the default controllers of the building in parametric form (e.g. $u_{RB,k}^{HW} = -\theta_1 T_k^{amb} + \theta_2$, with T_k^{amb} the average outside ambient temperature of the last 24 h, calculated at time k for a standard heating curve regulating the supply water temperature in a heating system, as shown in Figure 1-10) or new, more complex controllers like a heating curve including also the solar radiation and the office temperatures.

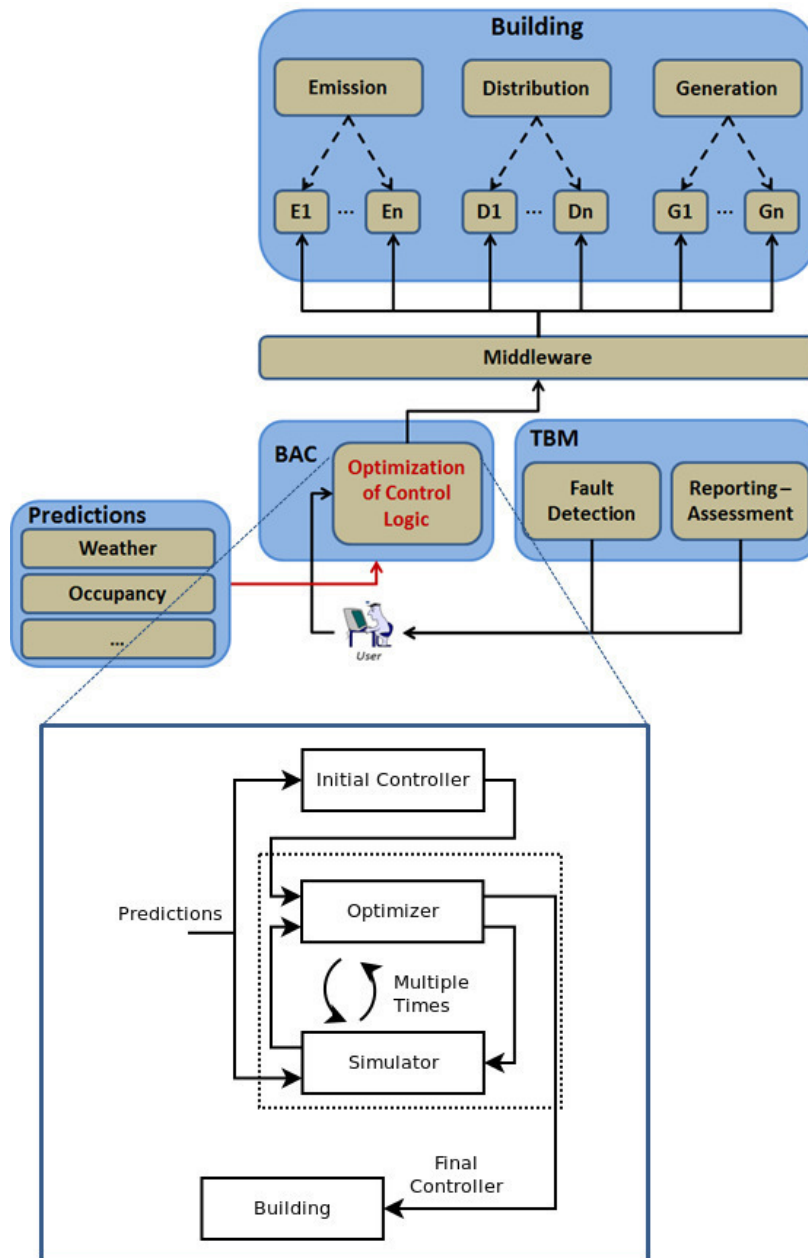


Figure 1-9: Model-assisted adaptive BACS design using detailed thermal simulation models

This parametric representation of the controllers allows our approach to be able to adapt in any control configuration of a given building (since for a given building equipped with a set of emission, distribution and generation systems, different providers can contribute controller libraries that define different control functions over the same controllable elements), while being able to handle controllers with special structure (e.g. Finite State Machines) in contrast to the classical MPC approaches.

1.2.3.2 Simulation Model Requirements

The proposed methodology relies on the availability of accurate enough models, able to predict the thermal state of the building and encapsulate all the relevant dynamics of the emission, distribution and generation systems. Of course, the level of accuracy cannot be quantified, since it varies

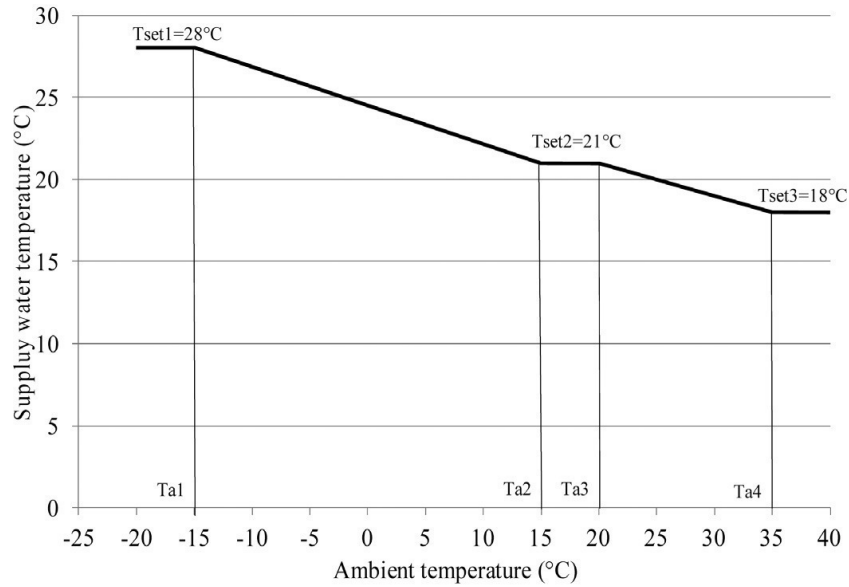


Figure 1-10: An example of a supply water temperature curve (Figure from GEOTABS project (Arteconi et al., 2014))

depending on the dynamics of the application building, the properties of the available HVAC and energy systems, as well as the expected fidelity of the BACS. Nevertheless, the model should be able to capture the relevant sensitivities and trends of the physical system and at the same time facilitate reduced simulation times, suitable for control design tasks. The balance between these requirements depends on the calculation methodologies utilized in each model type. From a generic point of view, Figure 1-11 illustrates the utilization of a model, facilitating a specific calculation methodology. Here, a set of inputs is provided to the model (typically control actions for all emission, distribution and generation systems) and a set of outputs reflecting the quality of the controller with respect to the cost function and the constraints defined for the problem.

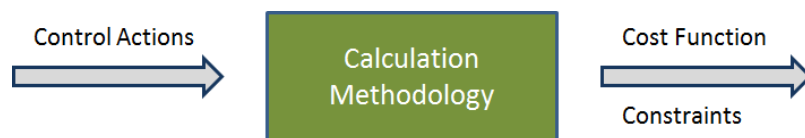


Figure 1-11: Simulation model view in this work

The complexity of building simulation stemming from the multitude of intertwined parameters along with the many and varying typology of energy-influencing and consuming elements makes the development of accurate simulation models a challenging and oftentimes formidable task. It is becoming quite common, especially during the design (or subsequent retrofitting) phases of a building lifecycle, that simulation models are employed to prognosticate energy performance and help identify salient problems with respect to energy design. The calculation methodologies used can range from “simple” quasi-steady-methods, as defined in ISO 13790:2008 (ISO, 2008) and related standards; to dynamic, implemented in energy-performance simulation zonal-type software like EnergyPlus or TRNSYS. Each calculation method supports different use cases and, as such, the modeling assumptions and the associated inputs can vary greatly in the levels of detail and information that has to be provided. In an attempt to rationalize the medley approaches one could use multiple classification criteria: the resolution of the spatial and temporal discretization, the mathematical structure of the models used, whether these models are created from data or using

first-principles, etc.

In general, building thermal and energy simulation programs use mass and energy balances (Moss, 2015) as a basis for estimation of the evolution of the values of variables referring to internal conditions (temperature, humidity, CO₂ concentration, luminance) and energy needs (total energy, maximum power demands) of building interiors. Energy conservation laws are used to investigate thermal energy transfers and exchanges among building elements, spaces, and systems, while mass conservation is used for evaluation of vapour-water transfers (humidity). Implicit in all the methodologies is the discretization of the pertinent conservation equations over pre-determined time intervals. Based on time-resolution criteria calculation methodologies can be classified into two categories:

- Static or quasi-static calculation methodologies. These methods assume average parameter values for a long period of time (typically a month or a season), and account for dynamic effects using empirical correlations and averaging correction factors. These types of calculation methods are especially useful for estimation on energy performance on an annual basis.
- Transient calculation methodologies. Transient calculation methodologies take a more granular approach using a time resolution which is comparable to the time-scale of time-varying effects that are being modelled. Consequently these methods are capable of capturing transient phenomena such as weather changes, occupancy variations, thermal loading effects, or the effects of building energy management systems.

The monthly-based calculation methodology described in ISO 13790:2008 is a prime example of a quasi-static calculation methodology. This fully-prescribed calculation methodology has been adapted – in the context of activities for the implementation of the EPBD (Maldonado et al., 2011) – by many EU member states to form at a national level an accepted calculation methodology for computing energy performance. In certain conditions, the calculation methodology can be validated against reality and relatively small deviations can be observed for annual predictions, but on the monthly scale these deviations can be significant. The sensitivity to input data is also discussed: uncertainties in the estimation of thermal properties or other input parameters can contaminate the results, and the propagation of these errors can yield sizable deviations in the end results. For this reason, in many cases, the calculation methodology is used to establish an ordering relation, that allows for meaningful comparisons (and thus establishing the rating system used in many countries), but with lesser expectations with regards to prognostication of real performance.

In the case where dynamic effects are important, like in the Control Design process defined in our methodology, the temporal resolution of a month is not sufficient to capture all relevant dynamics. In this case, smaller time steps are required and a different approach is essential. This has obvious benefits: certain physical effects like transfer of heat from building thermal masses or the dynamic effects of the operation of active climate control HVAC components happen on a time-scale which is comparable to the simulation time-step. It is then possible to use more detailed models that capture these dynamic interactions and there is no longer any need for averaging or using correlations and other correction factors. On the other hand the need for defining boundary conditions, at each time steps means that in many cases the problem definition has to be more detailed (at each time step) requiring, at this level of detail, information which may not be available.

An example of such model is the dynamic one described in (ISO, 2008). Here, as shown in Figure 1-12, a zone is represented as a thermal circuit with 5 thermal resistances and 1 thermal capacitance (5R1C). The thermal capacitance models thermal storage effects in the zone. The mathematical formulation of the problem in this case is an Ordinary Differential Equation to model the evolution of the temperature as a function of time. Upon discretization of the equation using a finite-difference scheme, e.g. an implicit scheme like the Crank-Nicolson method, one gets the equations for the evolution in time of the relevant temperature parameter. One obvious benefit in the model above is the ability to model the temperature in the walls and therefore it becomes possible to have estimates

of thermal comfort (as the radiant temperature is an important parameter for thermal comfort). In a multi-zone configuration one needs to set individually for each of these nodes the thermal system and combine it to form the overall thermal network. The number of capacitances in this case is proportional to the number of zones, and a system of Ordinary Differential Equations has to be integrated in time. In ISO 13790 such a methodology is described and the boundary conditions are selected to ensure compatibility between the monthly and dynamic models.

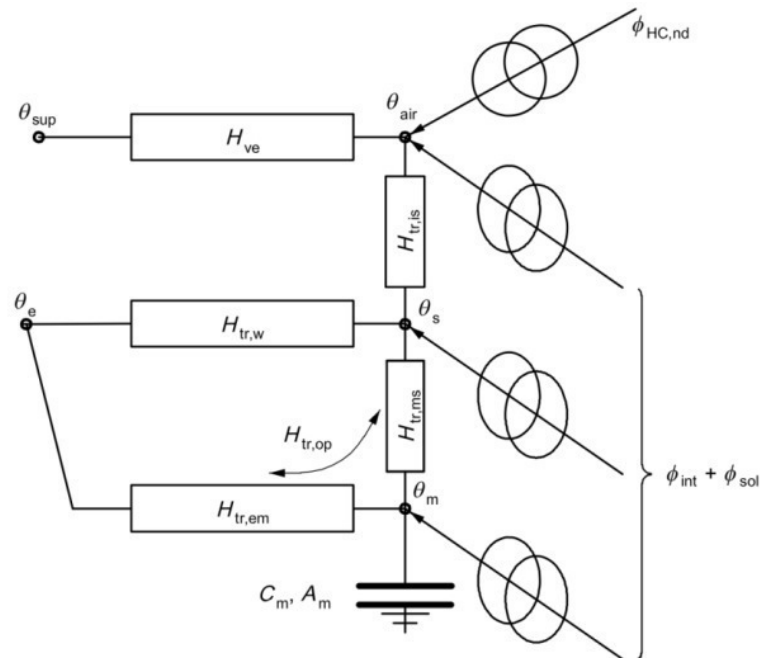


Figure 1-12: 5R1C Representation of a zone (ISO, 2008)

A similar approach is followed in TRNSYS 16: TRNSYS has a modular and extensible structure where different models for the building and its systems (called Types in TRNSYS lingo) are combined to form the problem description. Type 56, implements the multi-zone building model. There the geometrical and connectivity information for the zonal splitting is provided along with parameters for describing opaque and transparent building materials. The models used for the multi-zone building are more detailed than the simple RC above, including a star-shaped topology for approximating radiant exchange between zone surfaces along with the transfer function method for modelling transient conductive exchanges through walls. The integration time step can vary from 1 min to 1 h. This higher level of simulation detail is especially useful when one considers the coupled interaction of the building and energy systems; for this reason it has been extensively used as a simulation-aid tool for energy systems development and testing.

On the other hand, when predilection for temperatures in the zones or other dynamic effects exists, accurate modeling of thermal gains is essential. This is particularly important in cases of buildings with high solar gains e.g. due to a high glazing-wall ratio or due to the presence of solar atriums. To compute correctly solar gains and the evolution of temperature variables, a detailed consideration of the three-dimensional building geometry is necessary. For such reasons, state-of-the-art building simulation software today, uses the 3-D information of the building elements, to define geometrically the building spaces and surfaces, and uses this information to compute in more detail radiative transfer, e.g. due to solar gains. Examples of tools which implement such calculation methodologies are TRNSYS 17 and EnergyPlus. Both of these tools use detailed three-dimensional representation of geometric objects-building elements, and use detailed methods to compute such exchanges. At this level of modeling detail, obvious advantages are the capability to capture correctly radiant heat gains and exchanges. It also becomes possible to include the shading effects of neighbouring build-

ings, represented as external shading surfaces. Thus, for the work presented here, these types of models are utilized.

Shown in Figure 1-13 are the calculation methodologies discussed, on a diagram with the spatial and temporal discretization on its two axes. The classification based on the spatial discretization is important as it determines the level of modelling detail and the amount of information that has to be prescribed as input, when defining the geometry and other related information. The temporal discretization dimension is also important as it determines the integration time step, and consequently the granularity in which dynamically changing data (occupancy, weather, etc.) should be defined.

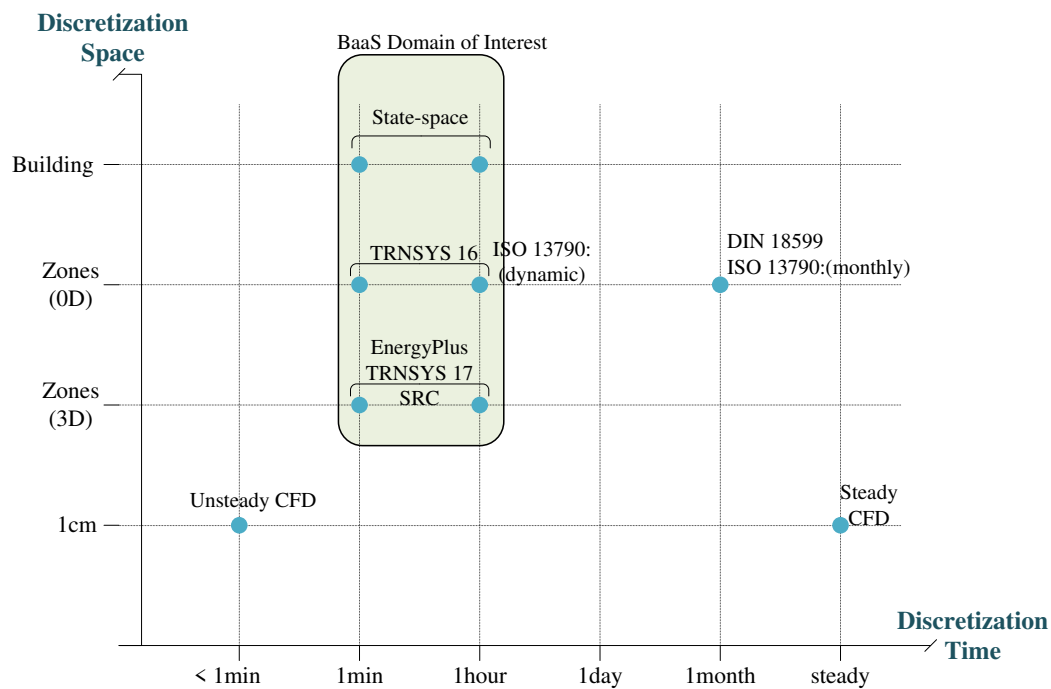


Figure 1-13: Comparison of different model types

1.2.3.2.1 Co-Simulation To facilitate the integration of different controllers within our Control Design approach, in each iteration of the algorithm (Figure 1-9) a different set of controllers has to be “injected” into the simulation model. This functionality is achieved using co-simulation and more specifically utilizing an actor-based library called Buildings Control Virtual Test Bed (BCVTB) (Wetter, 2011), which is based on Ptolemy II (Brooks et al., 2005) heterogeneous design and actor-oriented modeling open source environment. In Ptolemy, actors are hierarchical software entities (can include other actors) that execute concurrently and are able to communicate via messages through communicating ports. Here, the controllers are defined as actors in ptolemy (see for example an implementation of a simple heating curve in Figure 1-14) and they are evaluated at each simulation time-step to yield the new control action to be applied in the simulated building. These actions are sent through the co-simulation interface to the simulator and are included in the simulation of the building dynamics. This situation closely mimics what happens in the real building; the controller functions are evaluated at regular intervals at a supervisory level and the result is communicated to low-level control loops that implement this actuation command.

Next, the defined controllers need to be coupled with the simulation model in the BCVTB environment. The simulation models can be included as actors in BCVTB, thus we can define a composite actor containing the simulation model and the controllers, as shown in Figure 1-15. Note that the model calculates the cost function and the constraints and accepts control actions for each controllable element (e.g. valves, blinds, etc.) as inputs through an external interface.

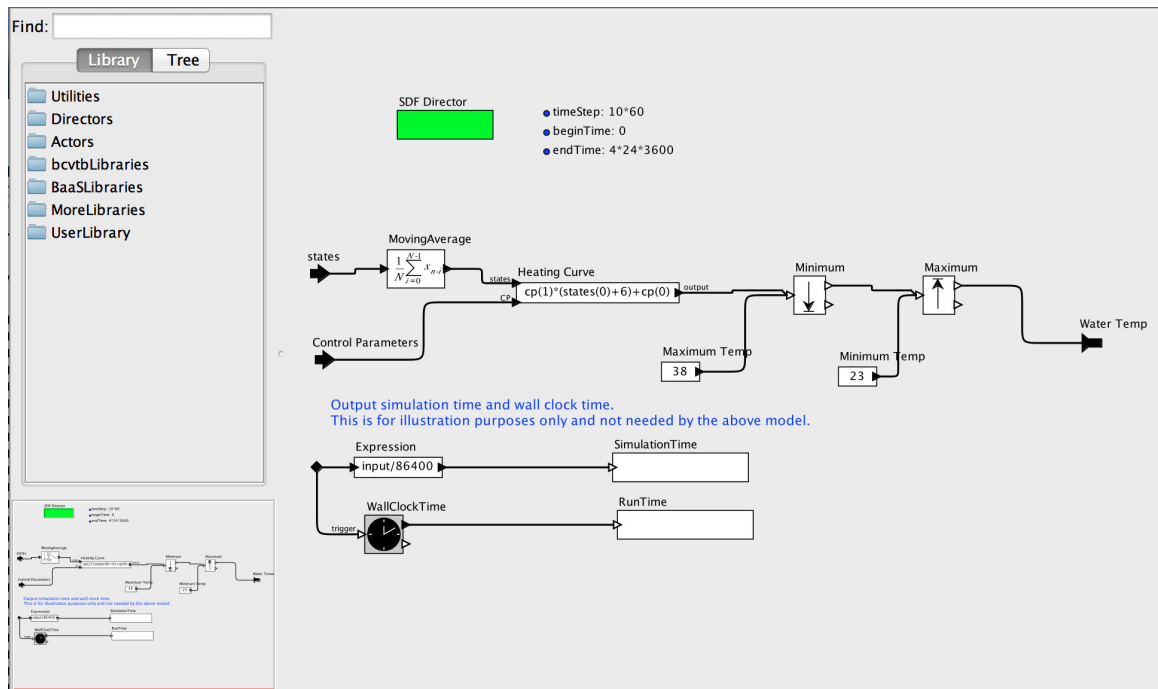


Figure 1-14: The Controller Actors in BCVTB

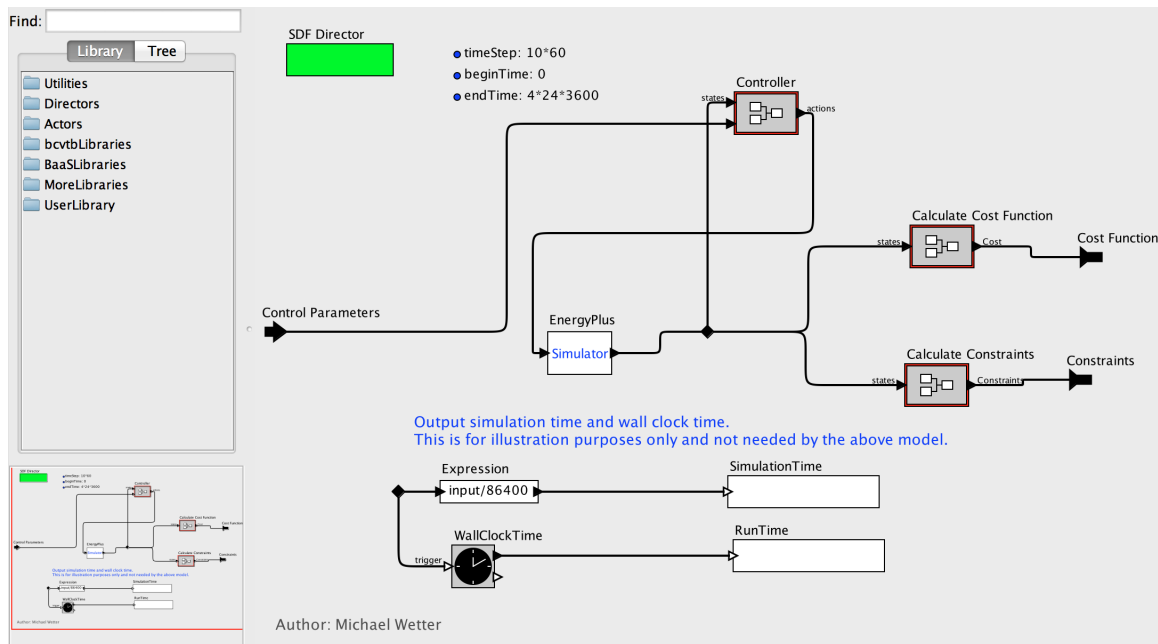


Figure 1-15: Coupling between the simulation model and the controller actors

In the final step, the Control Design process is setup as a BCVTB actor (e.g. implemented in Matlab). In this actor, the properties of the optimization algorithm are defined, such as the termination criterion and the bounds defining allowed values for the control parameters. The Control Design process is initiated either in scheduled intervals either as a response to an event and communicates the optimized controller parameters to the building.

1.2.3.2.2 The Warming-Up Process The iterative nature of the optimization algorithm (as shown in Figure 1-9), requires evaluating a number of candidate controllers in the simulator and generating

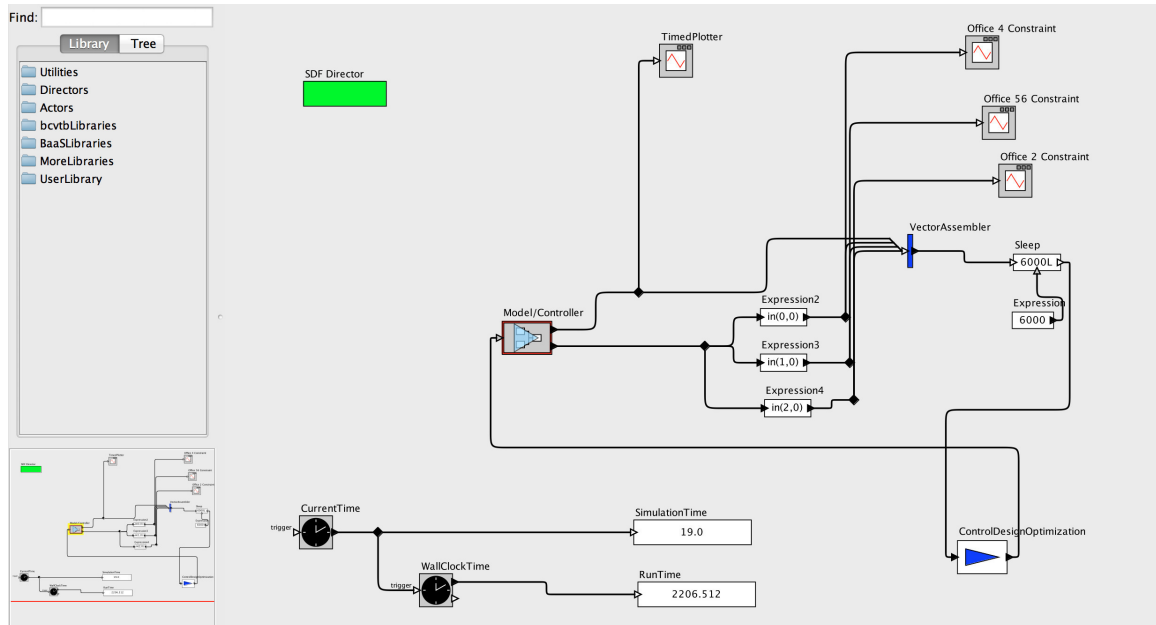


Figure 1-16: The Actors of the Model/Controllers and the Control Design in BCVTB

the meta-model in each iteration. Towards ensuring model accuracy, the initial thermal state of the building at the beginning of the Control Design process needs to be determined. Addressing this need is achieved again by the use of co-simulation, in which interfaces are introduced to allow data exchange between the simulation engine and external tools. The co-simulation is used to virtually “warm-up” the simulation model so that a correct estimate of the initial thermal condition of the building can be obtained.

In more detail, generally, the initial thermal state of the building can not be measured. While zone temperature and external condition information might be available from in-building sensors, the loading of the thermal masses and the wall temperatures are not known. To correctly estimate this state the actual simulation starts some days before the period of interest. So even though the period of interest is e.g. $I = [0, T]$, the simulation is performed for a larger interval $I_s = [-T_w, T]$; T_w is the warming up period and depends on the building time constant. For the period $[-T_w, 0]$ sensed data regarding zone temperature and weather conditions are passed through the co-simulation interface to the model. This allows for uncertainties related to the loading of the building thermal mass to disappear and a correct estimation of the initial thermal state of the building. Then, for the period from $[0, T]$ the building is simulated using the controller functions and available forecast data.

1.3 Novelty and Contributions of the Thesis

The contributions of the thesis, are inspired by the following fundamental questions:

1. Can existing thermostat-based controllers in buildings ensure comfortable interiors for the occupants (and save energy at the same time)?
2. Can we use detailed thermal simulation models in an on-line MPC setup?
3. Is continuous adaptation/re-design of the high-level supervisory control necessary (as in classical MPC) or for certain types of buildings and HVAC systems longer control design intervals (e.g. once per day) can be used?
4. Is MPC a viable technology option for any building?

In an effort to explore the above points, we have developed a model-based control design optimization methodology and framework, able to utilize detailed thermal simulation models of the building as surrogate models. In the heart of our framework lies a surrogate-based stochastic optimization scheme that is based on design-of-experiments principles, in order to facilitate a small number of calls to the simulation model.

We have applied our methodology to two office buildings with contrasting characteristics and different HVAC systems. Extensive experiments in both simulation and real world proved the efficiency of the proposed approach, while also led to significant insights regarding the posed research questions.

1.4 Publications

The work conducted for this thesis, has led in the following publications:

Journal publications

5. G.D. Kontes, G.I. Giannakis, P. Horn, S. Steiger and D.V. Rovas, “Using thermostats for indoor climate control in office buildings: the effect on thermal comfort”, Submitted to *Energies*, Under Review.
4. K.I. Katsigarakis, G.D. Kontes, G.I. Giannakis and D.V. Rovas, “Sense-Think-Act Framework for Intelligent Building Energy Management”, *Computer-Aided Civil and Infrastructure Engineering*, 31(6), 2016
3. G.D. Kontes, C. Valmaseda, G.I. Giannakis, K.I. Katsigarakis and D.V. Rovas, “Intelligent BEMS design using detailed thermal simulation models and surrogate-based stochastic optimization”, *Journal of Process Control*, 24(6), 2014
2. G.D. Kontes, G.I. Giannakis and D.V. Rovas, “Demand-Shifting using Model-Assisted Control”, *International Journal of Energy for a Clean Environment*, 14(1), 2013
1. K. Macek, J. Rojicek, G.D. Kontes and D.V. Rovas, “Black-Box Optimization for Buildings and its Enhancement by Advanced Communication Infrastructure”, *Advances in Distributed Computing And Artificial Intelligence Journal*, 2(2), 2013

Conference publications

20. G.I. Giannakis, G.D. Kontes, I. Korolija and D.V. Rovas, “Simulation-time Reduction Techniques for a Retrofit Planning Tool”, In 15th International Conference of IBPSA – Building Simulation 2017, August 07-09, 2017, San Francisco, California, USA.
19. G.F. Schneider, Y. Kalantari, G.D. Kontes, Gunnar Gruen and S. Steiger, “A Platform for Automated Technical Building Management Services Using Ontology”, In Lean & Computing in Construction Congress (LC3), July 04-07, 2017, Heraklion, Crete, Greece.
18. G.F. Schneider, Y. Kalantari, G.D. Kontes, S. Steiger and D.V. Rovas, “An ontology-based tool for automated configuration and deployment of technical building management services”, In Central European Symposium on Building Physics (CESBP) and BauSIM 2016, September 14-16, 2016, Dresden, Germany.

17. G.I. Giannakis, G.N. Lilis, M.A. Garcia, G.D. Kontes, C. Valmaseda and D.V. Rovas, "A methodology to automatically generate geometry inputs for energy performance simulation from IFC BIM models", In Building Simulation 2015, Hyderabad, India, December 7-9, 2015
16. K.I. Katsigarakis, G.D. Kontes, J. Rojicek, C. Valmaseda, J. Hernandez and D.V. Rovas, "An ICT platform for building analytics", In 10th European Conference on Product and Process Modelling (ECPPM), Vienna, Austria, September 17-19, 2014
15. G.N. Lilis, G.I. Giannakis, G.D. Kontes, and D.V. Rovas, "Semi-automatic thermal simulation model generation from IFC data", In 10th European Conference on Product and Process Modelling (ECPPM), Vienna, Austria, September 17-19, 2014
14. D.V. Rovas, K.I. Katsigarakis, G.D. Kontes, G.I. Giannakis and G.N. Lilis, "A Sense-Think-Act methodology for Intelligent Building Energy Management", In 30th International Conference on Applications of IT in AEC Industry (CIB W78 2013), Beijing, China, October 9-12, 2013
13. C. Valmaseda, M.A. Garcia Fuentes, J.L. Hernandez, K.I. Katsigarakis, G.D. Kontes and D.V. Rovas, "An Event-driven SOA-based Platform for Energy-efficiency Applications in Buildings", In 30th International Conference on Applications of IT in AEC Industry (CIB W78 2013), Beijing, China, October 9-12, 2013
12. G.I. Giannakis, M.F. Pichler, G.D. Kontes, H. Schranzhofer, and D.V. Rovas, "Simulation speedup techniques for computationally demanding tasks", In Building Simulation 2013, Chambéry, France, August 25-28, 2013
11. A. Constantin, J. Fütterer, R. Streblow, D. Müller, G.D. Kontes and D.V. Rovas, "Simulation assisted implementation of a model-based control parameter fine-tuning methodology for a nonresidential building with a complex energy system", In Building Simulation 2013, Chambéry, France, August 25-28, 2013
10. G.I. Giannakis, K.I. Katsigarakis, G.D. Kontes, and D.V. Rovas, "Co-simulation Setup for online Model-assisted Control Design", In CLIMA 2013, 11th REHVA World Congress, Prague, Czech Republic, June 16-19, 2013
9. E. Kontogianni, G.I. Giannakis, G.D. Kontes, and D.V. Rovas, "Comparing the impact of different thermal comfort constraints on a model-assisted control design process", In CLIMA 2013, 11th REHVA World Congress, Prague, Czech Republic, June 16-19, 2013
8. J. Rojicek, R. Fisera, G.D. Kontes, G.I. Giannakis, G.N. Lilis and D.V. Rovas, "Functional and technological definition of BIM-aware services to Assess, Predict and Optimize energy performance of buildings", In 2nd Central European Symposium on Building Physics, Vienna, Austria, September 9-11, 2013
7. G.I. Giannakis, K.I. Katsigarakis, G.D. Kontes and D.V. Rovas, "Model-assisted control through co-simulation for intelligent Building Energy Management Systems design", In 2nd Central European Symposium on Building Physics, Vienna, Austria, September 9-11, 2013
6. A. Constantin, J. Fütterer, R. Streblow, D. Müller, G.D. Kontes and D.V. Rovas, "Simulation-Assisted Adaption of a Model-Based Control Parameter Fine-Tuning Methodology For a Nonresidential Building with a Complex Energy System", Proceedings of International Symposium on Sustainable Energy in Buildings and Urban Areas (SEBUA), Kusadasi, Turkey, October 14-20, 2012
5. G.D. Kontes, G.I. Giannakis, E.B. Kosmatopoulos and D.V. Rovas, "Demand-Shifting Using Model-Assisted Control", Proceedings of International Symposium on Sustainable Energy in Buildings and Urban Areas (SEBUA), Kusadasi, Turkey, October 14-20, 2012

4. G.D. Kontes, G.I. Giannakis, E.B. Kosmatopoulos and D.V. Rovas, “Adaptive Fine-Tuning of Building Energy Management Systems Using Co-Simulation”, 2012 IEEE Multi-Conference on Systems and Control, Dubrovnik, Croatia, October 3-5, 2012
3. A. Constantin, J. Fütterer, D. Müller, D. Rovas, G.D. Kontes, “Implementierung einer modellbasierten prädiktiven Regelung für ein Nichtwohngebäude mit komplexem Energiekonzept – Simulationsergebnisse”, Proceedings of the 4th German-Austrian IBPSA Conference, Berlin, Germany, 2012
2. M. Pichler, A. Droescher, H. Schranzhofer, G.D. Kontes, G.I. Giannakis, E.B. Kosmatopoulos and D.V. Rovas, “Simulation-assisted building energy performance improvement using sensible control decisions”, 3rd ACM Workshop On Embedded Sensing Systems For Energy-Efficiency In Buildings (BuildSys11), Seattle, USA, November 2011
1. G.I. Giannakis, G.D. Kontes, E.B. Kosmatopoulos and D.V. Rovas, “A model-assisted adaptive controller fine-tuning methodology for efficient energy use in buildings”, Proceedings of the 19th IEEE Mediterranean Conference on Control and Automation, Corfu, Greece, June 2011

1.5 Funding

The research leading to these results has been partially funded by the European Commission FP7-ICT-2011-6, ICT Systems for Energy Efficiency under contract #288409 (BaaS) and by the European Commission FP7-ICT-2007-9.6.3, Energy Efficiency under the contract #248537 (PEBBLE).

In addition, I would like to gratefully acknowledge the use of the services and facilities of the Energie Campus Nürnberg and financial support through the “Aufbruch Bayern (Bavaria on the move)” initiative of the state of Bavaria and the MOEEBIUS project, a Horizon 2020 research and innovation program under grant agreement #680517.

THIS PAGE INTENTIONALLY LEFT BLANK

Chapter 2

Surrogate-based Stochastic Optimization

2.1 Formal Definition of the Optimization Problem

As described in the previous Section, the control design process utilizes an available model of the system, as well as forecasts for the weather conditions and occupancy patterns. This process is tasked to design energy-efficient controllers adapted to the thermal needs of the occupants of the building, by defining and solving a constrained optimization problem. To obtain the discretized equations we assume that the design process is to start at time t_0 and the prediction horizon is T . We select a set of $N - 1$ points $\{t_1, \dots, t_{N-1}\}$ with $t_i \in I \equiv (t_0, t_0 + T), i \in \{1, \dots, N - 1\}$ such that $t_0 < t_1 < t_2 < \dots < t_{N-1} < t_N \equiv t_0 + T$. Therefore a partition \mathcal{S} of I in N intervals $I_k = (t_{k-1}, t_k), k \in 1, 2, \dots, N$ is introduced. Then we can represent the simulation model as:

$$x_{k+1} = m(x_k, u_k, d_k), \quad (2.1)$$

where x_k is the vector of observable system states, u_k is the control vector, d_k are external to the system disturbances, like weather conditions and occupant actions, and k the discrete-time index. The goal is to discover series of control vectors that lead the system to optimized – with respect to a performance function J – behaviour.

Moreover, we assume a parametric smooth vector function π to represent the control law applied to the system at time k as follows:

$$u_k = \pi(\theta; x_k, d_k); \quad (2.2)$$

here $\theta \in \mathbb{R}^L$ is the vector of control parameters. A typical example of such parametric controller, is the heating curve adjusting the hot water temperature in buildings equipped with Thermally-Activated Building Systems (TABS) (Gwerder et al., 2008). Here, the sending water temperature u_k^{HW} at time k is obtained by the following equation:

$$u_k^{\text{HW}} = \theta_1 T_k^{\text{amb}} + \theta_2, \quad (2.3)$$

with T_k^{amb} the running average of the ambient temperature for the last 24 h. In this context, while the goal of the optimization process is to find a series of control vectors that lead the system to optimized – with respect to the cost function and the constraints – behaviour, this problem, under the effect of the control law (Eq. 2.2), is in turn transformed into the problem of discovering an optimal set of control parameters θ^* (e.g. parameters θ_1 and θ_2 of the heating curve defined above),

and leads directly to the definition of the following optimization problem:

$$\begin{aligned}
\theta^* &= \operatorname{argmin}_{\theta \in \mathbb{R}^L} \sum_{k=1}^N J(x_k, u_k), \\
&\text{subject to:} \\
u_k &= \pi(\theta; x_k, d_k), \\
x_{k+1} &= m(x_k, u_k, d_k), \\
u_k &\in \mathbb{U}, \\
x_k &\in \mathbb{X}, \\
C(x_k) &\leq 0,
\end{aligned} \tag{2.4}$$

where $\mathbb{X} \subseteq \mathbb{R}^m$, $\mathbb{U} \subseteq \mathbb{R}^n$ are constraint sets; and $C(x_k)$ a set of non-linear vector functions imposing the user comfort constraints.

Due to the utilization of detailed thermal simulation, solving this optimization problem can be a difficult task, since in many simulation engines interfaces for low-level access to simulation may not be available and optimization approaches exploiting low-level model information (Åkesson et al., 2010; Zavala, 2012) cannot apply. The system model is viewed as a black box function implementing a computationally expensive calculation procedure to compute state variables and evaluate the cost function and the constraints in the optimization process.

Due to the computational complexity of the high-fidelity models used (one simulation run can take up to 2 minutes) the use of global optimisation algorithms, like e.g. Genetic Algorithms (Arango et al., 2013), can be prohibitively expensive. To properly accommodate for the potentially high computational costs of evaluating the simulation models, we rely upon methods, such as trust-region (Wild and Shoemaker, 2013) and response-surface (Khuri and Mukhopadhyay, 2010) algorithms. In such methods, a less complex surrogate model (also referred to as response surface model or meta-model) of the (computationally expensive) simulation model is created, providing an approximation of the underlying function and assisting towards identifying optimized parameters to be evaluated on the expensive simulation model in the next iteration of the optimization algorithm. Utilizing the evaluation of these points, the region of the exploration and its “size” are constantly adapted, leading to a (local) optimum after a small number of simulation model calls (Regis and Shoemaker, 2005).

A high-level schematic of the optimization approach is shown in Figure 2-1. Here, an initial controller, as well as an initial size of the trust-region are provided and in each iteration of the algorithm: i) a set of control parameters is evaluated on the expensive simulation model with respect to the cost function and constraint values; ii) the meta-model(s) is(are) constructed using the available parameters-evaluation pairs; and iii) an optimization task is defined and solved on the meta-model(s), with the entire process being repeated until a termination condition is reached.

The definition of the algorithm does not pose any restrictions on the number of constraints. For example, we can define a complex building performance optimization task, requiring the minimization of the total energy consumption in the presence of thermal and visual comfort constraints. In such task, the controller would combine the control of the Heating, Ventilation and Air-Conditioning system of the building as well as daylight control, where separate models for the detailed thermal simulation and visual comfort (e.g. Radiance (Raphael, 2011)) could be utilized. Once the control design process is complete, the optimized control parameters θ^* are communicated to the building and the parameters of the controllers of the real building are updated with the new ones (e.g. the θ 's in Eq. 2.3).

It is conceivable that the selection of a proper approximator plays crucial role on the efficiency of the approach. The approximators need to be accurate, with low computational complexity for training

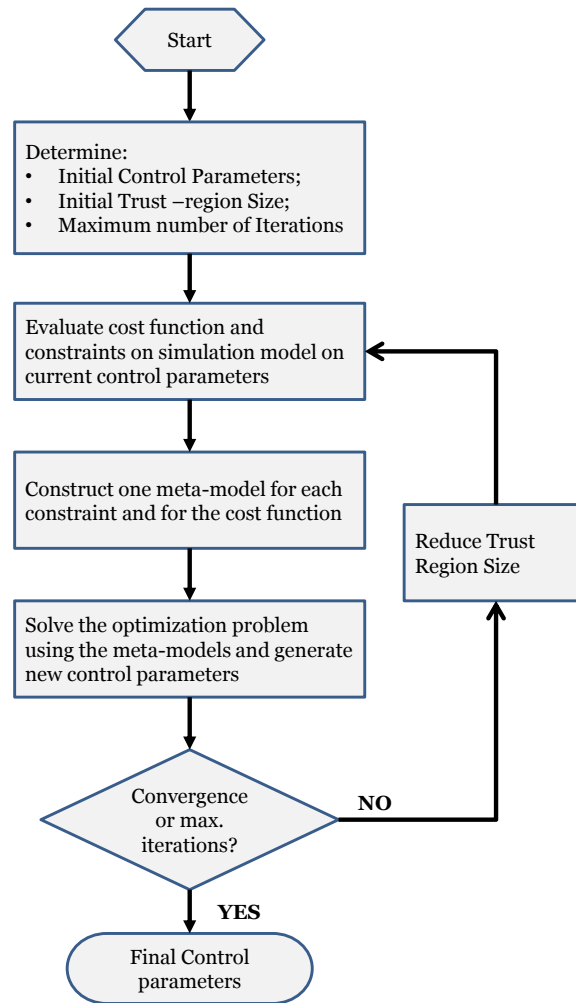


Figure 2-1: Flow-diagram of the Optimization Algorithm

and prediction, and should be “generic” enough to require minimum configuration when deployed in different buildings. For these reasons, we employ two non-parametric approximators: the Support Vector Machines (SVM) for regression, also known as Support Vector Regression (SVR) (Scholkopf and Smola, 2002; Vapnik, 2000; Vapnik et al., 1997), and the Gaussian process (GP) models (Rasmussen and Williams, 2006). Using these approximation approaches, the constrained optimization problem of Eq. 2.4 is solved using two methodologies that are tailored to each estimator type: the Cognitive Adaptive Optimization with Constraints (CAO-C) algorithm (Kontes et al., 2014) for the SVM and the Bayesian Optimization (BO) algorithm (Shahriari et al., 2016), adapted to the GPs.

We have selected to use non-parametric models for constructing the surrogates. Here, in contrast to parametric models that assume a fixed model structure and a finite set of parameters (like e.g. polynomial functions or neural networks), thus bounding the expressiveness of the model, non-parametric models assume an infinite-dimensional vector of parameters, where the amount of information that can be captured from the model grows as the amount of data grows. In addition, non-parametric models allow us to use the same models in all the experimental setups, regardless of the type of the building, the specifics of the HVAC system, the modeled quantity (e.g. energy consumption or Fanger values), etc., whereas in the case of parametric models, a laborious manual model selection process has to be performed.

2.2 Cognitive Adaptive Optimization with Constraints (CAO-C)

2.2.1 Support Vector Machines as Meta-Models

Let's assume that we have a sequence of l training samples $[(z_1, y_1), \dots, (z_l, y_l)]$, with $z \in \mathbb{R}^d$ and $y \in \mathbb{R}$. In general, we are required to design a regression function $\hat{y}(z)$ that predicts the targets y with at most ε deviation from the actual values, neglecting prediction errors smaller than ε , and at the same time assuring that the function is as smooth as possible. In the simple case of linear regression, the formulation of the regression function would be the following:

$$\hat{y}(z) = \langle w, z \rangle + b, \quad (2.5)$$

with $w \in \mathbb{R}^d$, $b \in \mathbb{R}$ and $\langle \cdot, \cdot \rangle$ denoting the inner-product operation defined in \mathbb{R}^d . The regularization requirement for this function corresponds to small w , thus, more formally, we can construct the following convex optimization problem:

$$\begin{aligned} & \text{minimize} && \frac{1}{2} \|w\|^2, \\ & \text{subject to} && \begin{cases} y_i - \hat{y}(z_i) \leq \varepsilon \\ \hat{y}(z_i) - y_i \leq \varepsilon, \end{cases} \end{aligned} \quad (2.6)$$

with $\hat{y}(z_i) = \langle w, z_i \rangle + b$ from (Eq. 2.5). Since this problem can be infeasible, we introduce slack variables $\xi + \hat{\xi}$ and penalize inaccurate target predictions using the ε -sensitive loss function:

$$|\xi|_\varepsilon = \begin{cases} 0, & \text{if } |\xi| < \varepsilon \\ |\xi| - \varepsilon, & \text{otherwise.} \end{cases} \quad (2.7)$$

This leads to the definition of an ε -sensitive loss tube (shown in Figure 2-2), while the introduction of the slack variables leads to the following formulation of the problem:

$$\begin{aligned} & \text{minimize} && \frac{1}{2} \|w\|^2 + C \sum_{i=1}^l (\xi_i + \hat{\xi}_i), \\ & \text{subject to} && \begin{cases} y_i - \hat{y}(z_i) \leq \varepsilon + \xi_i \\ \hat{y}(z_i) - y_i \leq \varepsilon + \hat{\xi}_i \\ \xi_i, \hat{\xi}_i \geq 0 \\ \varepsilon \geq 0. \end{cases} \end{aligned} \quad (2.8)$$

Here, $\hat{y}(z_i) = \langle w, z_i \rangle + b$ from (Eq. 2.5) as before, while $C > 0$ is a parameter regulating the trade-off between the flatness of the regression function and the ‘‘tolerance’’ to predictions with deviation larger than ε .

While this problem is well-posed, it is usually difficult in practice to determine a suitable loss function parameter ε , without knowledge on the desired accuracy of approximation a-priori. Due to this, in the present work we use the ν -SVR variation of the SVR process defined in (Scholkopf et al., 2000), where a new parameter $0 \leq \nu \leq 1$ is introduced to regulate the trade-off between the size of ε tube, the model complexity and the slack variables. In (Scholkopf et al., 2000) it is proven that ν is an upper bound on the fraction of errors and a lower bound of the fraction of Support Vectors (i.e. of samples that lie on or outside the ε -sensitive tube). This way, the following new optimization

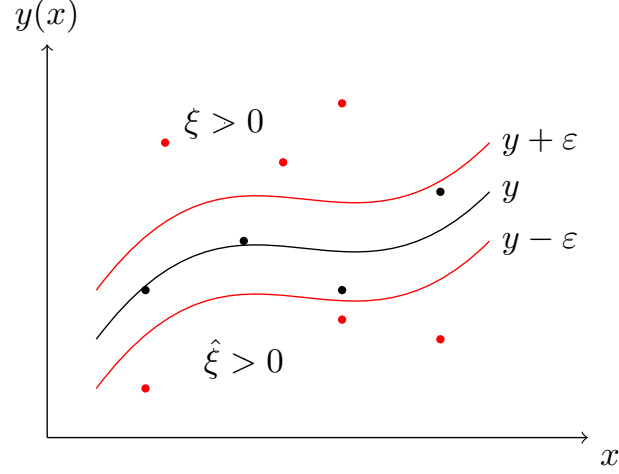


Figure 2-2: The ε -sensitive tube

problem is defined:

$$\begin{aligned}
 & \text{minimize} && \frac{1}{2} \|w\|^2 + C\nu\varepsilon + \frac{C}{l} \sum_{i=1}^l (\xi_i + \hat{\xi}_i), \\
 & \text{subject to} && \begin{cases} y_i - \hat{y}(z_i) \leq \varepsilon + \xi_i \\ \hat{y}(z_i) - y_i \leq \varepsilon + \hat{\xi}_i \\ \xi_i, \hat{\xi}_i \geq 0 \\ \varepsilon \geq 0. \end{cases} \quad (2.9)
 \end{aligned}$$

This problem can be solved in its dual form, introducing Lagrange multipliers $a_i, \hat{a}_i, \mu_i, \hat{\mu}_i, \beta \geq 0$ and defining the Lagrangian:

$$\begin{aligned}
 \mathcal{L} = & \frac{1}{2} \|w\|^2 + \frac{C}{l} \sum_{i=1}^l (\xi_i + \hat{\xi}_i) - \sum_{i=1}^l (\mu_i \xi_i + \hat{\mu}_i \hat{\xi}_i) \\
 & + C\nu\varepsilon - \beta\varepsilon - \sum_{i=1}^l a_i (\varepsilon + \xi_i + \hat{y}(z_i) - y_i) \\
 & - \sum_{i=1}^l \hat{a}_i (\varepsilon + \hat{\xi}_i - \hat{y}(z_i) + y_i). \quad (2.10)
 \end{aligned}$$

After calculating the saddle point of the Lagrangian (Bertsekas et al., 1999) and substituting to the dual problem, we get the ν -SVR Optimization Problem (Scholkopf and Smola, 2002), where, by applying the Karush-Kuhn-Tucker conditions (Bertsekas et al., 1999), the final estimator $\hat{y}(z)$ is given by the equation:

$$\hat{y}(z) = \sum_{i=1}^l (a_i - \hat{a}_i) \langle z_i, z \rangle + b. \quad (2.11)$$

The exact solution process of the Lagrangian is beyond the scope of this work, but we refer the interested reader to (Scholkopf and Smola, 2002) for a detailed description.

Moving one step forward, in order to provide non-linear properties to the regression function, a first approach would be to pre-process the training data z_i by a map $\Phi : \mathbb{R}^d \mapsto \mathcal{F}$ in some feature space, as in (Kosmatopoulos, 2009). Here, in contrast, noting that the algorithm depends only on the inner-products between the z_i 's (Scholkopf and Smola, 2002) implies that it suffices to know the kernel function $\mathcal{K}(z_i, z_j) : \langle \Phi(z_i), \Phi(z_j) \rangle$ rather than Φ explicitly. This allows to reformulate

the problem and acquire the kernelized version of (Eq. 2.11):

$$\hat{y}(x) = \sum_{i=1}^l (a_i - \hat{a}_i) \mathcal{K}(z_i, z) + b. \quad (2.12)$$

The most popular kernel functions are the linear, the polynomial, the sigmoid and the radial-basis functions (RBF), but for our approach we use the RBF kernel, defined as:

$$\mathcal{K}(z_i, z) = \exp(-\gamma \|z_i - z\|^2). \quad (2.13)$$

From the problem definition described above, it is obvious that the accuracy of the estimator depends on the selection of the parameters C , ν and γ . Calculating these parameters by hand can be rather difficult, since proper values might vary during each step of the algorithm, thus, in order to approximate appropriate values for the parameters, model selection is applied. As suggested in (Lin et al., 2001), a “grid” with exponentially growing parameters (e.g. $C = [2^{-15}, 2^{-14}, \dots, 2^{15}]$) is defined and each tuple of parameter values is tested using n -fold cross validation (Kohavi, 1995; Mosteller, 2006). In this setting, the dataset is divided into n subsets: $n - 1$ of them are used as a training set and the remaining one as a test set. The process is repeated n times and finally, the tuple with the best performance (e.g. with the lowest Mean Square Error) is used for the training of the estimator. The grid search method is preferred over other more sophisticated parameter search methods, since for small datasets is fairly fast, could be more accurate (due to thorough search over the parameter space) and is easily parallelizable (Lin et al., 2001).

The importance of the model selection process becomes clear in Figure 2-3. Here, the SVM regression functions for different values of the the hyper-parameters C , ν and γ are shown, indicating that proper selection of the parameters is crucial for the prediction quality of the regressor. Apart from that, Figure 2-3 also illustrates another appealing property of the SVM regression, since SVM regressors approximate the area far from the data samples with an unbiased flat line, thus preventing selection of parameters that can lead to poor performance.

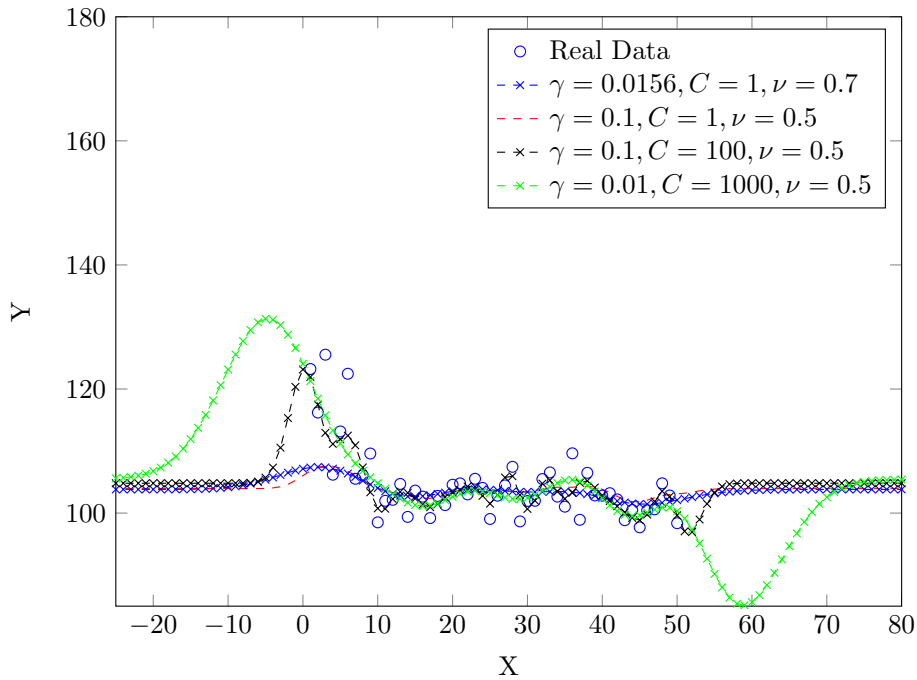


Figure 2-3: SVM regression with different values of the hyper-parameters C , ν and γ

2.2.2 Optimization over the Support Vector Machines Meta-Models

Since the proposed algorithm is iterative (as shown in Figure 2-1), we define $n \in \{0, 1, \dots, N_a\}$ as an index over the iterations and construct the meta-model of the cost function, as follows:

$$\hat{J}_n(\theta_n) = \vartheta_{n,J}^T \phi(\theta_n), \quad (2.14)$$

where \hat{J}_n denotes the approximation/estimation of J_n generated at the n -th iteration, ϕ denotes the RBF kernel functions and $\vartheta_{n,J}$ denotes the vector of *model parameter estimates* calculated at the n -th iteration. In the same way, we can define one surrogate model for each (comfort) constraint posed to the system, as follows:

$$\hat{C}_n(\theta_n) = \sum_{i=1}^{N_c} w_i \vartheta_{n,i,C}^T \phi(\theta_n); \quad (2.15)$$

\hat{C}_n denotes the approximation/estimation of C_n generated at the n -th iteration; i is an index over all different N_c constraints; ϕ denotes the RBF kernel functions as before; $\vartheta_{n,i,C}$ denotes the vector of *model parameter estimates* calculated at the n -th iteration for each constraint; and w_i is a normalization factor, indicating the relative importance of each constraint.

From here, we can optimize over the SVM meta-models using either local search or utilizing gradient information for efficiency.

2.2.2.1 Local Search Algorithm

Once the estimators are constructed, a local optimization task over the meta-models is defined, in which the best parameter vector (as predicted by the surrogate models) needs to be discovered and subsequently evaluated on the expensive simulation model. This optimization task is defined in an area with radius ρ_n around the current parameter set – following the trust-region methodology paradigm – with the radius decreasing in each iteration. In order to solve this optimization problem, traditional stochastic approximation techniques can be used. The low computational complexity of meta-model evaluation allows performing an exhaustive search over the trust region, by selecting M (a large number) candidate parameter sets, normally distributed around the current parameter set and within the current trust region:

$$\Theta_c = \{\theta^{(j)} | \theta_n + \alpha \zeta_n^{(j)}, j \in \{1, \dots, M\}, \zeta_n^{(j)} \sim \mathcal{N}(0, 1), \|\theta^{(j)} - \theta_n\| \leq \rho_n\}. \quad (2.16)$$

All candidate solutions in Θ_c are evaluated on the surrogate models of the cost function and the constraints and the best parameter vector are evaluated in the next iteration over the simulation model. The process repeats until convergence or a maximum number of iterations has been reached.

A detailed sketch of the process is shown in Algorithm 2.2.1. Here, the initial parameters set (θ_0), the maximum number of iterations (N_a) and the initial size of the trust region ($\rho_0 > 0$) are provided (line 1). Subsequently, for each iteration of the algorithm, the current set of parameters is evaluated on the simulation model, thus acquiring the cost function and constraints values for the current iteration (lines 3–4). Then, the SVM meta-models for the cost function and the constraints are constructed, using all previous evaluations on the simulation model (lines 5–6), while the size of the trust region is reduced appropriately (line 7). Inside this region, a set including a large number of candidate solutions is generated randomly (lines 8-9) and the best parameters of this set (as evaluated on the meta-models) is selected (line 10) to be evaluated on the simulation model during the next iteration of the algorithm. The best parameter set is determined using the process shown in lines 14–27. Initially, the parameters that perform best on the cost function meta-model are selected

(line 17). If these parameters do not violate the constraints (as predicted by the constraints meta-model) the process terminates, while if a constraint is violated, the parameter set is removed from the set and the process repeats (lines 18–22). If all candidate parameter sets violate the constraints, the parameters that give the fewest violations are selected (lines 24–26). Note here that in line 17 we do not solve a new optimization problem in each iteration of the inner loop. The list of control parameters is pre-sorted based on their performance on the cost function and in each iteration the parameter set with the lowest value is selected.

Algorithm 2.2.1 Random-search-based Cognitive Adaptive Optimization with Constraints Algorithm

```

1: Input:  $\theta_0, N_a, \rho_0 > 0, \alpha$  ▷ Initial parameters
2: for  $n = 0 : N_a$  do
3:    $J_n = J(\theta_n)$  ▷ Evaluate cost on the simulator
4:    $C_n = C(\theta_n)$  ▷ Evaluate constraints on the simulator
5:    $\hat{J}_n(\theta_n) = \vartheta_{n,J}^T \phi(\theta_n)$  ▷ SVM meta-model of the cost function
6:    $\hat{C}_n(\theta_n) = \sum_{i=1}^{N_c} w_i \vartheta_{n,i,C}^T \phi(\theta_n)$  ▷ SVM meta-model of the constraints
7:    $\rho_n = \frac{1}{(n+1)} \rho_0$  ▷ Trust region size update
8:    $\Theta_c = \{\theta^{(j)} | \theta_n + \alpha \zeta_n^{(j)}, j \in \{1, \dots, M\}, \dots$  ▷ Generate candidate parameter sets
9:    $\dots \zeta_n^{(j)} \sim \mathcal{N}(0, 1), \|\theta^{(j)} - \theta_n\| \leq \rho_n\}$ 
10:   $\theta_{n+1} = \text{BESTCONTROLLER}(\Theta_c, \hat{J}_n, \hat{C}_n, M)$  ▷ New controller
11: end for
12: Output:  $\theta_{N_a}$  ▷ The final controller
13:
14: function BESTCONTROLLER( $\Theta_c, \hat{J}_n, \hat{C}_n, M$ )
15:    $\Theta'_c = \Theta_c$ 
16:   for  $j = 1 : M$  do
17:      $\bar{\theta} = \underset{\theta_c \in \Theta_c}{\text{argmin}} \hat{J}_n(\theta_c)$  ▷ The parameter set with the minimum value for  $\hat{J}_n$ 
18:     if  $\hat{C}_n(\bar{\theta}) > 0$  then ▷ If a constraint is violated
19:        $\Theta_c = \Theta_c - \{\bar{\theta}\}$  ▷ Remove that element from the set
20:     else
21:       break;
22:     end if
23:   end for
24:   if  $\Theta = \emptyset$  then ▷ If all  $\theta_c$  violate the constraints
25:      $\bar{\theta} = \underset{\theta'_c \in \Theta'_c}{\text{argmin}} \hat{C}_n(\theta'_c)$  ▷ Choose the one with the less violations
26:   end if
27:   Return:  $\bar{\theta}$ 
28: end function

```

Note here, that usually a set of initial parameter vectors is generated to assist to construct an accurate enough initial meta-model. These initial samples can be either randomly selected or generated in a more structured manner, (e.g. using Latin Hypercube Sampling (LHS) (Tang, 1993) in our case).

2.2.2.2 Gradient-based Algorithm

On the other hand, and since a local optimal solution is pursued, the Kiefer-Wolfowitz stochastic approximation or Finite-Difference Stochastic Approximation (FDSA) algorithm (Kiefer and Wolfowitz, 1952) can be applied. Here, in each iteration n of the algorithm, the gradient of the control

parameters towards the minimum is estimated using finite differences and a line-search on the direction of the gradient is performed.

A sketch of the process is shown in Algorithm 2.2.2. Again, as in Algorithm 2.2.1, the initial parameters set (θ_0), the maximum number of iterations (N_a) and the initial boundaries of the trust region ($\rho_0^{\min} > 0$ and $\rho_0^{\max} > 0$) are provided (line 1). Subsequently, for each iteration of the algorithm, the current set of parameters is evaluated on the simulation model, thus acquiring the cost function and constraints values for the current iteration (lines 3–4). Then, the SVM meta-models for the cost function and the constraints are constructed, using all previous evaluations on the simulation model (lines 5–6). In line 7 the finite difference widths are adapted, while in lines 8 and 9, a new objective function is defined, combining the cost function and the constraint, and its gradient is calculated. Using this gradient information, in line 11 a set of candidate controllers, residing along the line defined by the gradient of the objective function and inside the adapted trust-region limits (line 10) are generated. The best controller of the set (calculated as before in lines 17–30) is used for the next iteration of the algorithm (line 13) and the process repeats until the termination criterion applies. Again, we generate a set of initial samples using Latin Hypercube Sampling (LHS).

Algorithm 2.2.2 Gradient-based Cognitive Adaptive Optimization with Constraints Algorithm

```

1: Input:  $\theta_0, N_a, \rho_0^{\min} > 0, \rho_0^{\max} > 0, \alpha, \alpha_1, \alpha_2$  ▷ Initial parameters
2: for  $n = 0 : N_a$  do
3:    $J_n = J(\theta_n)$  ▷ Evaluate cost on the simulator
4:    $C_n = C(\theta_n)$  ▷ Evaluate constraints on the simulator
5:    $\hat{J}_n(\theta_n) = \vartheta_{n,J}^T \phi(\theta_n)$  ▷ SVM meta-model of the cost function
6:    $\hat{C}_n(\theta_n) = \sum_{i=1}^{N_c} w_i \vartheta_{n,i,C}^T \phi(\theta_n)$  ▷ SVM meta-model of the constraints
7:    $\Delta\theta_n = \frac{1}{n^{1/3}}$  ▷ Finite Difference widths
8:    $\hat{G}_n(\theta_n) = \alpha_1 \hat{J}_n(\theta_n) + \alpha_2 \hat{C}_n(\theta_n)$  ▷ Construct combined objective function
9:    $\hat{\nabla}_{\theta} \hat{G}_n(\theta_n) = \frac{\hat{G}(\theta_n + \Delta\theta_n) - \hat{G}(\theta_n - \Delta\theta_n)}{\Delta\theta_n}$  ▷ Gradient Estimation
10:   $\rho_n^{\min} = \frac{1}{(n+1)} \rho_0^{\min}, \rho_n^{\max} = \frac{1}{(n+1)} \rho_0^{\max}$  ▷ Trust region size update
11:   $\Theta_c = \{\theta^{(j)} | \theta_n + \alpha \hat{\nabla}_{\theta} \hat{G}_n(\theta_n)\}, j \in \{1, \dots, M\}, \dots$  ▷ Generate candidate parameter sets
12:   $\dots \rho_n^{\min} \leq \|\theta^{(j)} - \theta_n\| \leq \rho_n^{\max}$ 
13:   $\theta_{n+1} = \text{BESTCONTROLLER}(\Theta_c, \hat{J}_n, \hat{C}_n, M)$  ▷ New controller
14: end for
15: Output:  $\theta_{N_a}$  ▷ The final controller
16:
17: function BESTCONTROLLER( $\Theta_c, \hat{J}_n, \hat{C}_n, M$ )
18:    $\Theta'_c = \Theta_c$ 
19:   for  $j = 1 : M$  do
20:      $\bar{\theta} = \underset{\theta_c \in \Theta_c}{\text{argmin}} \hat{J}_n(\theta_c)$  ▷ The parameter set with the minimum value for  $\hat{J}_n$ 
21:     if  $\hat{C}_n(\bar{\theta}) > 0$  then ▷ If a constraint is violated
22:        $\Theta_c = \Theta_c - \{\bar{\theta}\}$  ▷ Remove that element from the set
23:     else
24:       break;
25:     end if
26:   end for
27:   if  $\Theta = \emptyset$  then ▷ If all  $\theta_c$  violate the constraints
28:      $\bar{\theta} = \underset{\theta'_c \in \Theta'_c}{\text{argmin}} \hat{C}_n(\theta'_c)$  ▷ Choose the one with the less violations
29:   end if
30:   Return:  $\bar{\theta}$ 
31: end function

```

2.2.3 Comparison to Previous CAO Versions

Previous versions of CAO algorithm¹ have been reported in the literature (Kosmatopoulos, 2009; Kouvelas et al., 2011). There, the meta-model is a manually-designed Polynomial-Like Universal Approximator (PLUA) (Kosmatopoulos et al., 1995) and the optimization over this model is performed using random sampling, as in Algorithm 2.2.1. In this version of the algorithm, there is no explicit handling of constraints, with the exception of application in multi-robot coordination (Renzaglia, 2012), where the random samples that fell on constrained regions of the sample space were either rejected or simply projected to the feasible region. The latter is not a viable option in our case, since a set of controller parameters that satisfy the constraints is not known a-priori or a set of such parameters may not even exist, i.e. the HVAC system is not able to satisfy all the (thermal, visual, etc.) comfort constraints.

In comparison to the original version of CAO, the utilization of SVM regression functions as the meta-model in our approach provides a more suitable estimator compared to the PLUA approximators. In fact, the semi-automatic construction of the ν -SVR allows defining the meta-models in a laborious-free manner, without necessitating a priori knowledge on the nature of the underlying function or manually tuning estimator parameters (e.g. the number of the coefficients in the PLUA approximator) beforehand. In addition, even though many approximators (e.g. the PLUA) tend to exhibit poor extrapolation properties outside the hypercube where samples are available, SVM regressors approximate the area far from the data samples with an unbiased flat line, thus preventing selection of parameters that can lead to poor performance. as shown in Figure 2-3.

To add to this, the random sampling for the local search algorithm in the original version of CAO can be less efficient when a large number of control parameters are to be optimized and/or the optimization task has many constraints. This is due to the random generation of the candidate controllers (lines 8–9 of Algorithm 2.2.1), which can lead to a rejection of a large number of candidates that violate the constraints. To address this issue, the gradient-based optimization approach provides a more robust alternative.

2.3 Bayesian Optimization

In Algorithms 2.2.1 and 2.2.2 (and in all trust-region approaches in general), the size of the trust region is used to balance the exploration/exploitation trade-off. The problem here is that the initial size of the trust region and the properties that regulate the adaptation of this size in each iteration are ad-hoc parameters that require fine-tuning. As pointed out in (Frean and Boyle, 2008): “a more sophisticated search method might attempt to capture regularities about the nature of the search space (rather than merely fitting the existing data), and then use that model more sensibly than simply suggesting the highest predicted point for the next sample. The tendency to explore uncharted territory and collect new information about the problem’s structure once local territory has been mapped should be an emergent property of a good search algorithm, not a heuristic to be wired in as a quick fix for premature convergence. This naturally leads us to consider statistical models, where we have a full predictive distribution rather than a single prediction at each search point.” GP models inherently support these properties (Frean and Boyle, 2008).

2.3.1 Gaussian Processes as Meta-Models

A Gaussian Process is a collection of random variables, any finite number of which have a joint Gaussian distribution and is completely specified by its mean function and covariance function.

¹Also called Adaptive Fine Tuning (AFT) in some publications

The mean and covariance functions of a process $f(z)$ are defined as (Rasmussen and Williams, 2006) :

$$\begin{aligned} m(z) &= \mathbb{E}[f(z)], \\ k(z, z') &= \mathbb{E}[(f(z) - m(z))(f(z') - m(z'))] \end{aligned} \quad (2.17)$$

and we write the Gaussian Process as (Rasmussen and Williams, 2006) :

$$f(z) \sim \mathcal{GP}(m(z), k(z, z')). \quad (2.18)$$

As stated in (Brochu et al., 2010), we can consider that GPs are analogous to functions, but instead of returning a scalar $f(z)$ for any z , a GP returns the mean and variance of a normal distribution (Figure 2-4) over the possible values of $f(\cdot)$ at z .

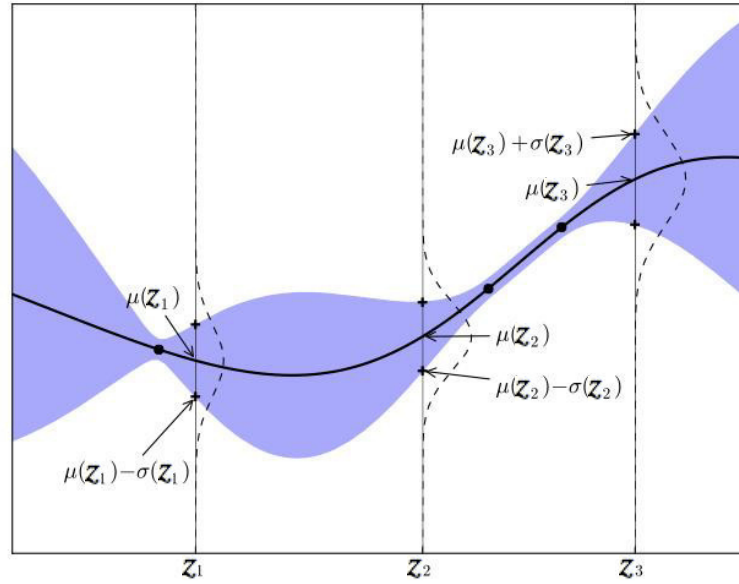


Figure 2-4: A simple GP with three observed points (Brochu et al., 2010).

Let's assume a dataset \mathcal{D} consisting of l pairs of $[(z_1, y_1), \dots, (z_l, y_l)]$, with $z \in \mathbb{R}^d$ and $y \in \mathbb{R}$. If we want to sample from the prior, we choose $z_{1:l}$ and sample the values of the function at these indices to produce the pairs $(z_{1:l}, \hat{y}(z_{1:l}))$, where $\hat{y}(z_{1:l}) = f(z_{1:l})$. The function values are drawn according to a multivariate normal distribution $\mathcal{N}(0, \mathbf{K})^2$, where the kernel matrix is given by:

$$\mathbf{K} = \begin{bmatrix} k(z_1, z_1) & \dots & k(z_1, z_l) \\ \vdots & \ddots & \vdots \\ k(z_l, z_1) & \dots & k(z_l, z_l) \end{bmatrix}. \quad (2.19)$$

Now, if we want to evaluate the value $\hat{y}(z_{l+1})$ of a new point z_{l+1} , then $f(z_{1:l})$ and $f(z_{l+1})$ are jointly gaussian:

$$\begin{bmatrix} f(z_{1:l}) \\ f(z_{l+1}) \end{bmatrix} = \begin{bmatrix} \mathbf{K} & \mathbf{k} \\ \mathbf{k}^T & k(z_{l+1}, z_{l+1}) \end{bmatrix}, \text{ with} \quad (2.20)$$

$$\mathbf{k} = [k(z_{l+1}, z_1), \dots, k(z_{l+1}, z_l)].$$

From here, we can arrive at an expression for the predictive distribution (Rasmussen and Williams,

²For simplicity we will assume a zero mean function in this Section.

2006):

$$\begin{aligned}
P(f(z_{1:l})|\mathcal{D}_{1:l}, z_{l+1}) &= \mathcal{N}(\boldsymbol{\mu}_l(z_{l+1}), \boldsymbol{\sigma}_l^2(z_{l+1})), \text{ with} \\
\boldsymbol{\mu}_l(z_{l+1}) &= \mathbf{k}^T \mathbf{K}^{-1} \mathbf{f}_{1:l} \text{ and} \\
\boldsymbol{\sigma}_l^2(z_{l+1}) &= k(z_{l+1}, z_{l+1}) - \mathbf{k}^T \mathbf{K}^{-1} \mathbf{k}.
\end{aligned} \tag{2.21}$$

The choice of the covariance function is crucial, as it determines the smoothness properties of the samples and encodes prior assumptions on the underlying function. Although the simplest and most commonly used is the Squared Exponential (SE) covariance function, defined as:

$$k_{\text{SE}} = \exp\left(-\frac{r^2}{2d^2}\right), \tag{2.22}$$

a plethora of covariance functions are available (Rasmussen and Williams, 2006), while it is also possible to design new covariance functions by combining existing ones (Duvenaud, 2014). This implies that the selection of a proper covariance function is a non-trivial task, even though some semi-automatic selection processes have been reported (Duvenaud et al., 2013).

In all the tests we have performed with synthetic benchmarks and building simulation models we have found that the rational quadratic covariance function was able to tackle efficiently any approximation task. The Rational Quadratic (RQ) covariance function is defined as:

$$k_{\text{RQ}}(r) = \left(1 + \frac{r^2}{2ad^2}\right)^{-a}, \tag{2.23}$$

with $d, a > 0$ being the hyperparameters. This covariance function is equivalent to an infinite sum of squared exponential covariance functions with different length-scales d .

2.3.2 Optimization over the GP Meta-Models

In the GP setup, the problem of balancing the exploration/exploitation trade-off is treated in a structured and semi-automatic manner through the use of acquisition functions. The role of an acquisition function is to guide the search for the optimum (Brochu et al., 2010). Typically, acquisition functions are defined such that high acquisition corresponds to *expected* high values of the objective function, either because the prediction is high, or because the uncertainty is high, or both. Maximizing the acquisition function is used to select the next point at which to evaluate the function. In our methodology, we use the Expected Improvement (EI) (Mockus et al., 1978) and the Upper Confidence Bound (UCB) (Srinivas et al., 2009) acquisition functions.

For the Expected Improvement (Frean and Boyle, 2008), we define the predicted improvement at a point z_i as $I(z_i) = f(z_i) - y_{\text{best}}$ for a maximization problem, with y_{best} being the sample with the best value (maximum) so far. The prediction at z_i is normally distributed ($f(z_i) \sim \mathcal{N}(m(z_i), \sigma^2(z_i))$) from Eq. 2.21), thus the improvement should follow the same distribution:

$$I(z_i) \sim \mathcal{N}(\boldsymbol{\mu}(z_i) - y_{\text{best}}, \boldsymbol{\sigma}^2(z_i)). \tag{2.24}$$

Now, the expected improvement at z_i can be computed analytically (Brochu et al., 2010; Frean and Boyle, 2008; Jones et al., 1998) as follows:

$$\begin{aligned}
EI_{\text{max}}(z_i) &= \sigma(z_i) [u\Phi(u) + \phi(u)], \text{ with} \\
u &= \frac{\boldsymbol{\mu}(z_i) - y_{\text{best}}}{\boldsymbol{\sigma}(z_i)}.
\end{aligned} \tag{2.25}$$

The functions $\Phi(\cdot)$ and $\phi(\cdot)$ are the normal cumulative distribution and the normal cumulative function respectively:

$$\Phi(u) = \frac{1}{2} \operatorname{erf}\left(\frac{u}{\sqrt{2}}\right) + \frac{1}{2}, \quad \phi(u) = \frac{1}{\sqrt{2\pi}} \exp\left(-\frac{u^2}{2}\right). \quad (2.26)$$

In case we are only allowed few iterations of the BO algorithm (as in our application in buildings due to the online nature of the Control Design process), we may need to favor exploitation over exploration after some iterations. To achieve this, and in contrast to the approach followed in (Jones, 2001; Lizotte, 2008), we define a convex combination of the *expected* function value at z_i and the mean of the GP prediction at z_i , as follows:

$$\hat{y}(z_i) = p(y_{\text{best}} + EI_{\max}(z_i)) + (1 - p)\mu(z_i). \quad (2.27)$$

Here, p is defined as:

$$p = \left(\frac{\gamma}{\delta} - \beta\right)^l, \quad (2.28)$$

with l the samples in the dataset. In all our experiments in buildings, we use $\delta = 0.99$, $\gamma \in [0.95, 0.98]$ and β depends on the size of the dataset. This treatment is an analogy to the classical trust-region approach.

In the Upper Confidence Bound (UCB), we can define our confidence on the *expected* function value on a point z_i as:

$$\hat{y}(z_i) = \mu(z_i) + \kappa\sigma(z_i). \quad (2.29)$$

Here, although a methodology for tuning κ based on multi-armed bandit setups has been reported (Srinivas et al., 2009), we have successfully used the same function for κ as with p in Eq. 2.28.

The intuition behind the semi-automatic exploration of the parameter space using the two acquisition functions can be summarized as follows:

- The value of the acquisition function is maximum when the GP model predicts a larger value compared to the best value in the dataset and the variance is high;
- The value of the acquisition function is high when the GP model predicts a high value compared to the best value in the dataset and the variance is high.
- The value of the acquisition function is low when the GP model predicts a low value compared to the best value in the dataset and the variance is low;

A detailed sketch of the BO process is shown in Algorithm 2.3.1. Since BO algorithm is also iterative, we define $n \in \{0, 1, \dots, N_a\}$ as an index over the iterations. Here, in line 1 the initial control parameters (θ_0) are provided. Subsequently, for each iteration of the algorithm, the current set of parameters is evaluated on the simulation model, thus acquiring the cost function and constraints values for the current iteration (lines 3–4). Following, one GP meta-model is constructed for the cost function and each of the constraints, using all previous evaluations on the simulation model (lines 5–6). Note that in contrast to the CAO setup (Algorithms 2.2.1 and 2.2.2) the constraints in this approach are not combined to form a single constraint function. In line 7, the best controller of the entire process (with the “best” controller evaluated as in the CAO setup), along with the acquisition functions of all GP meta-models are passed to a commercial constrained non-linear optimization solver in line 8.

For the last part, we use the Matlab function implementing the constrained Sequential Quadratic Programming algorithm defined in (Spellucci, 1998; Tone, 1983). Utilizing this commercial package allows for better constraint handling (no need to define proper weights over each constraint), while enables parallel execution, speeding-up the control design process.

Algorithm 2.3.1 Bayesian Optimization Algorithm

```
1: Input:  $\theta_0, N_a$  ▷ Initial parameters
2: for  $n = 0 : N_a$  do
3:    $J_n = J(\theta_n)$  ▷ Evaluate cost on the simulator
4:    $C_n = C(\theta_n)$  ▷ Evaluate constraints on the simulator
5:    $\hat{J}_n(\theta_n) = \mathcal{G}_{\mathcal{P}_{n,J}}(\theta_n)$  ▷ GP meta-model of the cost function
6:    $\hat{C}_n^{\{1,2,\dots,N_c\}}(\theta_n) = \mathcal{G}_{\mathcal{P}_{n,C}^{\{1,2,\dots,N_c\}}}(\theta_n)$  ▷ GP meta-model of the constraints
7:    $\theta_b = \text{BESTCONTROLLER}(\theta_n, J_n, C_n)$  ▷ Get best simulated controller so far
8:    $\theta_{n+1} = \text{SQP}(\theta_b, \text{Acq}(\hat{J}_n(\theta_n)), \text{Acq}(\hat{C}_n^{\{1,2,\dots,N_c\}}(\theta_n)))$  ▷ Use Sequential Quadratic Pro-
9:   ▷ -gramming to generate new
10:  ▷ controller.  $\text{Acq}(\cdot)$  is the Acquisition
11:  ▷ function defined in Eq. 2.27 or Eq. 2.29
12: end for
13: Output:  $\theta_{N_a}$  ▷ The final controller
14:
15: function BESTCONTROLLER( $\Theta_c, \hat{J}_n, \hat{C}_n$ )
16:    $\Theta'_c = \Theta_c$ 
17:   for  $j = 1 : n$  do
18:      $\bar{\theta} = \underset{\theta_c \in \Theta_c}{\text{argmin}} \hat{J}_n(\theta_c)$  ▷ The parameter set with the minimum value for  $\hat{J}_n$ 
19:     if  $\hat{C}_n(\bar{\theta}) > 0$  then ▷ If a constraint is violated
20:        $\Theta_c = \Theta_c - \{\bar{\theta}\}$  ▷ Remove that element from the set
21:     else
22:       break;
23:     end if
24:   end for
25:   if  $\Theta_c = \emptyset$  then ▷ If all  $\theta_c$  violate the constraints
26:      $\bar{\theta} = \underset{\theta'_c \in \Theta'_c}{\text{argmin}} \hat{C}_n(\theta'_c)$  ▷ Choose the one with the less violations
27:   end if
28:   Return:  $\bar{\theta}$ 
29: end function
```

Chapter 3

Experiments

In order to verify the efficiency of the proposed methodology, a hierarchy of experiments has been designed, facilitating simulation-based studies and real building experiments in two study buildings. The simulation-based studies are used to evaluate the potential of the proposed approach in a controlled and disturbance-free environment, while the goal of the real building experiments is to study the behaviour of the control design process under real-world conditions, influenced by user- and weather-induced stochasticity.

The two buildings used for the experiments has been chosen carefully, in order to cover as many different types of buildings and HVAC systems as possible. Thus, the first building is located in Crete, in a region characterized by long-hot summers and cool/cold-humid winters and long periods of sunlight for most of the year. It is a lightweight building, with high infiltration rates, and served by radiators for heating and AC units for heating and cooling. The second building is located in Kassel, Germany, and represents the archetype of a heavyweight building, with high thermal mass. It is equipped with TABS systems for heating. This diverse portfolio of buildings will help identify the performance of the algorithm under different building and HVAC system dynamics, varying microclimatic conditions, different user culture, etc.

3.1 Description of the Test Buildings

3.1.1 TUC Building

The Technical Services Building is located at the Campus of the Technical University of Crete in Chania, Greece. The region is characterized by long-hot summers and cool/cold-humid winters and long periods of sunlight for most of the year. The heating period starts in late November and ends in March, while the cooling period begins in May and ends in September.

The building has two floors and a basement with a total surface area of 450 m² and it hosts the offices of the Technical and Building Services Department of the University. As can be seen in the building plans (Figure 3-1), the building is divided in 10 offices and has an unusual triangular shape with a corridor running along its longer side, it has large openings and an atrium. The external walls are constructed by concrete, brick and stone wool as insulation material with the exception of some specific parts in the front and back of the building that are constructed by concrete only. Some of the internal partitions are brick, some concrete and others added later on to separate the space are constructed by gypsum plastering. The U-values of the external, internal walls and windows are relatively high which makes for a lightweight construction, easily affected by external weather variations.

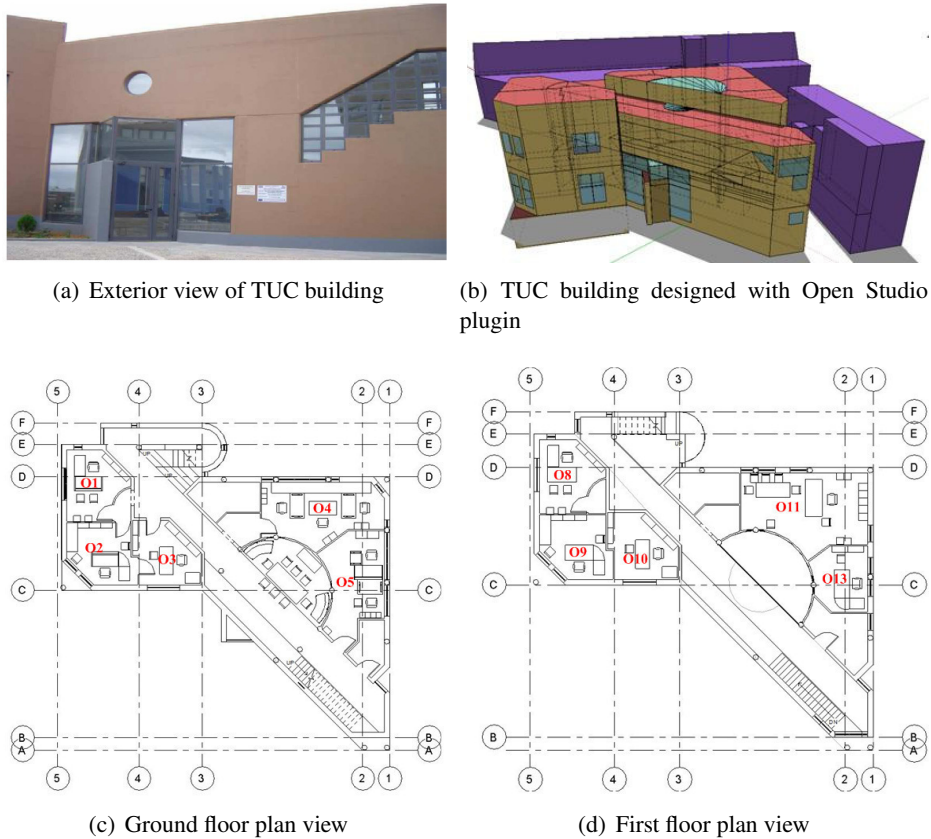


Figure 3-1: The TUC building

The ventilation and infiltration are based on window openings and cracks, expressing the air tightness of the building. A low air tightness is assumed for TUC building due to its construction and its exposure to high (mostly northerly) winds. The low insulation standards combined with a solar atrium contribute to overheating during the summer months and moderate (because of the mild climate) heating demands during the winter months. Concerning the efficiency of the building, in addition to thermal-comfort problems for the building users, the energy consumption is high, at $130 \text{ kWh/m}^2\text{a}$ based on energy audits and simulation results.

3.1.1.1 HVAC System and Available Sensing Infrastructure

A set of radiators is installed in each office for heating, with the heating demands being covered by a campus-wide district heating system. The connection between the campus-wide boiler and TUC building is achieved through underground pipes in two central points and then from these points hot water is distributed from the pipes to the radiators of each zone. To isolate the operation of each thermal radiator, a manually operated valve is located at the inlet node of each radiator. For the experiments conducted in this thesis, thermoelectric hot water valves installed on each of the water loops allow independent control of hot water flow, where each loop consists of thermal bodies (radiators) connected in series by pipes, as shown in Figure 3-2.

In normal operation mode there is no building-level control of the heating system, but heating depends upon hot water supply by the central campus boiler. In the particular building, two bypass three-way valves are installed (on each side), to isolate the building (when no heating demands are there) and in addition, thermoelectric valves installed on each of the water loops permit a more detailed control of heating supply to the associated radiator elements. Based on measurements and actual operation, the availability schedule of the central heating system is from (approx.) 5:30 in the

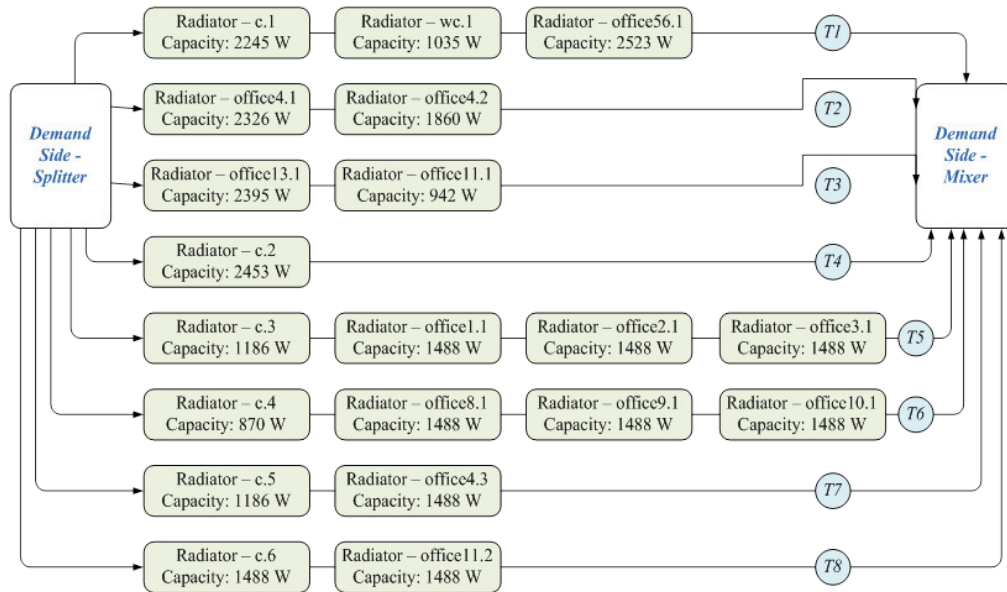


Figure 3-2: Central heating system branches and the corresponding flow valves (T1-T8)

morning to pre-heat the building and hot water supply is turned off at 11:30-12:00. This schedule is applied for “cold” days during the heating period. In heating mode, the AC units are activated only when the capacity of the radiators is not sufficient to reach the desired the thermal comfort level within a zone. That means that whenever the employees do not feel comfortable, they operate the split-type unit even if the radiators are heating the zone.

In summer, cooling is provided by Air Conditioning (AC) units. There is one available AC in each office and their operational schedule and the setpoint temperature are manually determined by the occupants. That means that whenever the users feel uncomfortable, they switch-on the AC unit and choose the desired setpoint temperature. For the experiments conducted in this thesis, the following operating parameters in each AC unit were controllable:

- On/Off;
- Set-point [18, 19, ..., 30] °C;
- Function mode (heating or cooling);
- Fan speed [0, ..., 100] %.

Finally, in each office room of the TUC building the following sensing elements were installed:

- Radiant and ambient temperature sensors;
- Relative Humidity sensor;
- Presence detection sensor;
- Contact sensors in all windows and doors;
- Single-phase energy meters for measuring the electrical power consumption of each AC unit.

3.1.1.2 Building Performance Optimization Potential

The availability schedule of the boiler is controlled by one person in charge who decides whether the heating should be on and for how long. This is far from optimal for a number of reasons: heating

might be supplied when it is relatively warm outside; due to differing thermal losses, demands on a per building or a per zone are not correctly accounted for; and unoccupied spaces or offices are heated according to the central schedule. This is the situation applicable to all buildings in the TUC campus. In addition, many winter days in Crete are characterized by relatively cold and humid mornings, where heating is required, followed by warmer and sunny afternoons, where no heating is necessary. In these cases, continued heating according to a fixed schedule leads systematically to overheating. In the absence of a forecast, it is hard to *a priori* determine when the heating system should be turned off.

Regarding the AC units operation, measurements have shown that in warm days of summer, the occupants set the temperature at low levels leading to overcooling of the building. The main reason for this behaviour is the fact that during peak hours, high solar gains greatly increase the radiant temperature in each office which correlates with the thermal comfort of the occupants. The reaction of the occupants is to reduce the setpoint to a low value in order to cool the space as fast as possible. Next, when the office gets too cool for their preferences, they increase the setpoint to a higher value. This manually-tuned bang-bang control is repeated throughout the day, leading to increased energy consumption and poor thermal comfort conditions.

The methodology presented in this thesis can assist towards alleviating the energy- and comfort-related problems of the building. The availability of a thermal simulation model, along with weather and occupancy forecasts and the automatic design of the control strategy can be utilized towards predicting and optimizing the operation of TUC building, by controlling the building in a proactive manner.

3.1.1.3 Available Thermal Simulation Model

The building is simulated using EnergyPlus simulation engine (Crawley et al., 2001). A detailed representation of its geometry was created according to the floor plans, presented in Figure 3-1, using OpenStudio plugin for SketchUp, a user interface of EnergyPlus thermal simulation engine, which allows for the automatic creation of the idf (EnergyPlus input) files. To account for shading from nearby buildings the shapes of nearby buildings were introduced. Furthermore, based on the building construction data, templates were created for each of the walls (internal partitions, external walls, roof etc.) detailing thermal characteristics.

Heat gains due to infiltration and ventilation can be significant and as such a detailed modeling of the infiltration/ventilation was performed using EnergyPlus Airflow Network (Walton, 1989). The Airflow Network model provides the ability to calculate multizone airflow driven by outdoor wind and forced air during HVAC system operation. To correctly account for internal gains due to occupant presence and their thermal sensation, activity data were collected for the building and imported. The types of data imported include occupant density (people/m²) on each zone, metabolic rates for office activities and occupants' clothing insulation. Computer and equipment gains were also introduced for each zone of the building while, lighting data were imported regarding the type of lights, energy requirement, visible and radiant fractions.

The indoor relative humidity is affected by five factors: internal moisture gains, ventilation, infiltration, removal with space - conditioning equipment, and moisture absorption into (or desorption out of) the materials; however, the last term is often neglected by building thermal simulation models (Woods et al., 2013). Towards a more accurate prediction of indoor relative humidity, the effective capacitance (EC) method is adopted in TUC buildings' thermal simulation model, estimating the moisture absorption into the materials; here, a moisture capacitance multiplier equal to 15 was used to combine this term with the zone air (Woods et al., 2013).

For providing a simplified simulation model for control design purposes, the building is divided into

three sub-buildings, as shown in Figure 3-3, each simulated separately in parallel, using as boundary condition for each sub-building contact surface the temperature of the corresponding surface, resulting from the adjacent sub-building's simulation. In other words, suppose that wall A is a common surface of sub-buildings 1 (A1) and 2 (A2). Then, at the end of sub-building:1 simulation, the temperature profile of surface A1 is applied as boundary condition to surface A2 so as to simulation of sub-building:2 run. More information regarding the simplified simulation model can be found in (Giannakis et al., 2013).

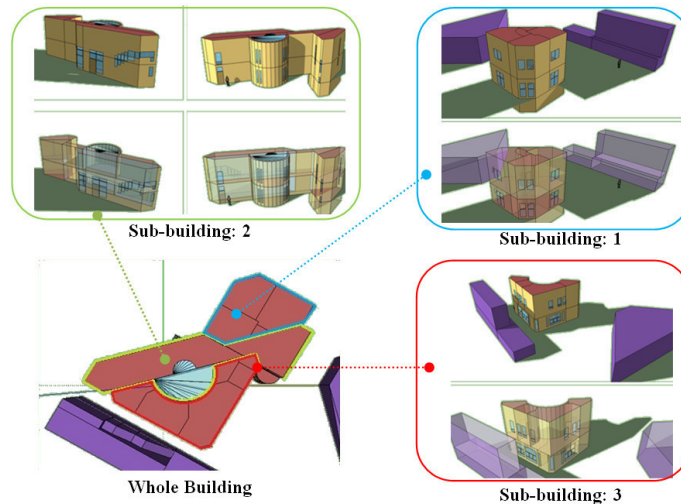


Figure 3-3: Simplified TUC simulation model for control

3.1.2 ZUB Building

The three-floor ZUB building located in Kassel (Germany), shown in Figure 3-4, has as main orientation a 20° SE. It is a low-energy office building, characterized by high thermal mass, sufficient air tightness and a south facing facade with a high glazing ratio (62 %). It is a well insulated building, since the U-value of the exterior walls is 0.11 W/m²K and the windows are triple glazed with a U-value of 0.6 W/m²K.

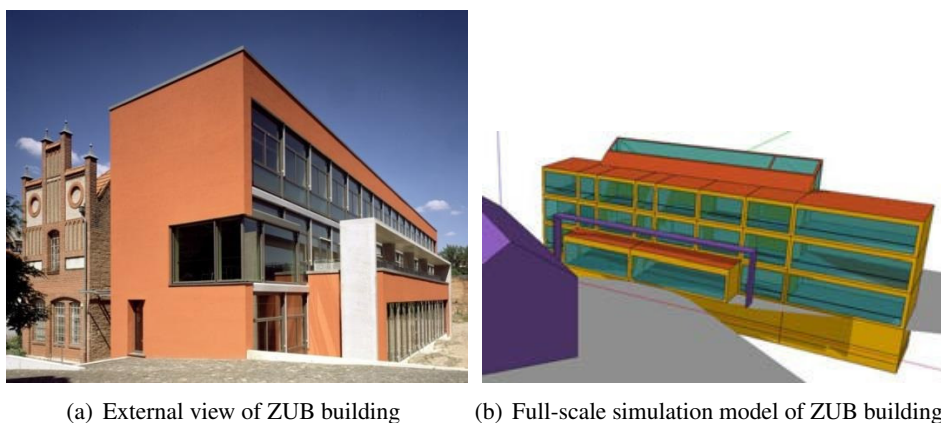


Figure 3-4: ZUB building and simplified Tower model views

3.1.2.1 HVAC System and Available Sensing Infrastructure

The ZUB building is equipped with radiant slabs situated in ceilings and floors of each room (Figure 3-5) with the two systems operated independently, and in combination with the Air Handling Unit that control the external air renovations.

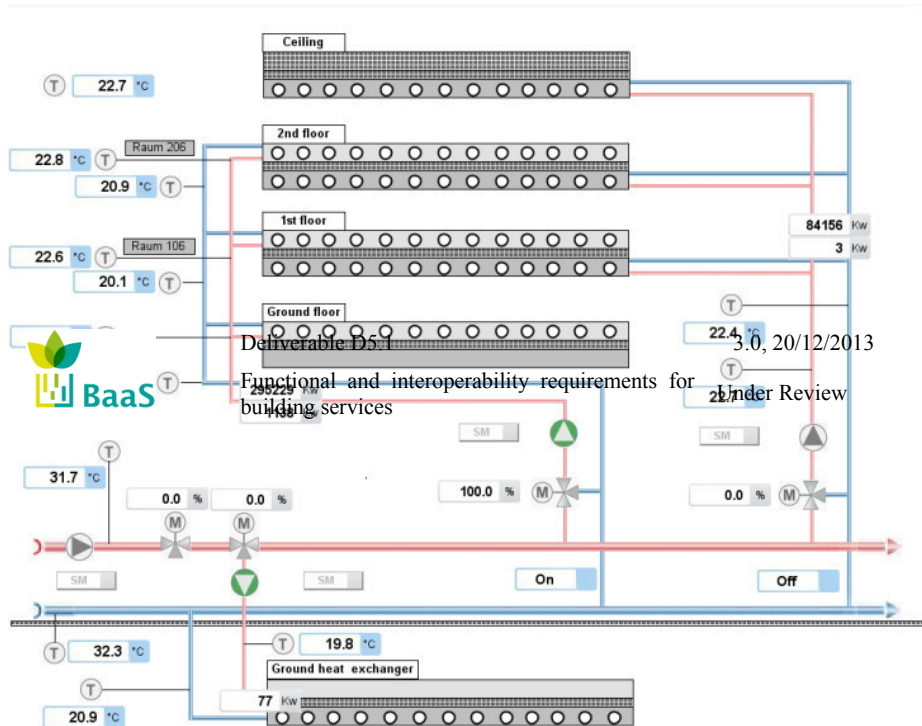


Figure 3-5: Schema of the radiant distribution in ZUB building

Both systems share a common distribution system that delivers cooling from an active ground exchanger during warm periods and heating provided by the Kassel's University district heating ring during the cold season.

The baseline TABS control strategy is generated by a simple set of rules. Here, the central building setpoint is set at 21°C constantly and only the inlet water temperature of the TABS varies and is calculated based on the 24 hours running average external temperature using a predefined curve, as seen in Figure 3-6.

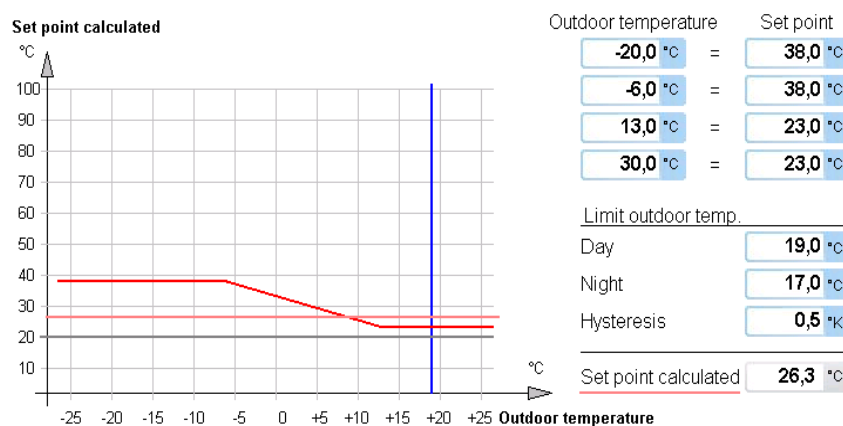


Figure 3-6: Supply water temperature curve for ZUB building

The underlying assumptions behind this control strategy are: i) that the 24-hour average of the outside temperature is indicative of the future external conditions, as days tend to have similar weather conditions – an assumption which is not always valid; and ii) that the average outside temperature can be an indicator of the building heating demand. The first assumption is invalidated on “turning days,” i.e. consecutive days with large variations of the average temperature. In these days the building can be under- or over-heated, as the sending temperature is higher or lower than the one required leading to an undersized or oversized system. The second assumption fails to include two critical factors affecting the heating demands of ZUB building: the solar radiation (which in the case of ZUB affects the thermal behaviour of the building more than the external temperature) and an estimation of the current thermal state (loading of the thermal mass) of the building. The latter is useful in cases the building is already heated (or even under-heated) in order to adjust the strategy accordingly.

The following controllable elements are available to the occupants:

- Setpoint offset ($\pm 2^\circ\text{C}$ in each office. This setpoint modifies the central setpoint of the building and regulates the operation of the radiant slab’s 2-way valves;
- blind angle and position;

Finally, two office rooms (106 and 206) have been equipped with additional sensors for research purposes. In these rooms, the following sensors have been installed:

- three temperature sensors at different heights inside the room to evaluate stratification;
- a relative humidity sensor;
- a radiant temperature sensor.

3.1.2.2 Building Performance Optimization Potential

The building is designed in a way that permits the effective utilization of solar radiation that passes through the glass façade in cold winter days; this energy is stored into the heavy masses that surround the occupied space. This design characteristic leads to low energy demands for space heating during the winter heating season which starts in November and continues to April. A downside is that in case there are many sunny days during the heating period, the building might overheat. This situation is particularly egregious on days with cold nights followed by sunny afternoon. In this case, heating is required during the night (even when the building is unoccupied) to ensure proper thermal loading of the thermal mass, so that when occupants enter the offices in the morning comfort requirements are met. Heating for longer period than required can easily lead to overheating problems during noon, forcing the users to open the windows, and leading to unnecessary energy use.

One of the control inefficiencies of the building is the manual operation of the blinds. In this case, when the offices are occupied, the users can either completely take down the blinds, effectively blocking solar radiation using the mechanical shading systems, or progressively adjust the angle of the shading and manually open the window in an effort to maintain indoor thermal comfort. During weekends there typically is no occupancy and therefore the blinds are not operated. In addition, the configuration of the BMS resets the blinds during the weekend according to a pre-defined seasonal rule. Without the user intervention over the weekend, the position of the blinds can lead to harvesting solar energy when it is not really required and may lead to overheating and discomfort on Mondays.

Apart from the manual operation of the blinds, another non-trivial task occurring during weekends is the proper operation of the central system. The system is active during unoccupied periods; this prevents the building from getting too hot or too cold during weekends. This way, large peaks on

Monday mornings for heating or cooling the building can be largely avoided. This strategy would make sense on certain very cold days as the capacity of the system would not be sufficient to cover the increased Monday-morning demands of all the buildings in the district heating loop. But, on the other hand, depending on the specific weekend weather conditions, the defined setpoint can increase energy losses, while for milder days a small peak on Monday morning may be preferred over operating the system over the entire weekend. The problem becomes more complex since the delivery of energy inside the building rooms is mostly realized through radiant systems, active floors and ceilings, which have a long time constant, thus the reaction time on operational control decisions is quite long, which makes difficult to maintain the internal comfort levels through a hand-tuned control strategy that ignores weather forecasts.

Again here, the availability of a thermal simulation model, along with the automatic design of the control strategies can assist towards operating the TABS system in an intelligent and proactive manner, thus saving energy and preventing comfort-related problems.

3.1.2.3 Available Thermal Simulation Model

As detailed simulation of indoor temperatures of the full-scale model increases computational complexity, a “tower” of three offices upon each other is cut-out, since the whole building can be viewed as a parallel expansion of the simple “tower” sub-model in one dimension. Here, the outer surfaces are actually adjoining rooms’ surfaces, which are defined as “boundary walls,” and the adjacent constructions that have a shading effect on the tower, but are not included in the thermal simulation, are modeled as shading groups. The tower is shown in Figure 3-7. It consists of 3 offices (25 m² each) and an adjacent Atrium. Here, the East and West walls of the building are modeled as heavy external walls with a total thickness of 0.5 m and U-value of 0.113 W/m²K, with the same construction also used for the side walls of the Atrium.

An identical occupancy schedule is assumed for all 3 offices of the Tower model from Monday to Friday. The offices are occupied with 2 persons each from 8:00 to 17:00, while the internal gains are set according to the VDI 2078 (class 1 at 23 °C) (Verein Deutscher Ingenieure, 1977). More information regarding the simplified simulation model can be found in (Giannakis et al., 2013).

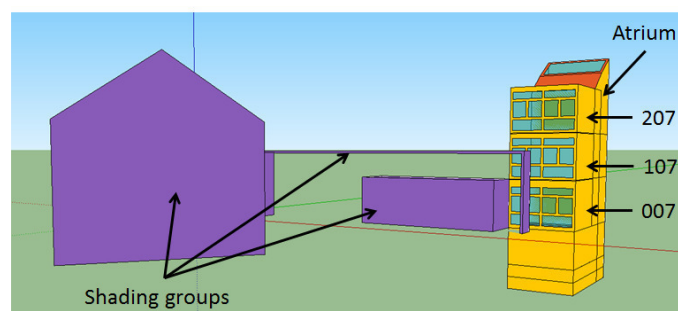


Figure 3-7: South-East view of the Tower model with external shading groups

3.2 Thermal Comfort Study

In current practice, the operative temperature values defined in ISO 7730 comfort limits (Table 1.1) are used as reference values for programming room thermostats, with the difference that the measured temperature is usually not the operative temperature but rather the dry-bulb air temperature. This practice is based on two assumptions: i) the values of air and operative temperatures in each

building space are (more or less) identical; and ii) maintaining the operative temperature within some predefined bounds throughout occupied periods suffices to ensure thermal comfort for the occupants, since usually still-air internal environments with moderate humidity levels are assumed.

Both of these assumptions are not without issues. First, the assumption that air temperature can be a proxy for operative temperature is true only if the radiant temperature which is linked to building surfaces temperatures is not too different. This is very frequently the case in buildings with TABS systems; in this case local discomfort can be minimized and an almost uniform vertical temperature distribution can be achieved that matches the ideal comfort temperature profile. Even in this case solar and internal gains can lead to discrepancies between radiant and air temperature. Second, the assumption that pre-defined and static bounds for the operative temperature alone suggests that this is the dominant factor, but neglecting other personal (clo value) and environmental (humidity) factors can be pernicious.

In order to investigate the ability of thermostats controlling the indoor air temperature to maintain comfortable interiors in our test buildings, an experimental protocol is designed in simulation level. Working in simulation will allow us to evaluate the results under the same boundary conditions and without having any deviations due to specific thermostat control settings. In addition, we have intentionally selected two buildings that represent the two “extrema” of the spectrum regarding their thermal characteristics. This will allow us to quantify the significance of thermal mass in the air/operative temperature mismatch (and in maintaining comfortable interiors in general). Our research findings could be generalized for all the building types in between.

3.2.1 The Experimental Setup

Summer and winter operation simulation experiments were performed for the TUC building. In each mode, two numerical experiments were performed: one assuming a thermostat which regulates heating or cooling based on dry-bulb air temperature measurements, representing current practices; and one, based on operative temperature control. In winter operation, heating is delivered to the spaces using radiators, whereas in summer operation, cooling is delivered by the AC units in each office. These experiments provide some insights to the first assumption in Section 3.2.1, namely quantify the impact on thermal comfort when air temperature is used as a proxy. Also the discussion contributes to development of some understanding on the effect different types of systems (radiant or air-based) have on thermal comfort.

In the case of the ZUB building only winter experiments were performed; in summer the building is naturally ventilated and set point control is not relevant. Heating is delivered using the TABS system that can be independently controlled in each office; a ventilation system is serving all offices, maintaining acceptable indoor air quality. This allows us to evaluate the effect of internal and solar gains on the comfort conditions in the offices.

For both buildings, the Fanger PPD index is utilized to evaluate the thermal comfort levels, with the values of the Fanger index at each time step of the simulation being a simulation output for both EnergyPlus and TRNSYS simulation engines. Even though according to ISO 7730 both buildings should belong to Class C (see Table 1.1), as they are existing buildings, the thermal properties of ZUB building allow to reach Class A comfort levels, at least in simulation where the internal gains and occupant behaviour are deterministic. This means that for the experiments below, we define a 15% Fanger PDD limit for TUC building and a 6% Fanger PPD limit for ZUB building.

For all the experiments both in TUC and ZUB building, we have selected to operate the heating system continuously during night and day. This is due to the simple structure of the controllers applied, which can lead to poor tracking of the temperatures when switching to different comfort bounds

during the transition between unoccupied to occupied periods, due to the inability to incorporate weather and occupancy predictions (Maasoumy and Vincentelli, 2014).

In the remainder of the Section, the results from all the experiments for TUC and ZUB building are illustrated.

3.2.1.1 TUC Building

For the summer experiments, the period between July 1st and July 16th was examined, using a meteorological weather file (Remund et al., 1999) for the simulation. This period is characterized by hot days, with the average temperature at 26.9 °C, the minimum temperature at 20.4 °C and maximum temperature at 35 °C. The blinds and the windows of the building are considered always closed and the operative/air thermostat temperature set point (controlling the AC units in each office) is set at 24.5 °C for the entire simulation period (day-night), following the mean operative temperature shown in Table 1.1 for summer.

For the winter experiments, the period between January 1st and January 16th was selected using the same weather file. Here, we have some sunny days, with the average temperature at 11.9 °C, the minimum temperature at 5.6 °C and the maximum temperature at 17 °C. The windows in all offices are considered closed, but the blinds are always open to exploit the solar gains for heating. The operative/air temperature set point (controlling the radiators in each office) is set at 22 °C for the entire simulation period (day-night), again according to the mean operative temperature provided in ISO 7730 (Table 1.1) for winter.

The results of offices 04 and 08 are presented in the ensuing discussion. The two offices selected are representative of the thermal behaviour of other offices in the building: office 04 is south-facing and receives high solar gains both during summer and winter, while office 08 is north-facing, is more exposed to wind and receives the least amount of solar gains of all offices.

Starting with the summer experiments, Figure 3-8 illustrates the results for office 08 using the air temperature thermostat control, where it is obvious that the selected control strategy manages to maintain comfort at acceptable limits, as indicated by the Fanger PPD values. Note that the operative temperature is higher compared to the air temperature, as expected, due to the lightweight construction of the building and the type of the HVAC system (air and not radiant system): here the air system cools the zone air but the radiant temperature remains higher, leading to higher operative temperatures.

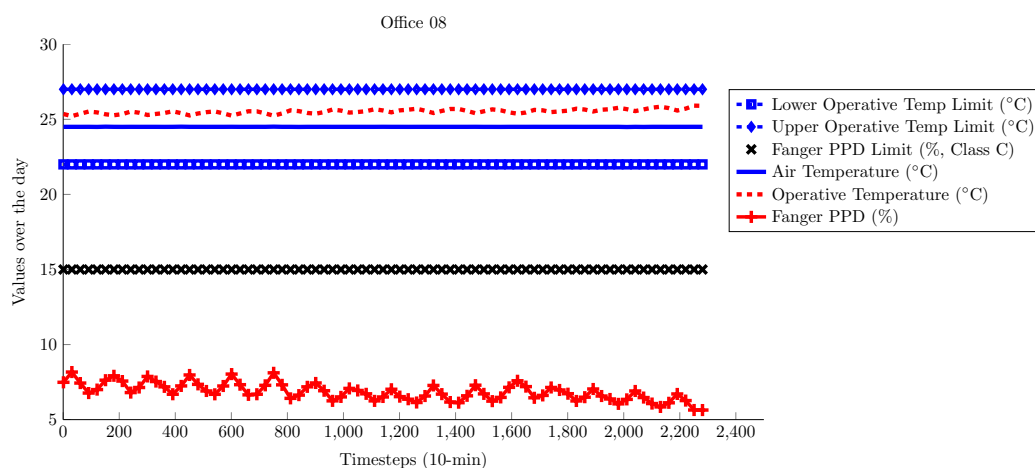


Figure 3-8: Summer results for office 08 using air temperature thermostat set at 24.5 °C

Figure 3-9 shows the results from the same experiment for office 04. Similar behaviour with respect to both comfort levels and the incompatibility of air and operative temperatures as with office 08 is observed, but in this case the operative temperature values exhibit higher variability, fluctuating between day and night, due to the significantly higher solar gains that office 04 receives compared to office 08.

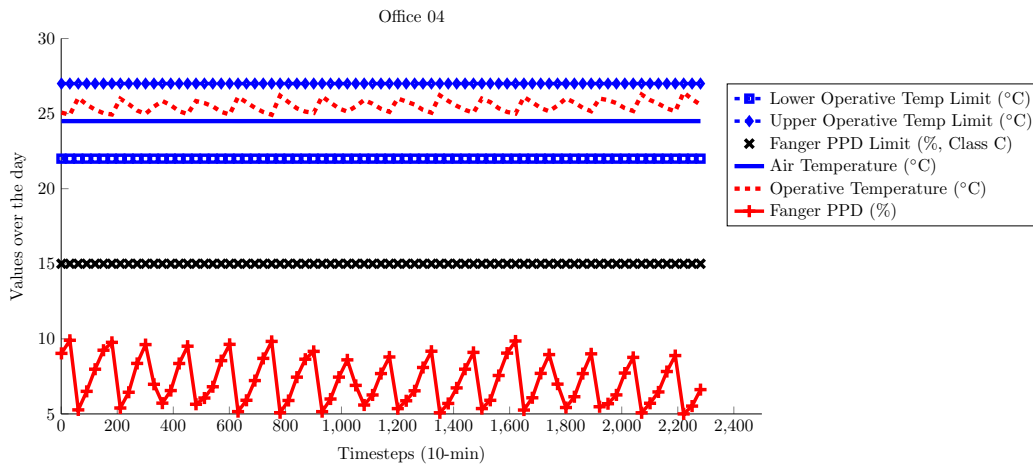


Figure 3-9: Summer results for office 04 using air temperature thermostat set at 24.5 °C

For operative temperature control in the summer experiments, where the thermostat control mode has been modified properly to enable operative, instead of air, temperature control (set point values refer to the desired operative temperatures), the results for Office 08 are shown in Figure 3-10. It is obvious that the operative temperature is still higher compared to the air temperature, but also attains lower values compared to the results of the air temperature control shown before (Figure 3-8). Here, the Fanger PPD values lay on the upper comfort bound due to over cooling.

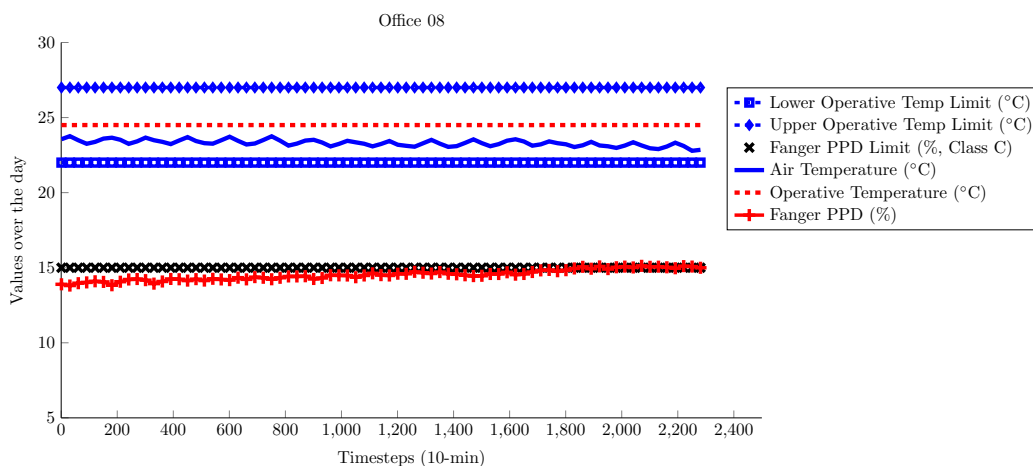


Figure 3-10: Summer results for office 08 using operative temperature thermostat set at 24.5 °C

Controlling the operative instead of air temperature leads to similar results for Office 04 as well (Figure 3-11), where the control strategy is characterized by higher discomfort than before (Figure 3-9), again due to overcooling.

The fact that even though the operative temperature in both offices is set equal to the design temperature suggested in the ISO 7730 (shown in Table 1.1) leads to overcooling should not come as a surprise. The acceptable temperature and comfort bands in the ISO example tables have been calculated under specific assumptions for all other influencing factors, namely clo value, metabolic

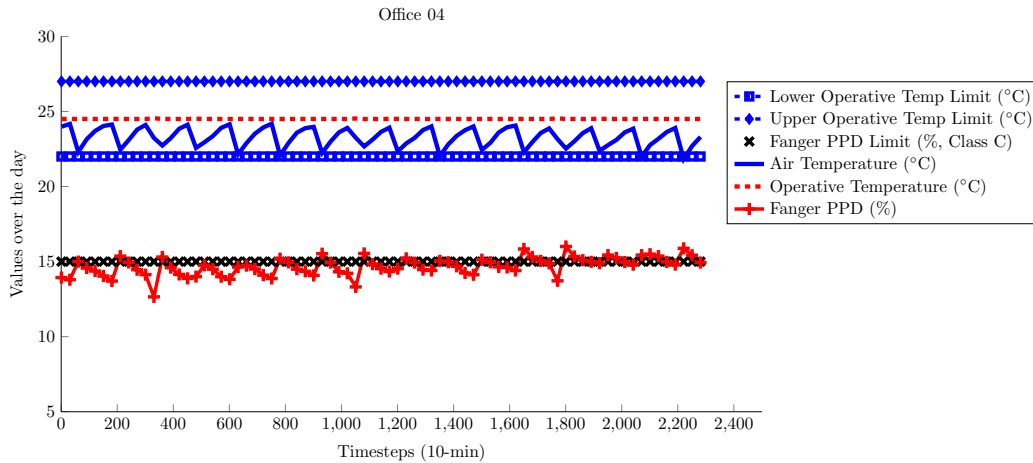


Figure 3-11: Summer results for office 04 using operative temperature thermostat set at 24.5 °C

rate and relative humidity levels (constant at 60%). For the experiments presented here, although personal factors are defined according to similar assumptions, the relative humidity levels are not constant, but dynamically calculated by the EnergyPlus simulation engine, resulting to relative humidity values between 40% and 48% approximately for the entire simulation period. These values are substantially lower compared to the relative humidity level assumed in Table 1.1. Here, higher values of the PPD index are due to the fact that Fanger comfort model takes into account the heat loss by evaporation of sweat from the human body skin; due to sweating effects, when the relative humidity gets higher, occupant thermal sensation is expected to be hotter than the actual temperature.

Towards further investigating the impact of relative humidity to the desired operative temperature for thermal comfort, we use the psychrometric chart of Figure 1-6 as a guideline. Here, taking into account the shaded polygon corresponding to the cooling season ($clo = 0.5$), we can see that for lower relative humidity values, operative temperature values higher than 24.5 °C are required in order to move closer to the center of the polygon. Thus, we perform another experiment using 25.5 °C as the setpoint to the operative temperature thermostat. Results shown in Figs 3-12 and 3-13 highlight the better comfort levels for both offices, a fact which indicates that taking into account the humidity levels in a building when designing the respective operative temperature comfort bounds is crucial for capturing the actual thermal comfort profile of the specific building.

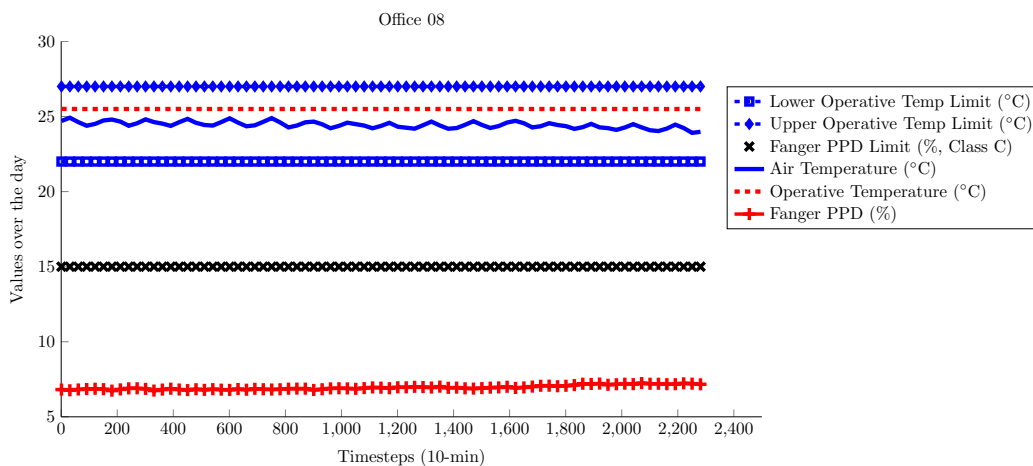


Figure 3-12: Summer results for office 08 using operative temperature thermostat set at 25.5 °C

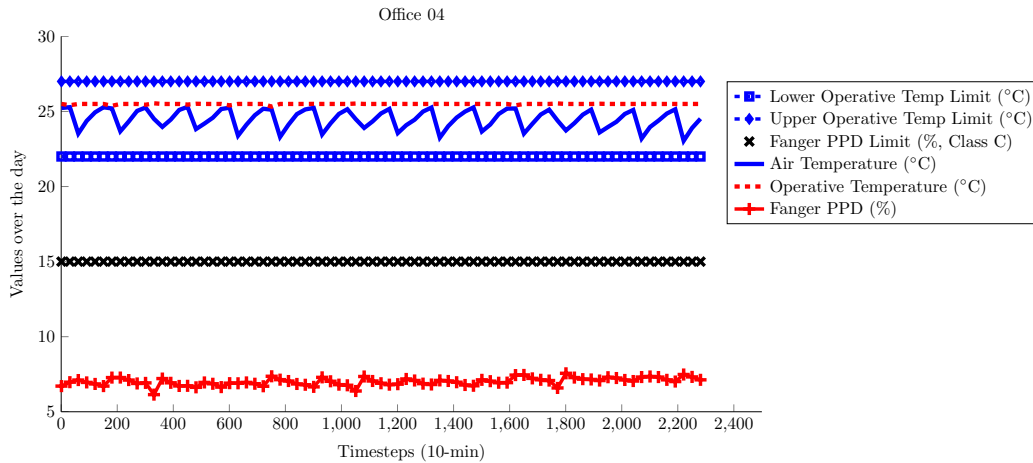


Figure 3-13: Summer results for office 04 using operative temperature thermostat set at 25.5 °C

For the winter experiments, Figure 3-14 illustrates the results obtained for Office 08, where Fanger PPD values are within the acceptable limit for this type of building most of the time. Note here that the operative temperature is lower compared to the air temperature throughout the simulation period. This is expected, since even though the HVAC system is based on radiant heating (radiators) and a part of the heating energy is absorbed by the walls, the lightweight construction and the poor insulation of the building lead to lower wall temperatures (thus lower radiant temperature) compared to the air temperature of the zone. The relative humidity in the office varies from 30% to 50% depending on the external conditions, thus affecting the comfort as with the summer experiments, with this effect being more obvious in the first two days of the experiment, where the relative humidity is around 30%.

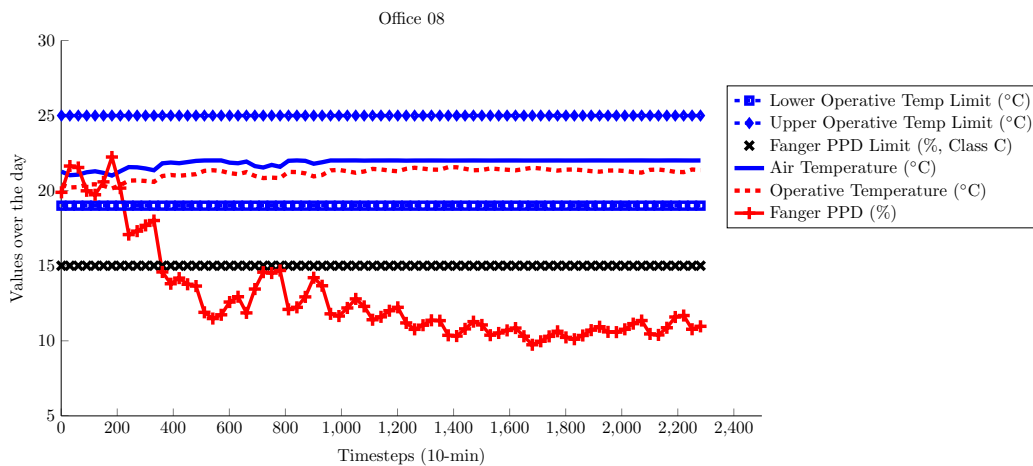


Figure 3-14: Winter results for office 08 using air temperature thermostat set at 22 °C

Office 04 results for the same experiment are shown in Figure 3-15, leading to the same conclusions: Fanger PPD values remain within acceptable limits for most of the time, while the air temperature is higher compared to the operative temperature. On the other hand, we can notice some spikes on both air and operative temperatures, which are due to the high solar gains office 04 is exposed to (unlike office 08) on days with clear sky. Note that for the first two days of the experiment, relative humidity is around 30%, thus leading to increased discomfort as in the case of office 08 above.

As with the summer set of evaluations, the same experiments are conducted controlling the operative temperature instead of the zone air temperature. Here, as illustrated in Figure 3-16 for Office 08,

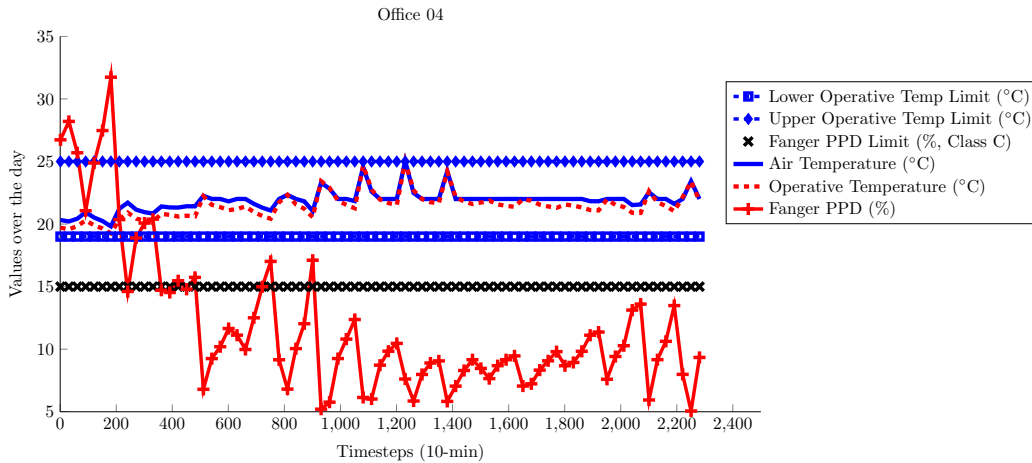


Figure 3-15: Winter results for office 04 using air temperature thermostat set at 22 °C

the air temperature is higher than the operative temperature as with the air temperature thermostat control, but both naturally acquire higher values compared to the previous experiment for the same office (Figure 3-14), which leads to more comfortable interior conditions as indicated by the Fanger PPD levels.

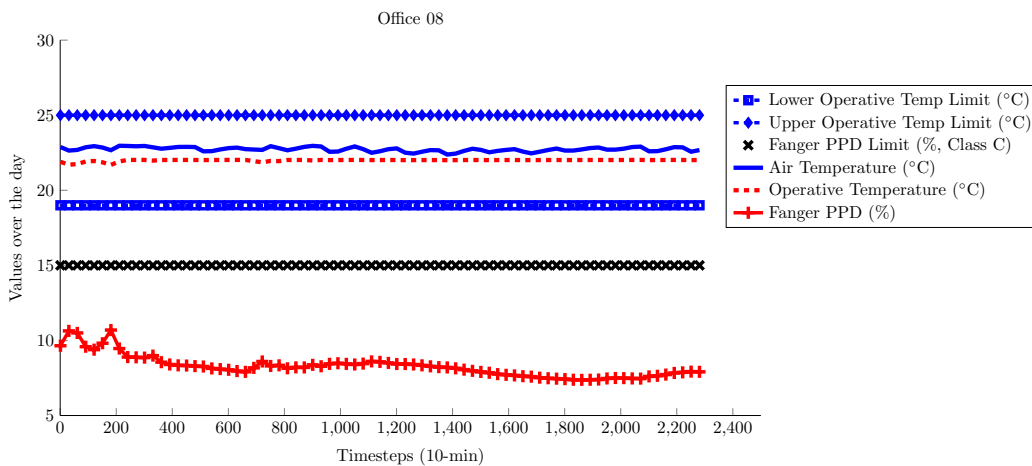


Figure 3-16: Winter results for office 08 using operative temperature thermostat set at 22 °C

The same comfort improvement due to the increased values of operative temperature, is also observed in Office 04 results (Figure 3-17). Of course, as with the previous winter experiment controlling the air temperature in the same office (Figure 3-15), both operative and air temperatures show periodic increments due to the high solar gains on less cloudy days.

The results from these experiments confirm our initial hypotheses: i) controlling the air temperature does not provide a structured method for controlling the operative temperature; and ii) the suggested operative temperature comfort band calculated in ISO 7730 for fixed clo value, metabolic rate and relative humidity levels needs to be adapted to the particularities of each target building.

In order to provide a clear illustration of the difference in the thermal comfort conditions between air and operative temperature control in TUC building, a parametric study for the same summer and winter days as before and with different air and operative temperature setpoints has been performed. The impact on comfort is evaluated using both the percentage of comfort violations and the average Fanger PPD values in the entire experimental period. For the latter, the standard deviation of the Fanger PPD values is also presented to provide an estimate on the variability of the comfort levels

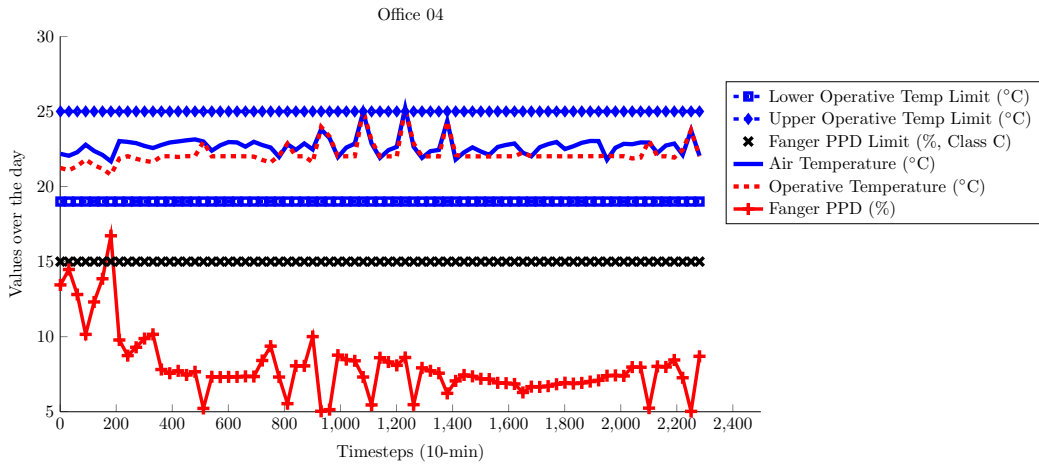
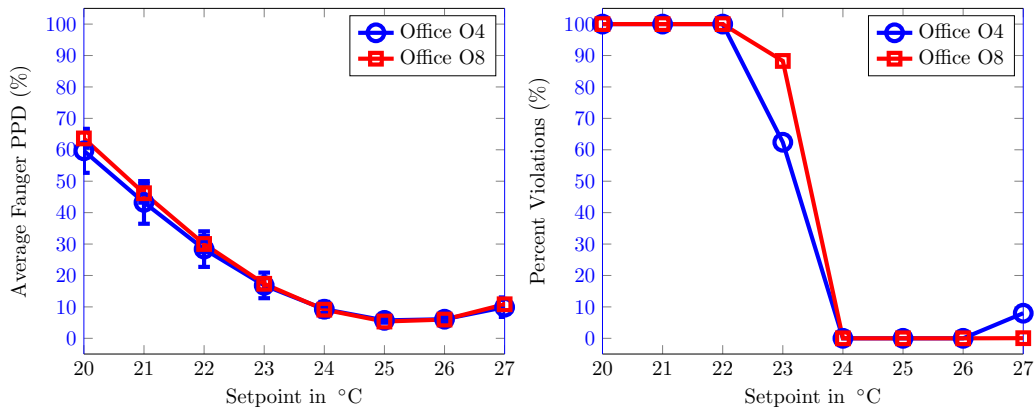


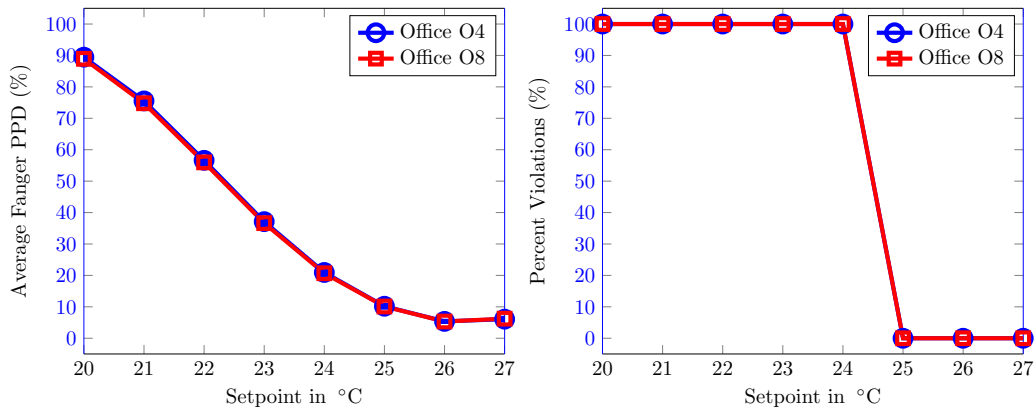
Figure 3-17: Winter results for office 04 using operative temperature thermostat set at 22 °C

throughout the experiment. The results for all cases are shown in Figs 3-18 and 3-19 for Offices 04 and 08 as before and for summer and winter respectively.

For the summer study, the in-equivalence of the two control strategies (air over operative temperature) is apparent, since for the air temperature control all setpoints between 24 °C and 26 °C lead to comfortable interiors for both offices, while for the operative temperature this interval is shifted between 25 °C and 27 °C.



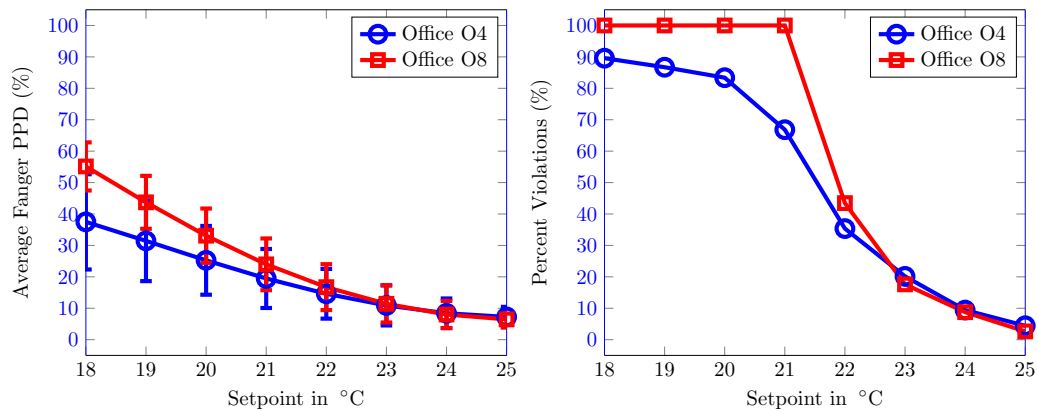
(a) User comfort evaluation for different air temperature setpoints for summer period



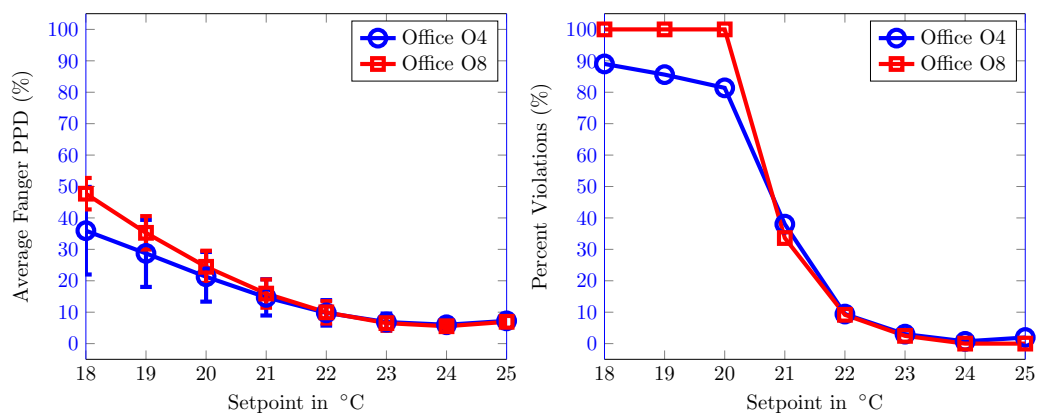
(b) User comfort evaluation for different operative temperature setpoints for summer period

Figure 3-18: Summer Experiments with different setpoints

The same conclusion is derived from the winter results, since here the best air temperature setpoint is 25°C, while it is 24°C for the operative temperature. Apart from this, another interesting observation here is the high variability of the Fanger PPD values (as indicated by the high standard deviation) due to the internal occupant and equipment gains and – mostly for Office 04 – the solar gains throughout the entire simulation period, as well as the slow dynamics of the heating system (radiators).



(a) User comfort evaluation for different air temperature setpoints for winter period



(b) User comfort evaluation for different operative temperature setpoints for winter period

Figure 3-19: Winter experiments with different setpoints

Concluding with the experiments conducted in TUC building, we have been able to confirm the inability of widely-used air temperature control methodologies to provide a structured and systematic way of representing and controlling thermal comfort in buildings, as well as the necessity to constantly adapt thermal comfort constraints based on the actual environmental (humidity) and personal (e.g. clo value) influencing factors, rather than myopically adopting the – calculated under steady-state conditions – operative temperature constraints in the example tables included in ISO 7730.

3.2.1.2 ZUB Building

In ZUB building, only winter experiments are performed using air temperature thermostat control. The period between January 25th and February 4th is selected, while a meteonorm weather file (Remund et al., 1999) is used. In this period we have some days with clear sky, with the average temperature at 3.3°C, the minimum temperature at -5.4°C and the maximum temperature at 9.3°C.

In contrast to the experiments conducted in TUC building, ZUB building is intended to serve as

a testbed complying with the assumptions leading to Table 1.1 of ISO 7730. In this direction, an ideal ventilation system with a fixed airflow of 50% relative humidity has been implemented in all offices and the Atrium. In order to not affect the room temperature and the energy balance, the ventilated air (with an air-change rate of 0.7 l/h) has the same temperature as the respective room temperature. In reality, the building is not equipped with a de-/humidification system, so this approach is a theoretic workaround to obtain the desired humidity levels. In the same direction, although an airflow model (TRNFlow) of the building is available, it is disabled for this study to limit the disturbances affecting comfort. Instead, an infiltration rate of 0.1 l/h has been set for all offices due to cracks and openings in the building. Finally, the same clo value assumed in ISO 7730 has been defined in all experiments.

Here, a simple control approach was chosen. Each room has an on/off differential controller which is acting as a thermostat. The controller tries to maintain a user-defined set temperature within a certain dead band (± 1 °C) by switching the TABS-massflow on or off. An internal hysteresis is used to prevent oscillation, while the hot water sending temperature in this case depends on the mean ambient temperature over the last 24 h through a heating curve defined for the building (Rovas et al., 2014a).

In these experiments, windows are considered always closed, while the blinds are activated when the total radiation on the main facade rises above 500 W/m^2 and are deactivated when it falls below 300 W/m^2 . Here, closed blinds result in a reduction of the solar radiation in an office by 70%. The air temperature thermostat setpoint is set at 21 °C (lower limit for class A buildings according to ISO 7730 — see Table 1.1), implemented using the controller described above.

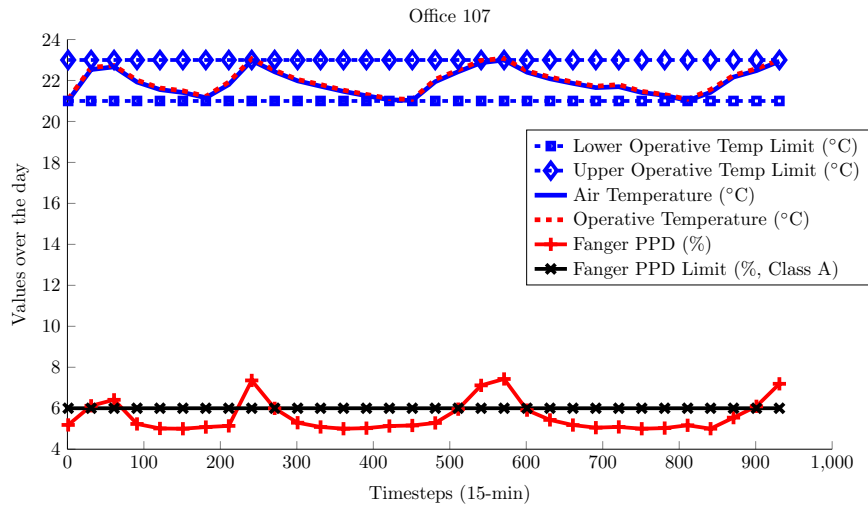
For ZUB building, two sets of air temperature control experiments are conducted, with the results shown in Figure 3-20, only for Office 107. The first setting forces the blinds always closed and no internal gains in order to ensure steady-state operation of the TABS, while the second includes internal gains and uses the default blinds control strategy of the building as described earlier. For both cases the air and operative temperatures coincide, due to the dynamics of the system and the heavy construction and insulation of the building. On the other hand, Figure 3-20(b) reveals the well-known overheating problem of buildings equipped with TABS due to internal and solar gains (Gwerder et al., 2008; Olesen et al., 2002), indicating the utilization of solutions facilitating weather and occupancy forecasts (Gwerder et al., 2008; Kontes et al., 2014; Oldewurtel et al., 2012) as an attractive option for control.

3.2.2 Conclusions

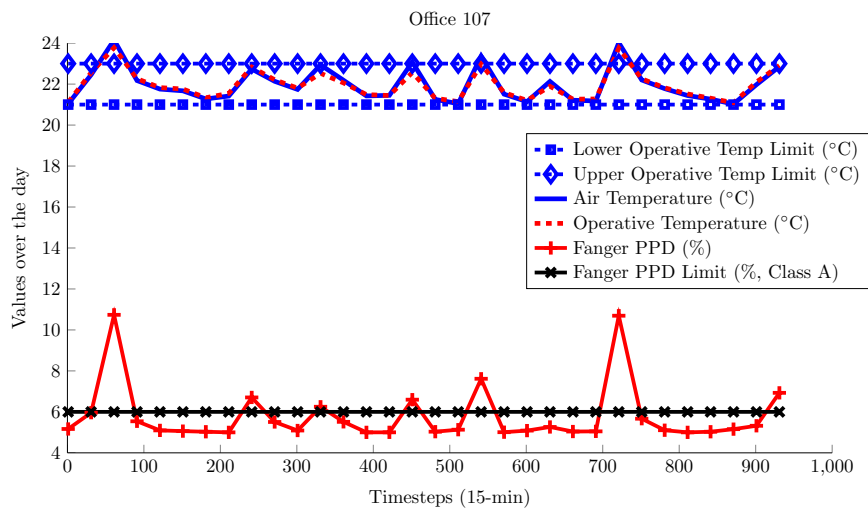
In this Section, an investigation on the ability of room thermostats to ensure comfortable building interiors has been performed. The wide use of such controllers is mainly based on two assumptions: i) that the operative temperature limits for comfortable interiors defined in ISO 7730 suffice to ensure user thermal comfort; and ii) that air and operative temperatures of building interiors coincide.

Regarding the first assumption, simulation results for an existing building in Crete indicate that neglecting other parameters influencing thermal sensation and designing controllers based on the indicative operative temperature limits of ISO 7730 can lead to invalid thermal sensation estimates. More importantly, the necessity for controlling (or at least accounting for) the humidity in building spaces has proven a crucial ingredient towards accurate estimation of thermal sensation, and thus towards efficient control of building indoor climate.

For the second assumption, experimental validation on the same building revealed an appreciable mismatch between indoor air and operative temperatures for both summer and winter tests, due to the dynamics of the HVAC system in each case (radiators for heating and AC for cooling season) and the construction and thermal properties of the building. On the other hand, we observed similar



(a) Results for office 107 using air temperature thermostat set at 22 °C, blinds always closed and no internal gains



(b) Results for office 107 using air temperature thermostat set at 22 °c

Figure 3-20: Results for office 107 of ZUB building

air and operative temperature values on a heavy construction building equipped with TABS leading to the conclusion that for specific construction and HVAC system dynamics, the air temperature measurements provide an accurate enough estimation of the operative temperature. Here, we can generalize that for buildings with high thermal mass this assumption holds, if proper care is taken to account for solar and internal gains in the control strategy, while as we move to buildings with lower thermal mass, there can be a considerable mismatch between air and operative temperatures in building spaces.

Due to the trade-off between energy consumption and thermal comfort, it is crucial to be able to represent (or predict) thermal sensation of the building’s occupants under different HVAC operation strategies — from all available comfort preserving strategies the one that requires the least amount of energy should be preferred. This suggests that the ability to calculate comfort indices such as Fanger, or even the ability to build personalized comfort models for the building occupants (Daum et al., 2011; Ghahramani et al., 2015; Lee et al., 2017; Malavazos et al., 2014; Sadeghi et al., 2017) should be features of an intelligent BACS.

3.3 Experiments on TUC Building

In this Section, the simulation-based and real experiments performed in TUC building are presented. The experimental process for the real experiments (also followed in the simulation-based experiments) is shown in Figure 3-21 and can be divided in three parts:

- The warming-up phase: here, historical sensor and weather data are collected by accessing the database, and using the co-simulation module are injected to the simulation model, to properly estimate the initial thermal state of the building;
- The control design phase: here, weather and occupancy forecasts are provided to the simulation model, thus enabling accurate evaluation of the candidate controllers produced by the optimization algorithm. The outcome of this phase is a new controller to be applied to the real building;
- The control application phase: here, the controller service is invoked and utilizing sensed data from the building and the weather station, calculates new control actions for all actuating components.

As can be witnessed from the results of this Section, conducting experiments on real buildings and evaluating the results can be quite complicated because of the many parameters and uncertainties involved. An important aspect in conducting the real experiments has been the ability to store and manipulate building data in a transparent way. This has been achieved using a middleware component that was developed for the purposes of the real experiments in TUC, the details of which are reported (Rovas et al., 2014b).

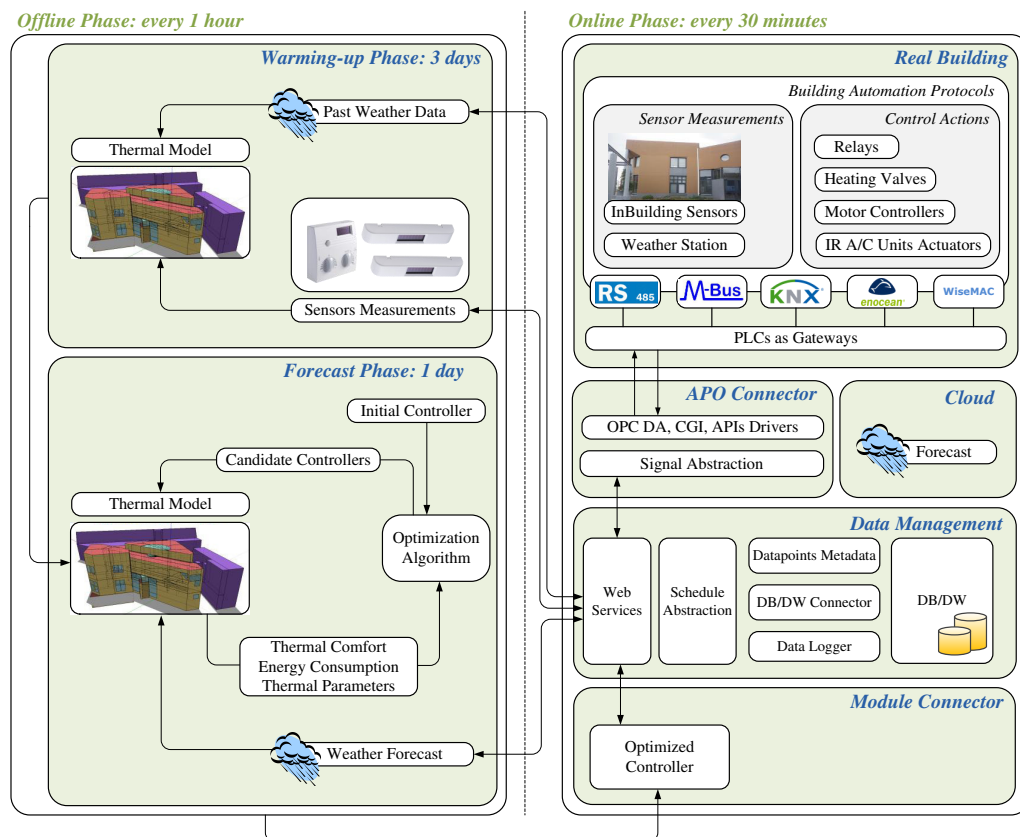


Figure 3-21: The Experimental Setup

3.3.1 Real Heating Experiment with Radiators

In this experiment, the heating demands are met by radiators, supplied with hot water from two inlets. The main objective of the test case is to verify applicability of the algorithm and to evaluate the “rationality” of the generated heating strategy, compared to the default operation. The experiment is not performed to the entire building, but to Offices 4 and 5, shown in Figure 3-22.

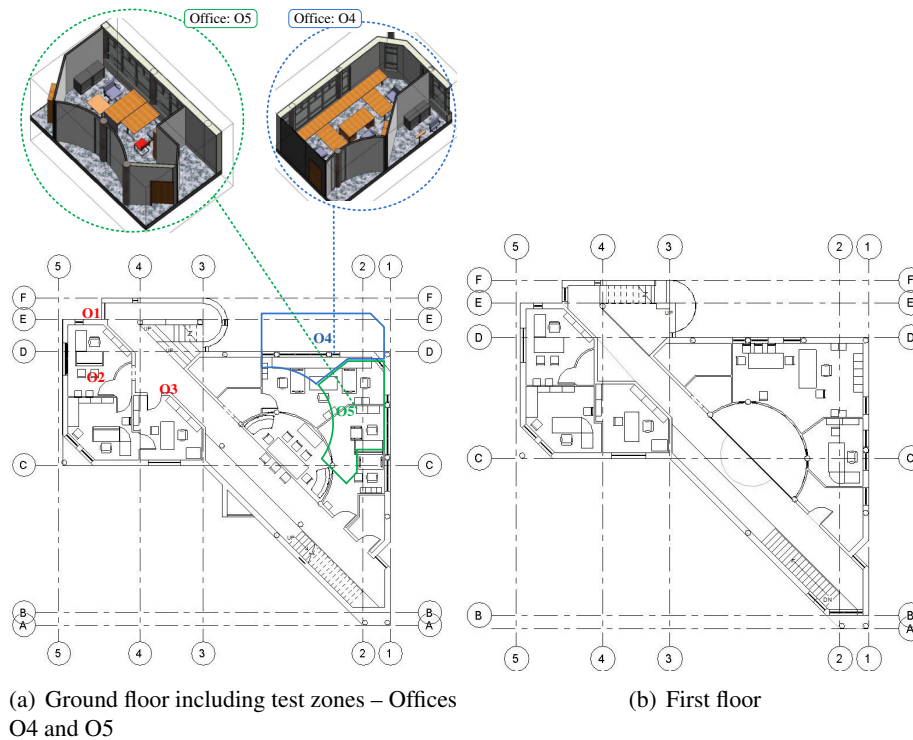


Figure 3-22: Floor plan of the experimental building and test zones

3.3.1.1 Experimental Setup

Two valves (T1, T2) are controlled, determining hot water flow to the radiators of offices O4 and O5 with total capacity 5.8kW and 4.2kW respectively (Figure 3-23). Even though the experimental setup does not include the entire building, it provides a demanding task, capable of evaluating the potential of the proposed approach. Office O4 is also served by a second line (T7 in Figure 3-23), which is considered uncontrollable for our experiment and is set to its default state (open). In this way, the algorithm needs to identify that there is another heating source in the room (a radiator of capacity of 1448 W) and schedule the controllable line to maintain acceptable comfort conditions and save energy at the same time. Moreover, as analyzed in Section 3.1.1, the central campus boiler is located outside of the building and serves a number of other facilities before the hot water reaches the Maintenance building. It is conceivable that the heating demands of the other buildings cannot be estimated without further information, thus the hot water temperature that reaches the building can fluctuate from the fixed value set to the thermal model. Here, the algorithm has to exploit actual in-building information in order to define control strategies able to overcome these disturbances. Finally, apart from the stochastic nature of the inlet hot water temperature, the proposed methodology needs to be able to react to all other unmodeled discrepancies, such as inexact weather and occupancy predictions and stochastic occupant behaviour.

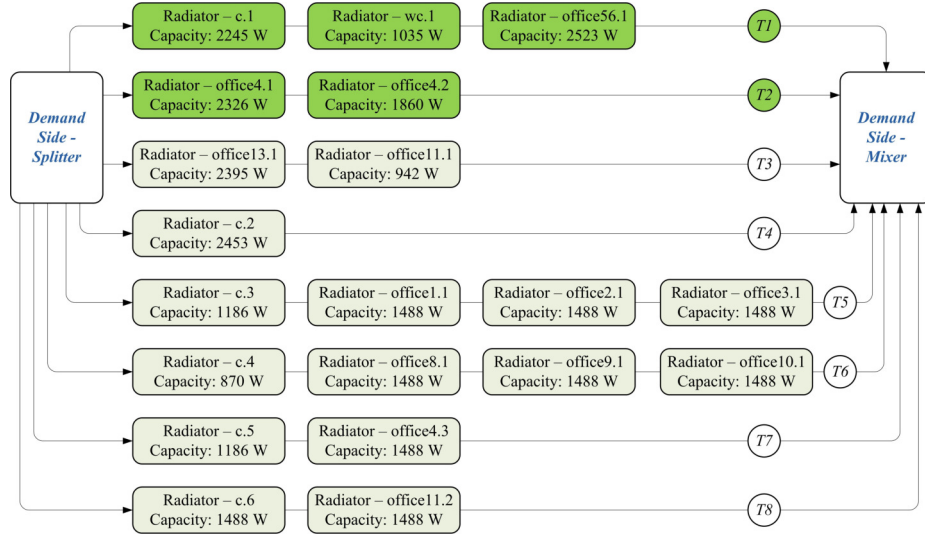


Figure 3-23: Central heating system branches and corresponding flow control valves

3.3.1.2 Formulation of the Control Design Problem

For the experimental setting above, the problem is related to determining the operation of the valves (open or closed) on each of the controllable lines (T1 and T2). Even though reliable weather and occupancy forecasts are available for periods longer than one day, a prediction horizon of one day ($T = 24$ h) has been selected; selecting larger T has no impact to the solution because of the low thermal capacity along with the poor insulation and air tightness of the building.

We build upon Eq. (2.4), to make the formulation of the optimization problem in the specific setup more precise. Let $i \in \{1, 2\}$ be an index indicating the controllable line, or correspondingly the room that this serves (Office 5 for $i = 1$, and Office 4 for $i = 2$), as shown in Figure 3-23. This way, we can define one controller for each line i as follows:

$$u_k^i = \begin{cases} 0, & \text{if } \frac{1}{1+e^{-(\theta^i)^T g(x_k)}} \leq 0.5 \\ 50, & \text{otherwise} \end{cases} \quad (3.1)$$

with u_k^i the position of each valve i (0: fully closed and 50: fully open) set at time instant k , and θ^i a set of coefficients for linearly combining a set of features $g(x_k)$. Here, g_1 is the outside temperature, g_2 the outside humidity, g_3 the global solar radiation, g_4 the wind speed, g_5 the wind direction, g_6 the occupancy, g_7 the office temperature, g_8 the office humidity and g_9 and g_{10} the square values of the office temperature and office humidity respectively. Since two lines are controlled in this experiment, $\theta = (\theta^1, \theta^2) \in \mathbb{R}^{20}$, and $u_k = \pi(\theta; x_k, d_k) = \begin{pmatrix} u_k^1 \\ u_k^2 \end{pmatrix}$ in Eq. (2.4).

For the comfort constraint, the Fanger PPD index is used, but we allow as a relaxation parameter in the solution of the optimization problem, values of the comfort index in each office to surpass this

limit for 15% of the time¹. This way, the comfort constraint for each office i is defined as follows:

$$c^i(\hat{x}) = \left(\frac{1}{N} \sum_{k=1}^N F_k^{i,v} \right) - D^i \leq 0, \quad (3.2)$$

with ;

$$F_k^{i,v} = \begin{cases} 0, & \text{if } F_k^i - F_k^s \leq 0 \\ 1, & \text{otherwise.} \end{cases}$$

here F_k^i is the Fanger PPD value at room i , F_k^s is the Fanger PPD limit for both rooms (15% for occupied periods and 100% for unoccupied), $F_k^{i,v}$ is 1 if the limit value is violated and 0 otherwise, D^i is the relaxation parameter for each room i , set to the maximum allowed discomfort time (15%) for both rooms and \hat{x} contains the states generated by the evolution of the model for all timesteps $k = 1 \dots N$.

Eq. (2.4) becomes for the particular problem:

$$\theta^* = \operatorname{argmin}_{\theta \in \mathbb{R}^{20}} \sum_{k=1}^N E_k, \quad (3.3)$$

subject to:

$$u_k^i = \begin{cases} 0, & \text{if } \frac{1}{1+e^{-(\theta^i)^T \cdot g(x_k)}} \leq 0.5 \\ 50, & \text{otherwise} \end{cases}, \quad \text{with } i = 1, 2$$

$$x_{k+1} = m(x_k, u_k, d_k),$$

$$C(\hat{x}) = \sum_{i=1}^2 w_i c^i(\hat{x}) \leq 0;$$

with E_k the energy consumption of the building² and $C(\hat{x}) \leq 0$ a function combining the comfort constraints of Eq. (3.2), with $w_i = 0.5$, $i = 1, 2$. An initial parameter vector (θ_0) is provided to Algorithm 2.2.1 and in each iteration a set of new parameters is generated and evaluated on the simulation model with respect to the total energy consumption and comfort constraints. Solution of Eq. (3.3), results in a set of controller parameters (θ^*) which are used to generate the controllers $u_k = \pi(\theta^*; x_k, d_k)$ to be applied to the actual building and the control design process restarts.

Algorithm 2.2.1 is used to solve the posed optimization problem. As the search space can be large, an intelligent selection of the initial set of parameters θ_0 can help accelerate convergence. In our case θ_0 was selected to mimic a behaviour functionally “near” the initial knowledge-based controller designed for the building at hand. This is achieved by performing an initial simulation following the existing rule-based control strategy and generating θ_0 by least-squared fitting over the simulated control actions (\hat{u}) and simulated building states (\hat{x}).

3.3.1.3 Results

For our experiment, a less cold week has been selected for the experiments in the real building, with the outside temperature fluctuating between 10 °C and 15 °C.

The control strategies produced by the proposed approach are evaluated against the performance of

¹This relaxation is only used for the solution of the optimization problem. The evaluation of the optimized controller is performed without posing this relaxation.

²We can only measure energy flows to the entire building and cannot determine the individual consumption in each study room. Note here though that using the same deterministic weather and in-building states in each iteration, only the different control decisions on Offices 4 and 5 can influence the total consumption of the building.

the actual rule-based strategy applied to the heating system of the building. Here, the central heating system serving all campus buildings is switched on every day at 05:30 to preheat the buildings and is switched off at 11:30–12:00, depending on the external conditions, while the valves controlling the lines inside each building remain open. This means that controllable elements of this experiment (T1, T2) would normally follow the centrally-selected strategy, thus the rule-based control strategy can be replicated and meaningful comparison between the two strategies can be made.

In addition to the controllable heating system shown in Figure 3-23, a collection of controllable elements manually operated by the users is also available in the building. These components include the doors and a number of openable windows in each office, blinds in all windows, as well as an AC split unit in each office. This implies that apart from providing the model with forecasts for the weather conditions and the occupancy, some assumptions have also to be made for the operation of these elements, acting as uncontrolled disturbances to the system. Blinds are assumed always open to exploit solar gains, while the same applies to the AC units, which are treated as back-up heating system operated by the users when feeling uncomfortable. We have to emphasize here that the above forecasts on the operation of the uncontrollable elements are inputs to the model used to estimate the future thermal state of the building. Any deviation from the predicted behaviour is considered disturbance and is treated by adjusting the behaviour of the system through the feedback control.

The heating experiment was initiated on February 26th and the system operated for 4 days. Given the physical constraints posed by the actuators (thermoelectric valves require 10min to change state) and the slow dynamics of the terminal units (radiators), actuation commands are sent every 30 min. Note that by solving the optimization problem new parameters θ^* are generated every 45 min, while Eq. (2.2) is evaluated with the current set of θ^* every 30 min to compute new valve positions.

The resulting control strategies are compared to the centrally-designed rule-based controller on the basis of total energy consumption and user comfort levels. For energy consumption, the comparison is performed at a simulation level, taking into account the total amount of time each strategy operates the radiators in each office, while for the user comfort the comparison is performed both at the simulation level – evaluating the Fanger PPD index values in each office using the detailed simulation model – and at the physical level, by determining if the users utilized the backup heating system (AC units).

In the remaining of the section, a comparison between the proposed methodology and the default campus-wide control strategy is provided. Here, the operating schedules for the valves are illustrated (with 0: fully closed and 50: fully open), along with the internal (simulated) and external temperatures (in °C), the actual occupancy of each office (scaled, with 0=no occupancy and 15=occupancy) and the predicted Fanger PPD levels ([0-100]%).

For room O4, the system selects to close the valve serving the controlled radiator (Figure 3-24), allowing the second radiator to cover the heating demands of the office. Comparing the resulting control strategy to the rule-based controller shown in Figure 3-25, it can be observed that both manage to maintain similar comfort levels throughout the entire study period (see also Figure 3-28 for a summary of the results), but the proposed methodology manages to save a significant amount of energy at the same time. This is due to the fact that the proposed approach correctly identifies that one radiator suffices for the heating demand of room O4 for the specific period, by utilizing information on the weather predictions and using the detailed thermal model of the building and past sensor data.

For room O5, the resulting strategy allows water flow for shorter periods (Figure 3-26) compared to the respective rule-based controller (Figure 3-27). During the entire availability period, the valve is opened only in the last (colder) day, where heating is necessary to maintain comfort, as predicted by the model. On 27/02 and 28/02 the system is operated in the morning only, while on 26/02 the room

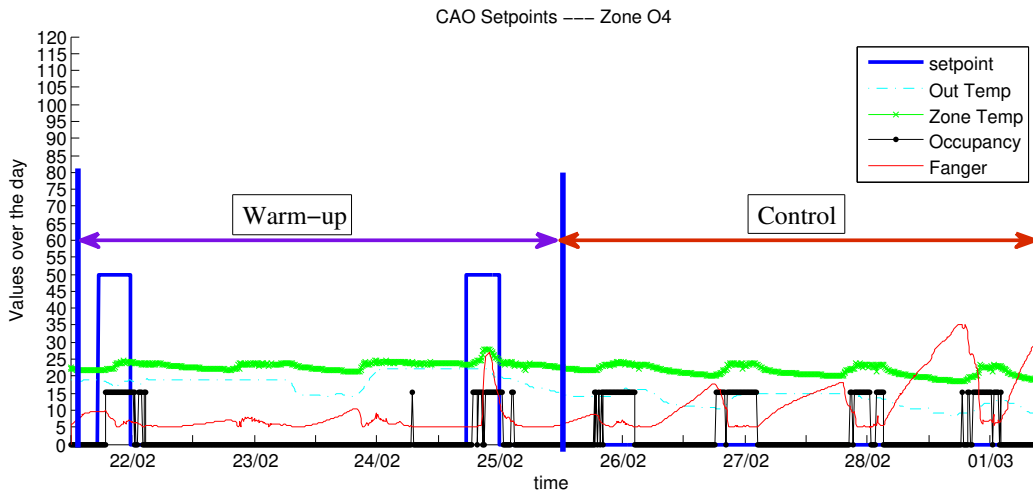


Figure 3-24: Optimized operation for Office O4

is heated only for a short period of time, when discomfort levels begin to rise. Overall, the proposed approach manages to effectively exploit the availability of the model and weather forecasts in order to predict – and treat when necessary – future discomfort.

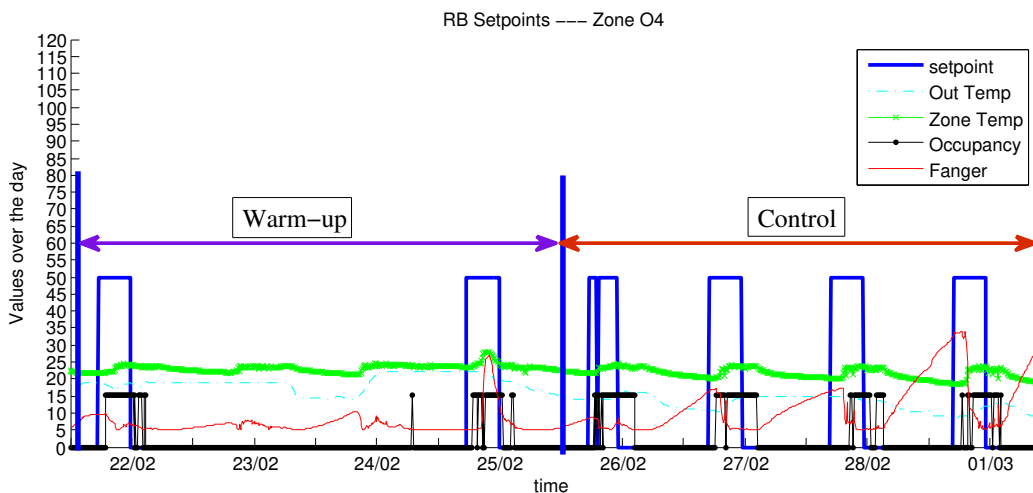


Figure 3-25: Rule-based control for Office O4

The rule-based controller on the other hand, would operate the heating system during the entire availability period, without achieving significant comfort improvement compared to the proposed approach, as shown in Figure 3-27. Both control strategies maintain comfort at acceptable levels, but in our approach the system was active for 32.2% less time (Figure 3-28).

Figure 3-28 summarizes the results of the heating experiment, comparing the control strategy produced by the proposed approach to the rule-based controller applied to the building. Both strategies prevent discomfort in both office rooms, but the methodology presented here managed to fulfill the task by closing the controllable valve of O4 for the entire test period and opening the valve in O5 for a total of 16.8 h in four days, while the rule-based controller would open both valves for 24.8 h on the same period. This intelligent operation of the two valves leads to 10.12% energy savings for the whole building, as computed using the validated detailed simulation model.

Regarding energy savings, the control strategy designed by the algorithm is evaluated against the performance of the actual rule-based strategy applied to the heating system of the building on the basis of the building total fuel (oil) consumption. Nevertheless, the controllable elements (valves

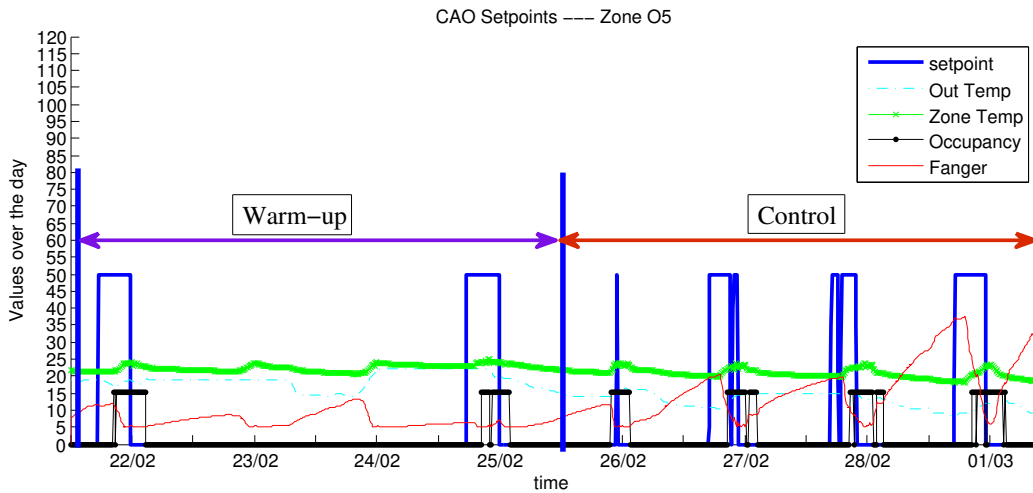


Figure 3-26: Optimized operation for Office O5

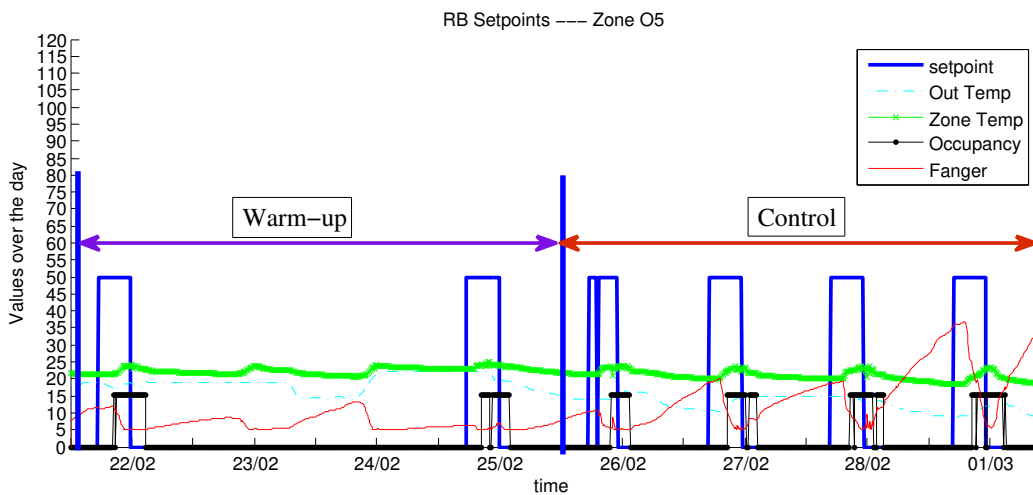


Figure 3-27: Rule-based control for Office O5

T1, T2 serving office O5 and O4 respectively) during the experiment, regulate the water flow in only two of a total of eight central heating system branches and as such, the result is not representative of the actual energy savings at the building level. Thus, apart from the total fuel consumption in the building, hot water energy supply at each controllable branch is also a criterion to evaluate the efficiency of the system.

Figure 3-29 depicts the hot water energy supply at each branch, as well as the hot water energy supply in offices O4, O5, for both the proposed approach and the rule-based controller. The proposed solution leads to 57.77% and 34.85% savings for offices O4 and O5, respectively.

Finally, it is important to emphasize that apart from the demonstrated savings and the user comfort evaluation on the simulation level, the backup AC units were not operated by the users at any time. This fact, combined with interviews with the occupants indicate that comfortable indoor conditions were achieved throughout the experiment.

3.3.1.4 Conclusions

Application of the proposed setup in TUC building has achieved 35% – 57% energy savings in two offices, compared to the default heating strategy of the building, while maintaining similar

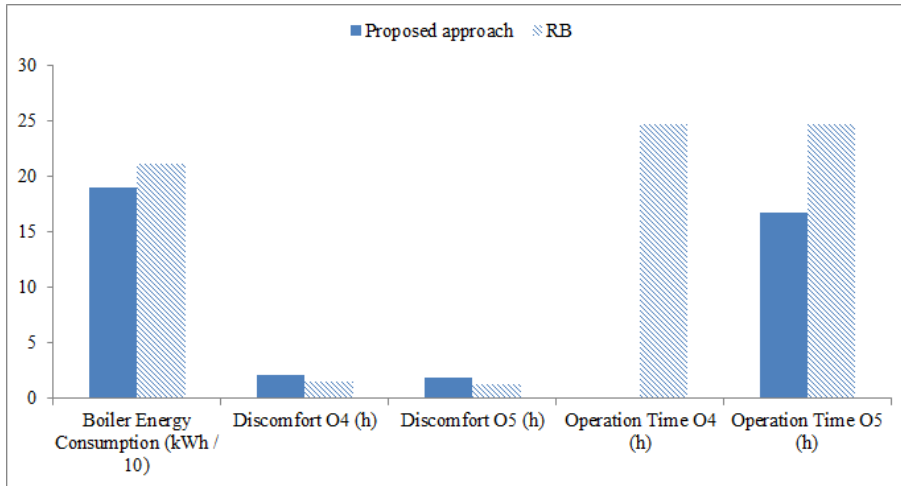


Figure 3-28: 22/02/2013 – 01/03/2013 real-building heating experiment results

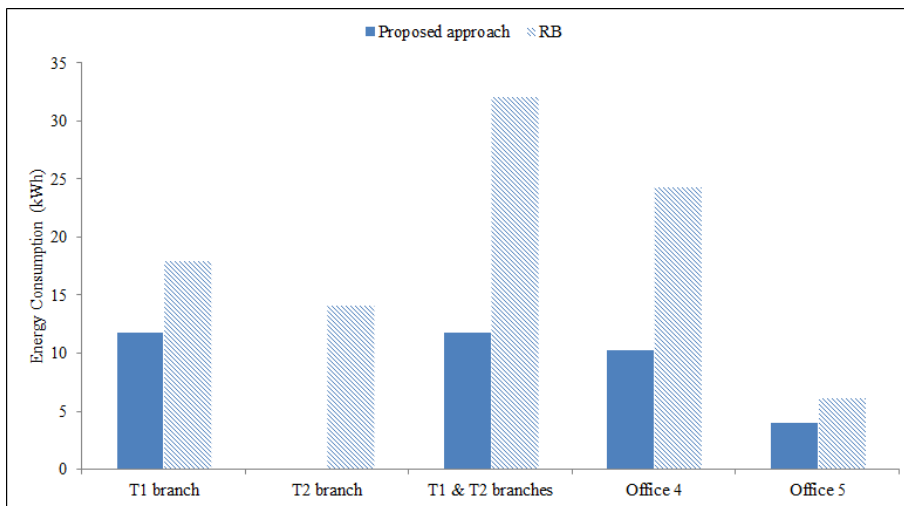


Figure 3-29: Heating experiment results — hot water consumption

indoor comfort conditions. While such high energy savings would not be realizable in an annual basis – and can, partly be attributed to the improper operation of the heating system under normal conditions (a situation which is very common in this and many other buildings), – what is perhaps more important is that the Control Design process managed to identify correct operational strategies. Nevertheless, the potential for inefficiency identification, along with the opportunities offered for balancing between thermal comfort and energy consumption offer a promising methodology for automatic design of BACS.

3.3.2 Real Heating Experiment with AC Units

A second real heating experiment was performed in TUC building, using the Air Conditioning (AC) units in each office for covering the heating demands, while the radiant system was inactive.

3.3.2.1 Experimental Setup

Our approach was applied on February 14th, 2014 in the building. On that day, the morning was relatively cold and humid, with heating required, followed by a warmer and sunny afternoon, with no heating necessary. On similar past days, the offices would be very cold in the morning causing comfort problems in the first hours of occupancy. The users would turn on the AC units upon arrival, very often selecting a very high setpoint, and would keep them operational until later in the day even when heating was no longer necessary, thus leading both to comfort problems (in the morning) and unnecessary energy consumption (later in the day).

The occupancy forecast assumes a fixed occupancy from 8 a.m. to 4 p.m., in agreement with the regular working hours of the building occupants. Weather forecasts are obtained from an external source by polling at regular intervals a web-service provided by the forecast provider. Uncontrollable elements (doors, windows and shading devices) are assumed fixed to either closed (doors and windows) or open (blinds) for the duration of the day. These forecasts are used as part of the simulation and control design process. In addition, a fault-detection module is monitoring occupancy in each of the rooms and turns-off the AC unit if users leave their office for a period of more than three minutes.

To accommodate user preferences, a setpoint correction interface with a rotary knob is activated in each room. A virtual sensor is introduced in the system that would receive an analogue value $[0, 270]^\circ$ (knob angle) and by mapping to the interval $[-3, 3]$ and rounding to the closest integer would return a discrete value in the range $(-3, -2, \dots, +3^\circ\text{C})$. For the heating experiments described here, the value of -3°C would indicate a preference by the user to turn off the AC unit. In all other cases, the setpoint communicated to the AC was the setpoint generated by our algorithm offset by the correction value provided by the corresponding virtual sensor.

Out of all the offices, three offices are selected for performing the active regulation experiments, while all other offices are assumed (in the simulation) to be operated by a simple “reasonable” rule based controller. The offices chosen for control by our algorithm are Offices 2, 4 and 5, shown in Figure 3-22. Office 2 is on the north side of the building and receives a small fraction of direct solar radiation, thus requires significant heating even during sunny winter days. Office 4 requires heating during the morning when the users enter, but receives high solar gains during noon that can lead to overheating, while office 5 is in between of the other offices in terms of heating demands. The different office characteristics, require our optimization algorithm to discover a different control strategy for each office, due to the different amount of solar gains. Un-modelled disturbances, and inexact weather and occupancy predictions along with stochastic user behaviour influence the quality of the controllers generated but to a smaller extent compared to open loop control approaches.

3.3.2.2 Formulation of the Control Design Problem

In each room the AC mode is set to “heating” and the fan speed to 50%. The setpoint is then calculated by the following controller function:

$$u_k^i = \theta_0^i T_k^{\text{out}} + \theta_1^i S_k + \theta_2^i T_k^{i,\text{in}} + \theta_3^i; \quad (3.4)$$

with i an index over the controlled offices, $u_k^i \equiv T_k^{i,\text{set}}$ the AC set point for office i at time k , T_k^{out} the outside temperature at k , $T_k^{i,\text{in}}$ the indoor air temperature of office i at k , S_k the global horizontal radiation measured by the weather station and θ the tunable control parameters (weights). As a starting point for the optimisation the following parameters are used: $\theta_0^i = \theta_1^i = \theta_2^i = 0$ and $\theta_3^i = 23^\circ\text{C}$, $i \in \{2, 4, 5\}$, representing a controller that maintains the internal temperature at 23°C for the entire occupancy period.

A warming-up period (as described in Section 1.2.3.2.2) of three days ($T_w = 72$ h) and a prediction horizon of one day ($T_p = 24$ h) are selected. Even though reliable weather and occupancy forecasts for longer than one day periods were available, for the lightweight building at hand and given the poor insulation and air tightness, longer prediction periods have no influence on the solution. In each control design cycle, historical office temperature and weather data are retrieved for the warming-up phase, while weather and occupancy forecasts are used for predicting the future thermal behaviour of the building. Once the control design process finishes and optimized controllers are generated (i.e. optimized weights θ^*), they are communicated to the building-side. There, every 30 minutes the controller service is invoked, and utilizing sensed data from the building and the weather station, using Eq. 3.4, new setpoints are calculated for each office. The actual temperature communicated to the AC units, is obtained from the calculated setpoint properly offset according to the user preferences in the manner described above.

For the experiment presented here, the task is to minimize the total electric consumption of the building while not violating the posed comfort constraints as expressed by the Fanger PPD index. Following the ISO recommendations for existing buildings of class C – like the TUC building – an acceptable limit for the Fanger PPD is 15%. In the experiment presented here, we formulate the thermal comfort constraints as stochastic constraints (Oldewurtel et al., 2012). First, we define the probability of discomfort P_d^i for each office i as follows:

$$P_d^i = \frac{\# \text{ of occupied timesteps with } F_k^i \geq 15\%}{\# \text{ of occupied timesteps}}, \quad (3.5)$$

where F_k^i is the Fanger PPD value in office i at time k . Next, we define the comfort constraint C^i for each office i as:

$$C^i = \begin{cases} 1 - P_d^i, & \text{if } 1 - P_d^i < \alpha \\ 1, & \text{if } 1 - P_d^i \geq \alpha \end{cases} \quad (3.6)$$

Here, we set $\alpha = 0.9$. Finally, we construct one constraint involving all offices, as required by the algorithm (Kontes et al., 2014) (2.2.2), as follows:

$$C = 1 - \prod_{i=1}^3 C^i. \quad (3.7)$$

For evaluating the results *measured* values from the offices are used: for the energy consumption measurements from the installed energy meters are collected, while for the calculation of the Fanger PPD index, in-room (air temperature, radiant temperature and relative humidity) and weather station (barometric pressure) measurements, along with default values for sensor measurements that are not available (e.g. indoor air velocity, clothing values, etc.) are combined. For a detailed analysis on the Fanger PPD calculations for TUC building please refer to (Rovas et al., 2014a).

3.3.2.3 Results

Starting with office 2, it is clear that the algorithm discovers that pre-heating is required to ensure comfortable interior when users (are predicted to) enter at 8 a.m. Therefore, the room is heated from 7 a.m. to 8 a.m. and the Fanger PPD values reach the acceptable limits (Figure 3-30). On the other hand, from the time the occupant enters the room (at 8:30 a.m.) and for the rest of the day, comfort levels are violated as Fanger PPD values range between 30% and 40% during occupancy period.

A closer look to the in-room conditions (Figure 3-31) reveals that although the radiant temperature reaches relatively high values during the pre-heating period and remains at the same levels throughout the day, the air temperature remains constant in significantly lower values. A review with the office user revealed that the office door remains open throughout the day, which results in the inabil-

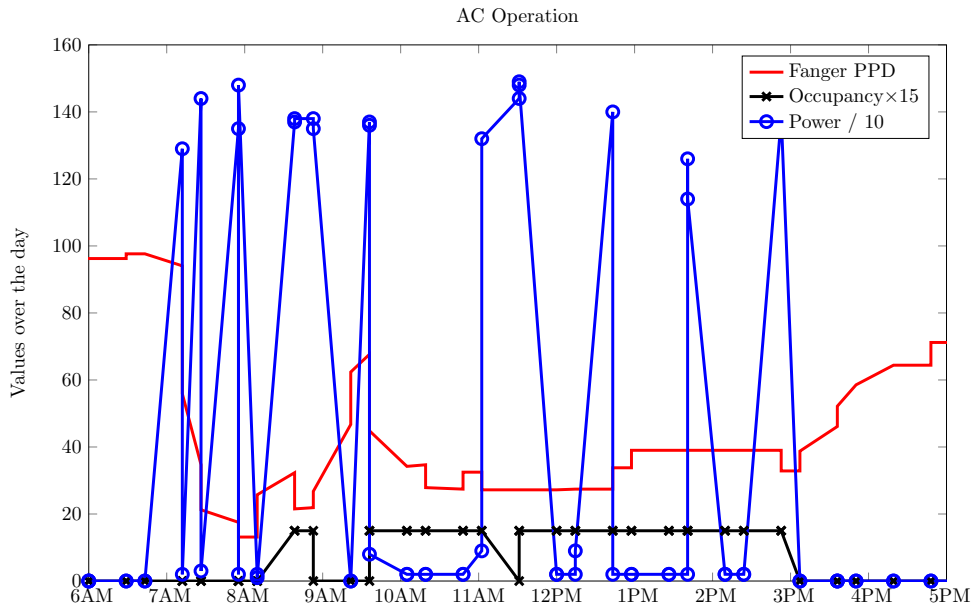


Figure 3-30: AC operation and comfort levels for Office 2

ity of the AC system to cover the heating demands, especially when not operating in full fan speed. This leads both in significant energy consumption and thermal discomfort as shown in Figure 3-30.

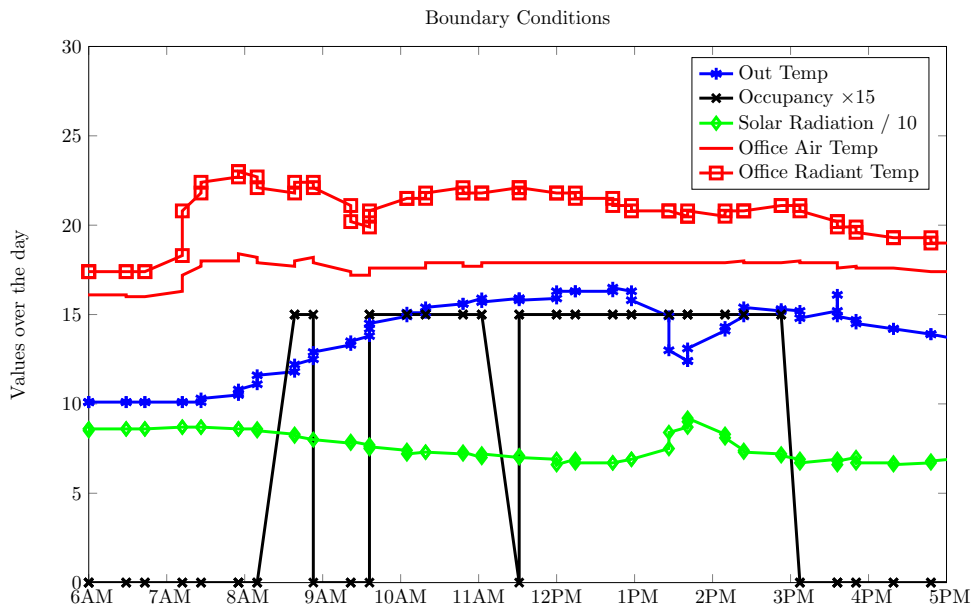


Figure 3-31: Weather and in-room conditions for Office 2

In Office 4 the optimized controller also applies a pre-heating strategy between 7 a.m. and 8 a.m., as shown in Figure 3-32, which terminates due to false occupancy signals from the occupancy sensor of the office between 7 a.m. and 8 a.m. On the other hand, when the users enter the office around 8:15 a.m. they open the door and windows as shown in Figure 3-33. A review with the users revealed that they naturally ventilate the office every morning (if weather conditions permit) — a strategy that cancels the effects of pre-heating and leads to unnecessary energy consumption. For the remaining of the day the optimized controller generates set points that lead to minimum use of the AC, since thermal comfort is preserved due to the high solar gains the zone receives.

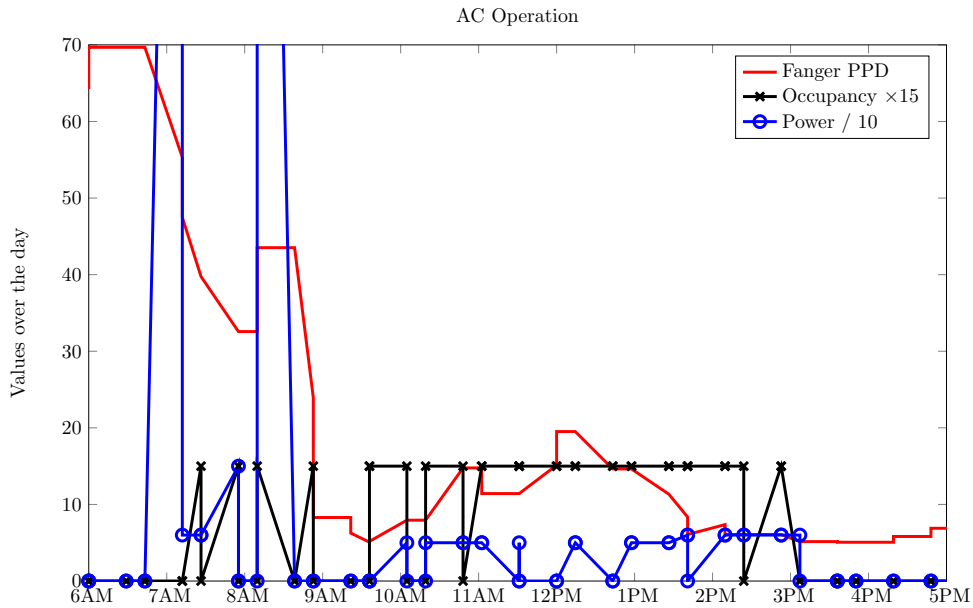


Figure 3-32: AC operation and comfort levels for Office 4

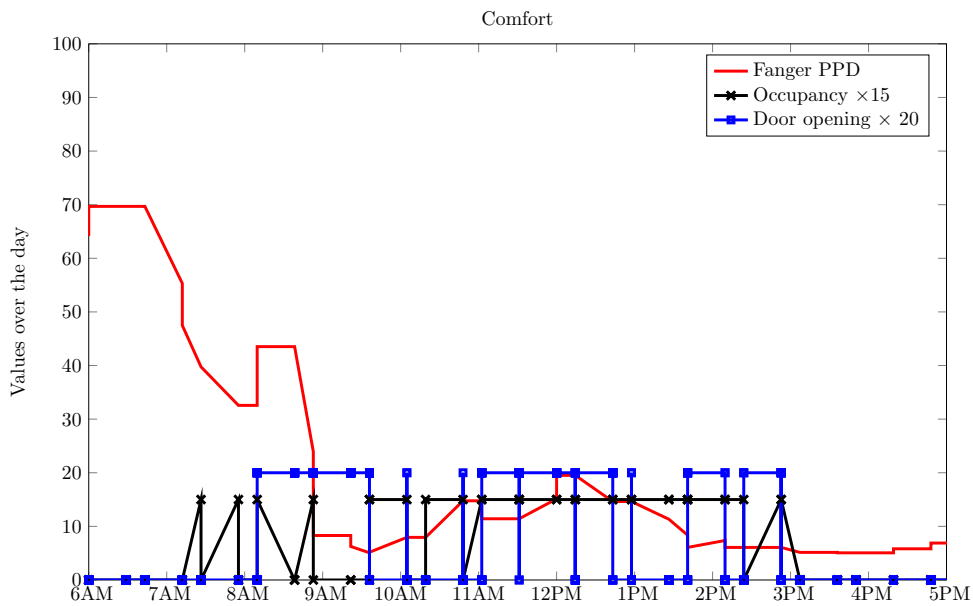


Figure 3-33: Door and windows opening schedules for Office 4

In office 5 the users cancel our system from the previous day by using the set point correction functionality, thus there is no heating operation during morning, as shown in Figure 3-34. The users allow the system to control the AC unit between 9 a.m. and 10 a.m., where the controller heats the room leading to comfortable interior.

Table 3.1 shows the overall energy consumption and comfort levels during occupied periods in each room. A significant amount of energy is consumed in office 2 without leading to improved comfort, since the office door remains open throughout the day. The users in office 5 did not allow any pre-heating in the morning, thus a small amount of energy is consumed in the office, accompanied by high discomfort levels. Office 4 is characterized by good comfort levels, as it receives high solar gains, and requires energy only for preheating in the morning — energy which is wasted by the occupant’s practice to naturally ventilate the office. What is also important, is that user acceptance

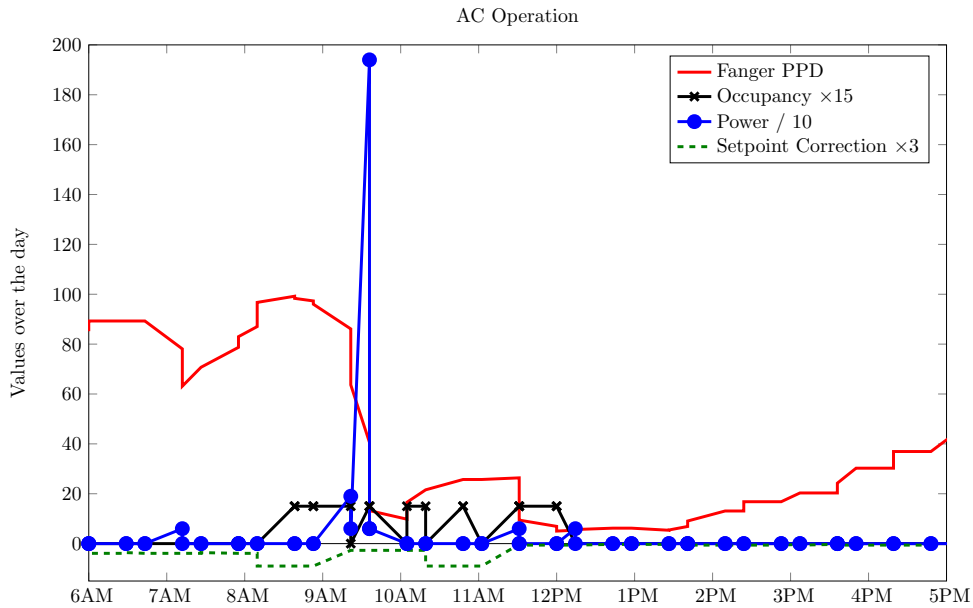


Figure 3-34: AC operation and comfort levels for Office 5

of the system has been good, with the occupants stating that indoor comfort in their offices has been better compared to the manual operation of the system in days with similar conditions, mostly due to the pre-heating in the morning.

Table 3.1: TUC AC heating experiment results

Office 2		Office 4		Office 5	
Energy Consumption (kWh)	Comfort Fanger PPD (%)	Energy Consumption (kWh)	Comfort Fanger PPD (%)	Energy Consumption (kWh)	Comfort Fanger PPD (%)
6.05	33.7	1.01	10.4	0.42	29

3.3.2.4 Conclusions

The effect of the user disturbances dictates the need for fault detection services that will complement the control design functionality. Here, analytics that would prevent heating the room if a door or window is left open would have reduced energy consumption in office 2, while services predicting user occupancy schedules and user behavior (such as opening the doors and windows *systematically* in the morning) would have prevented the pre-heating of office 4.

The philosophy and potential of our approach are evident in office 4 results. Here, the thermal simulation model of the building, using information from the weather forecast service, manages to *predict* the effect of the solar and internal gains in the thermal state of the office and in user comfort, with user comfort defined according to ISO 7730 and not as ad hoc upper and lower air temperature bounds. The control design service, utilizing the detailed model, is able to generate controllers (optimized parameters θ^*), that are able to achieve comfortable interiors with moderate energy consumption.

Nonetheless, despite this experiment is affected by the behaviour of the users and equipment faults, still indicates the rationality of the solution generated by the proposed approach. Here, in office 4 the model accurately predicts that the solar and internal gains suffice to cover the heating demand after 9 a.m. and the algorithm generates control parameters that lead to minimum AC usage for this

space. In addition, for office 2, even though the model assumes the office door closed and predicts different heating demand for the office throughout the day, the closed-loop nature of the controller allows to recover from the unpredicted event (open door) by heating the office.

3.3.3 Simulation-based Evaluations with AC Units

Since the real heating experiment in TUC using the ACs has been affected by user-induced and sensor faults, we setup two experiments, one for winter and one for summer where we apply the Control Design process in simulation, to evaluate the potential of the methodology. In both these experiments, the application of CAO algorithm (Algorithms 2.2.2 and 2.2.1) with the constraints defined for the real experiment above (Eq. 3.7) failed, due to the inability of the approach to handle the large number of constraints. Thus, the simulation-based evaluations have been performed using the Bayesian Optimization approach (Algorithm 2.3.1).

3.3.3.1 Control Design for one Winter Day

This experiment is setup for January 4th using a meteorological weather-file for Athens and 3 days for the warming-up period, while new setpoints are sent to the AC units every 10 minutes. The controllers used for the setpoint of each AC unit are:

$$u_k^i = \theta_0^i T_k^{\text{out}} + \theta_1^i S_k + \theta_2^i T_k^{i,\text{in}} + \theta_3^i; \quad (3.8)$$

with $i \in \{1, 2, \dots, 10\}$ an index over the controlled offices, $u_k^i \in [18, 30]^\circ\text{C}$ the AC set point for office i at time k adjusted every 10 minutes, T_k^{out} the outside temperature at k , $T_k^{i,\text{in}}$ the indoor air temperature of office i at k , S_k the global horizontal radiation measured by the weather station and $\theta \in \mathbb{R}^{40}$ the tunable control parameters (weights).

The users enter the building at 8 a.m. and exit at 4 p.m. and the controllers are applied one hour earlier to account for pre-heating, thus the building schedule (or Occupancy Mode) is defined between 7 a.m. and 4 p.m. For the rest of the day (Setback Mode), the setpoint is set at 30°C . For comparison, a standard rule-based controller is formulated, with the following logic:

$$u_k^i = \begin{cases} 23^\circ\text{C}, & \text{In Occupancy Mode} \\ 30^\circ\text{C}, & \text{In Setback Mode} \end{cases} \quad (3.9)$$

The task for the control design process is to minimize the total energy consumption of the building, while maintaining comfortable interiors according to Fanger index. Following the ISO recommendations for existing buildings of energy class C – like the TUC building – the acceptable limit for the Fanger PPD is 15%. In the experiment presented here, we formulate the thermal comfort constraints as stochastic constraints. First, we define the probability of discomfort P_d^i for each office i as follows:

$$P_d^i = \frac{\# \text{ of occupied timesteps with } F_k^i \geq 15\%}{\# \text{ of occupied timesteps}}, \quad (3.10)$$

where F_k^i is the Fanger PPD value in office i at time k . Next, we define the comfort constraint C^i for each office i as:

$$C^i = 1 - P_d^i < \alpha \quad (3.11)$$

For this experiment we study the performance of the algorithm under different values for the constraint relaxation, that is we set $\alpha = \{0.8, 0.85, 0.9, 0.95, 1.00\}$.

Figure 3-35 illustrates the results of the experiment. The RB controller (constant setpoint during

occupancy) is unable to utilize information on weather conditions and building properties (i.e. thermal properties, orientation, glazing area, etc.), thus leads to high discomfort to offices that do not receive high solar gains. The control design setup on the other hand, leads to similar comfort levels for all offices, but of course requires more energy to compensate for the comfort improvement.

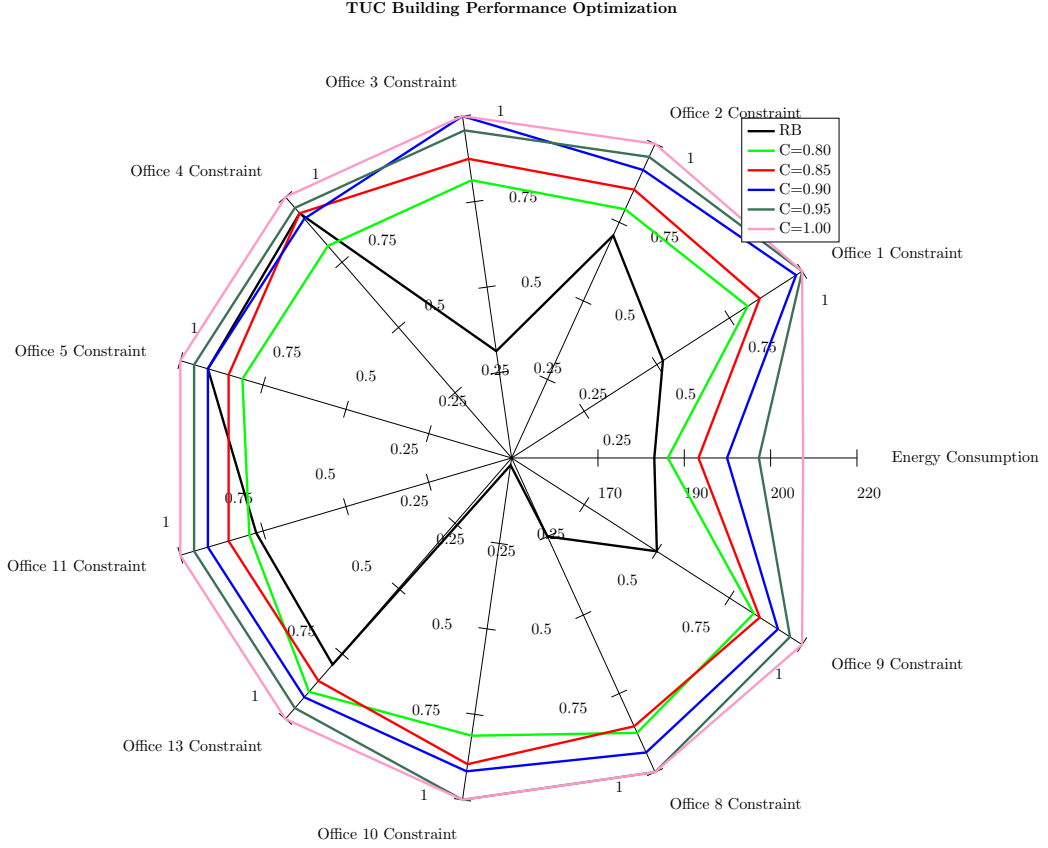


Figure 3-35: CAO controller performance for TUC building simulation study

The trade-off between energy and comfort is shown clearly in Figure 3-36, where the energy consumption that the proposed approach achieved for different constraint limits is illustrated. Here, the plotted value for the constraint is the average constraint for all offices.

3.3.3.2 Control Design for the Summer Period

A second simulation-based evaluation of the proposed approach has been performed (July – September), using the same meteorological weather file for Athens and the centralized approach of Algorithm 2.3.1 for the solution of the optimization problem. Here, the controllers used for the setpoint of each AC unit are the same as in Eq. 3.8:

$$u_k^i = \theta_0^i T_k^{\text{out}} + \theta_1^i S_k + \theta_2^i T_k^{i,\text{in}} + \theta_3^i; \quad (3.12)$$

with $i \in \{1, 2, \dots, 10\}$ an index over the controlled offices, $u_k^i \in [18, 28]^\circ\text{C}$ the AC set point for office i at time k adjusted every 10 minutes, T_k^{out} the outside temperature at k , $T_k^{i,\text{in}}$ the indoor air temperature of office i at k , S_k the global horizontal radiation measured by the weather station and $\theta \in \mathbb{R}^{40}$ the tunable control parameters (weights).

The users enter the building at 8 a.m. and exit at 4 p.m. and the controllers are applied one hour earlier to account for pre-cooling, thus the building schedule (or Occupancy Mode) is defined between 7 a.m. and 4 p.m. For the rest of the day (Setback Mode), the setpoint is set at 28°C . For

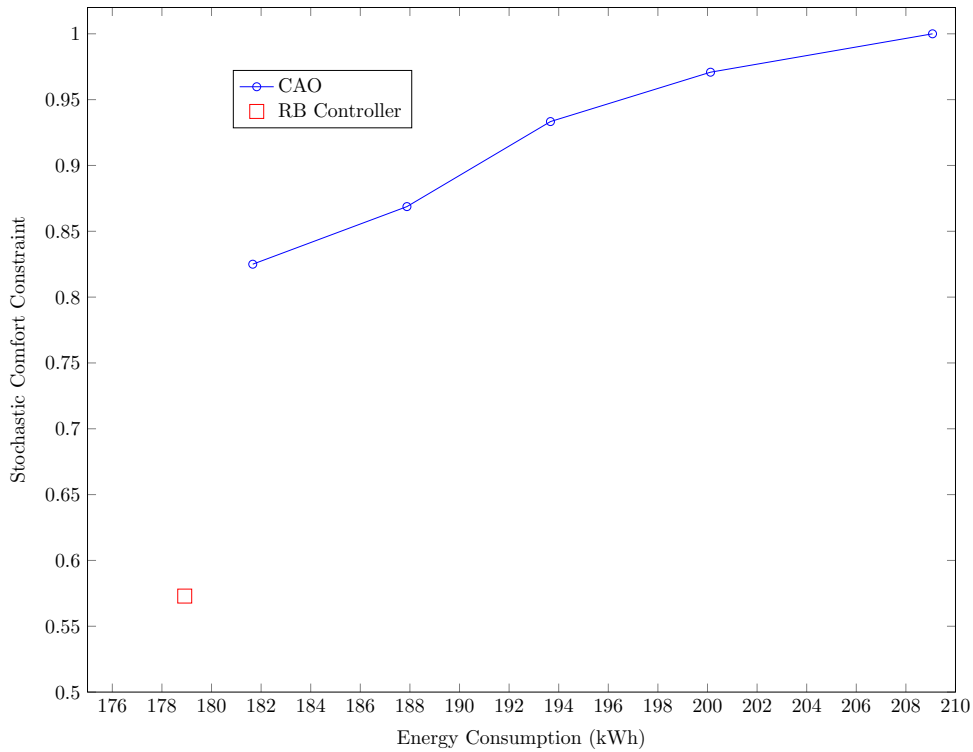


Figure 3-36: Energy consumption – Comfort trade-off

comparison, the same rule-based controller as in Eq. 3.9 is used, but here the setpoint in Occupancy mode is set at 24 °C, while for the Setback mode is set at 28 °C.

The task for the control design process is to minimize the total energy consumption while maintaining comfortable interiors in all offices. For the comfort, the constraint of Eq. 3.11 is used, while we require comfortable interiors for 90% of the occupied time, thus we set $\alpha = 0.9$.

Note here the limited flexibility of the control design process, since the generated controller is allowed to interact with the building only during the Occupancy Mode, while setting a constant setpoint for the rest of the day. In addition to this, the warming-up period for each day has been considered to be the same as applying the Rule-Based controller, assuming that due to the low thermal mass of the building and the high infiltration, the building thermally “resets” at night. Both these restrictions have been enforced to reduce the computational burden of the entire experiment, allowing distributed control design tasks.

Despite these constraints though, the energy consumption in almost all offices is reduced as shown in Figure 3-37, with the total reduction being around 17%.

3.3.3.3 Conclusions

In this set of experiments, the potential of the control design approach is evident. If there are no disturbances from the occupants, the proposed methodology is able to manage the trade-off between energy consumption and user comfort in a transparent and principled manner. In addition, the ability of the Bayesian Optimization algorithm to handle multiple constraints in a structured manner, compared to the manually-tuned weighting of CAO algorithm has become evident.

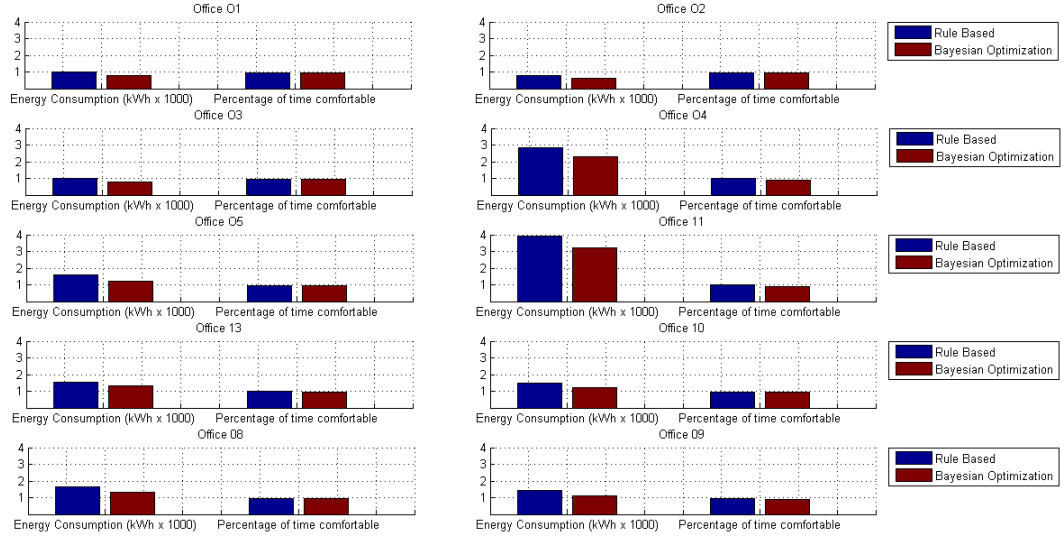


Figure 3-37: Simulation study on the efficiency of BO vs RB controller for the whole cooling season for TUC

3.4 Experiments on ZUB Building

3.4.1 Simulation-based Experiments on ZUB Building

A set of simulation-based control design experiments are performed on the Tower model of ZUB building (Figure 3-7), using a meteorological weather file from an area with similar climatic conditions to Kassel (Frankfurt am Main).

3.4.1.1 Experimental Setup

The building is considered occupied between 9 a.m. and 6 p.m. A standard rule-based controller is used to provide a baseline comparison to the efficiency of the controllers generated by the control design process. This controller adjusts: (i) the hot water sending temperature of the TABS system; (ii) the setpoint in each office, used as input to a low-level logic that controls the position of the valves in each circuit of the TABS; and (iii) the opening of the blinds in each office. In detail, for the water temperature the following heating curve is used:

$$u_{RB,k}^{HW} = -0.8(T_k^{amb} + 6) + 38, \quad (3.13)$$

with T_k^{amb} the average outside ambient temperature of the last 24h, calculated at time k . A new water temperature is calculated every 2 h.

For the zone setpoint of each controllable office i , the following controller is applied:

$$u_{RB,k}^{s,i} = \begin{cases} 21^\circ\text{C}, & \text{In Occupancy Mode} \\ 18^\circ\text{C}, & \text{In Setback Mode.} \end{cases} \quad (3.14)$$

The Occupancy Mode is defined between 5 a.m. and 5 p.m. and the controller generates a new setpoint every 1 h. Note that the controller regulates the position of the TABS valves in each office and is a proportional controller with a deadband of 1°C .

For the blinds, controlled every 2 h, a simple rule is used to define their state:

$$u_{\text{RB},k}^{\text{b},i} = \begin{cases} \text{Close,} & \text{If } S_k^{\text{S}} > 300 \text{ W/m}^2 \\ \text{Open,} & \text{If } S_k^{\text{S}} < 120 \text{ W/m}^2, \end{cases} \quad (3.15)$$

with S_k^{S} the 2-hour running average of the solar radiation on the south facade calculated at time k . Note here that closed blinds result in a reduction of solar radiation by 70%, i.e. the blinds cannot block the solar radiation completely.

In the control design setup, more complex controllers are formulated, while the sampling interval for each controller is the same as with the rule-based control. Here, the sending water temperature is controlled by the following heating curve:

$$u_{\text{CD},k}^{\text{HW}} = \theta_3^{\text{HW}} T_k^{\text{amb}} + \theta_2^{\text{HW}} S_k + \theta_1^{\text{HW}} \frac{1}{3} \sum_{i=1}^3 T_k^i + \theta_0^{\text{HW}}, \quad (3.16)$$

with T_k^{amb} the 24-hour running average outside air temperature, S_k the 2-hour running average of the global horizontal radiation and T_k^i the 24-hour running average of the zone air temperature of zone i , all calculated at time k . The water temperature setpoint is limited in the interval $u_{\text{CD},k}^{\text{HW}} \in [23, 38]^\circ\text{C}$.

The zone setpoint of each controllable office i , is calculated as:

$$u_{\text{CD},k}^{\text{s},i} = \begin{cases} \theta_3^{\text{s},i} T_k^{\text{amb}} + \theta_2^{\text{s},i} S_k + \theta_1^{\text{s},i} T_k^i + \theta_0^{\text{s},i}, & \text{In Occupancy Mode} \\ \theta_4^{\text{s},i}, & \text{In Setback Mode,} \end{cases} \quad (3.17)$$

with T_k^{amb} the 24-hour running average outside air temperature, S_k the 2-hour running average of the global horizontal radiation and T_k^i the 24-hour running average of the zone air temperature of zone i , all calculated at time k . During Occupancy Mode the setpoint is limited in the interval $[15, 28]^\circ\text{C}$, while during Setback Mode it is bounded in the interval $[10, 28]^\circ\text{C}$.

The controller of the blinds is based on the rule-based controller formulation, with:

$$u_{\text{CD},k}^{\text{b},i} = \begin{cases} \text{Close,} & \text{If } S_k^{\text{S}} > \theta_1^{\text{b},i} \\ \text{Open,} & \text{If } S_k^{\text{S}} < \theta_0^{\text{b},i}. \end{cases} \quad (3.18)$$

Here S_k^{S} is the 2-hour running average of the solar radiation on the south facade calculated at time k .

3.4.1.2 Formulation of the Control Design Problem

The task for the control design process is to minimize the total energy consumption of the building, while maintaining comfortable interiors according to Fanger index, by discovering optimized parameters for the controllers of the building (i.e. $\theta \in \mathbb{R}^{25}$). Following the ISO recommendations for existing buildings of energy class B – like ZUB – an acceptable limit for the Fanger PPD is 10%. In the experiment presented here, we formulate the thermal comfort constraints as stochastic constraints. First, we define the probability of discomfort P_d^i for each office i as follows:

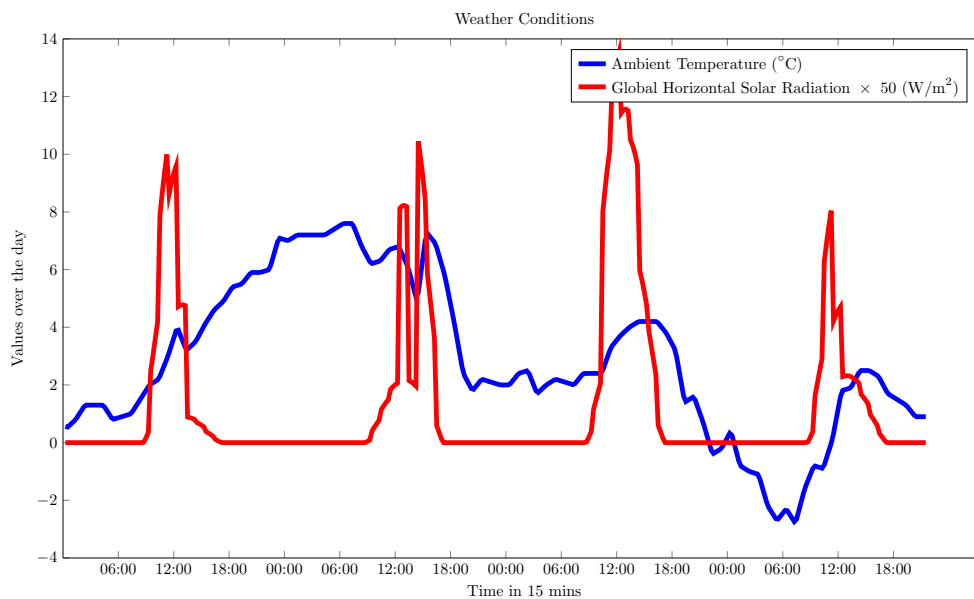
$$P_d^i = \frac{\# \text{ of occupied timesteps with } F_k^i \geq 10\%}{\# \text{ of occupied timesteps}}, \quad (3.19)$$

where F_k^i is the Fanger PPD value in office i at time k . Next, we define the comfort constraint C^i for each office i as:

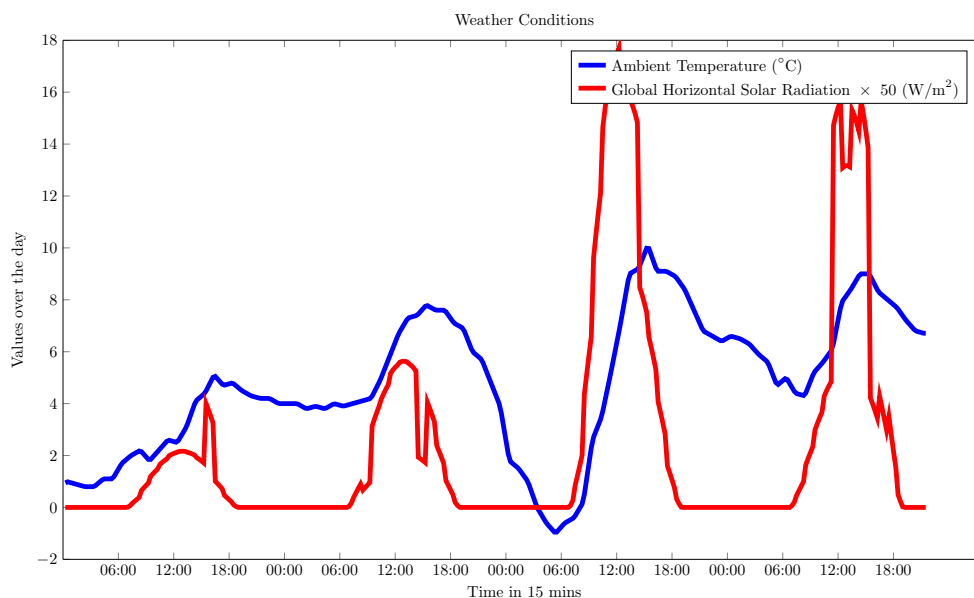
$$C^i = 1 - P_d^i < \alpha \quad (3.20)$$

Since one of the main goals of this experiment is to study both the efficiency of the control design approach in buildings with TABS and the thermal characteristics of ZUB building, different control design configurations are utilized, with $\alpha \in \{0.85, 0.90, 0.95, 1\}$.

A control design task is initiated for four winter (January 16th – January 19th) and four spring days (March 19th – March 22nd), characterized by a varying temperature profile and high solar gains (see Figure 3-38). The control design process is performed for different levels of constraint relaxation, using Bayesian Optimization (Algorithm 2.3.1) with the Expected Improvement criterion for the acquisition function (Eq. 2.25).



(a) Ambient temperature and global solar radiation during the test days of the January experiment



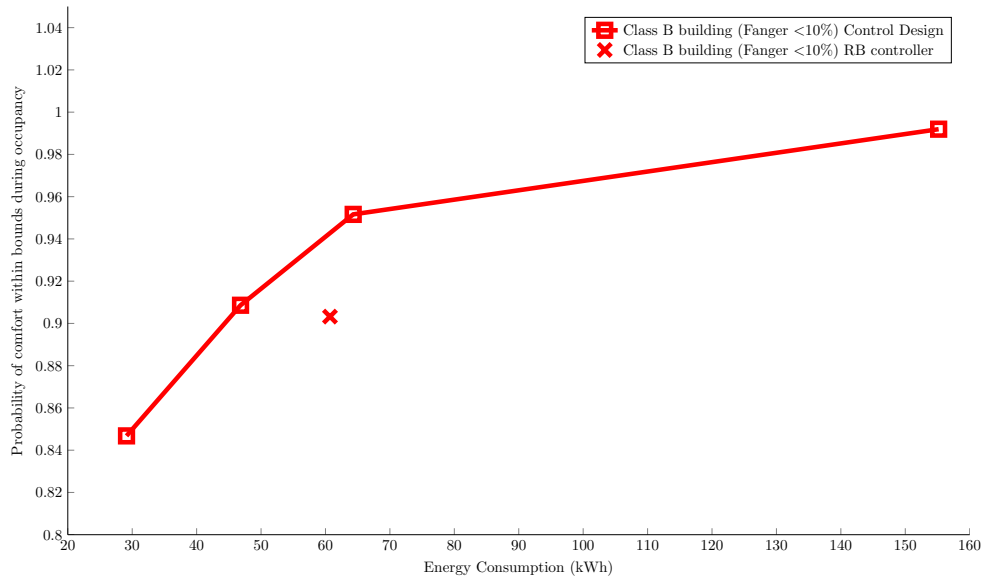
(b) Ambient temperature and global solar radiation during the test days of the March experiment

Figure 3-38: Weather data for the two simulation-based experiments on ZUB

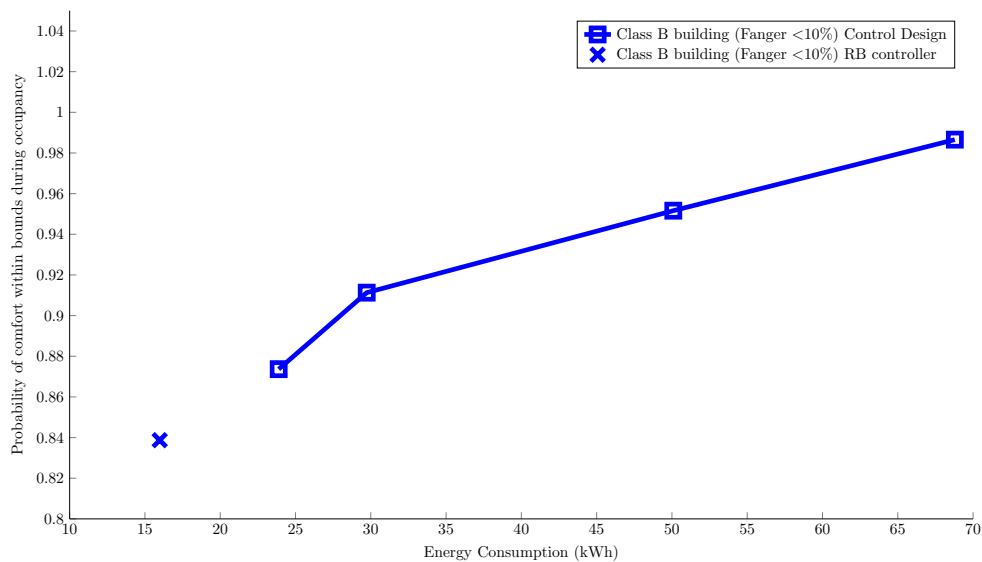
3.4.1.3 Results

An overview of the results for each experiment are shown in Figure 3-39. Here the y-axis represents the average probability of comfort for all three offices. A more detailed illustration of the energy consumption and probability of comfort for each office is shown in Figures 3-40 and 3-41.

In winter experiments, the optimized controllers manage to achieve similar comfort levels with the rule-based control strategy in all offices, while consuming less energy (approx. 22.8% savings), as shown in Figures 3-39(a) and 3-40(b). On the other hand, a significant amount of energy is required to ensure comfortable interiors (according to ISO 7730) with probability 1 at all times (see Figures 3-39(a) and 3-40(d)).



(a) Performance of ZUB under different levels of chance constraint relaxation, for the January Experiment



(b) Performance of ZUB under different levels of chance constraint relaxation, for the March Experiment

Figure 3-39: Performance of ZUB under different levels of chance constraint relaxation, for the simulation-based evaluations on ZUB building

A key insight on the efficiency of the proposed control design methodology is provided through

the analysis of Figure 3-40(a). Here, the simulation model has correctly identified that office 107 requires less heating compared to the other two offices, since it is on the first floor and surrounded by *heated* neighboring spaces, while offices 207 and 007 have cold boundaries with the external air and the ground respectively. Using this information, the control design process generates controllers that result in a control strategy that does not heat office 107, but the required level of comfort is achieved only through the effect of the internal and solar gains affecting the office.

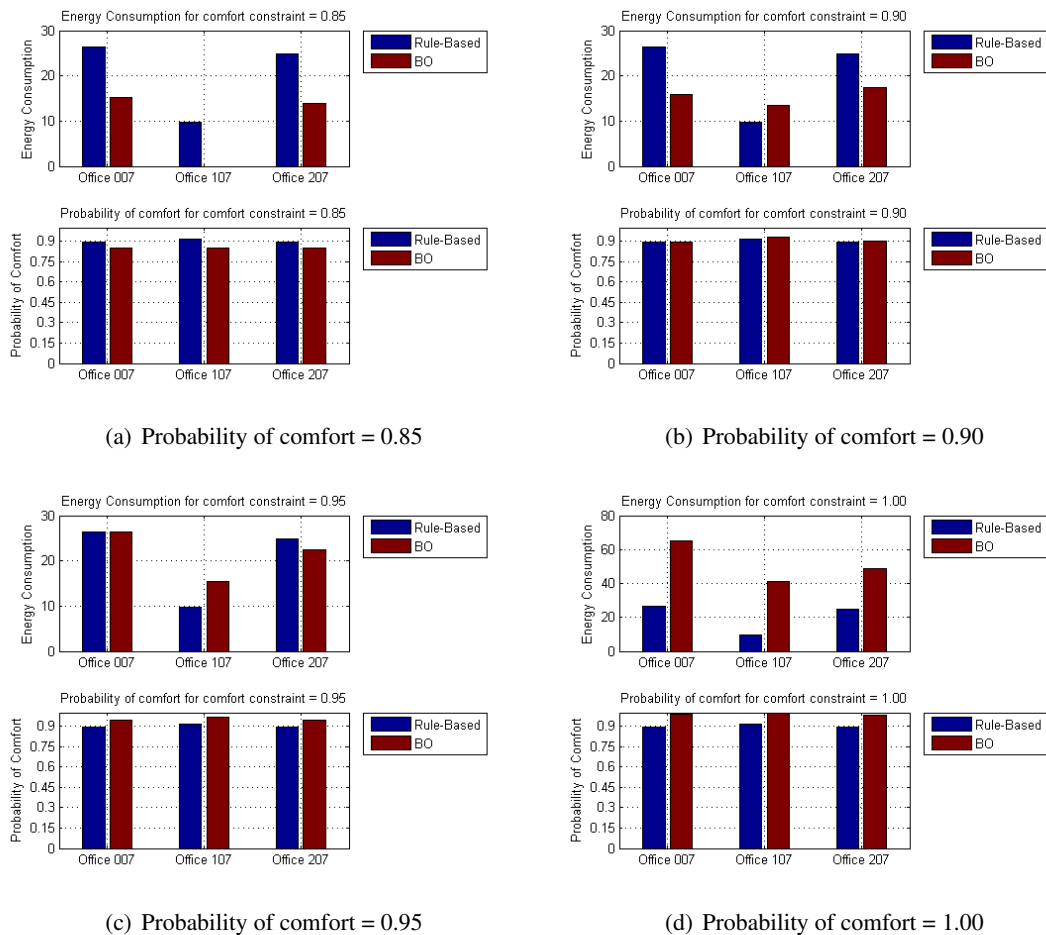


Figure 3-40: Performance of each office of ZUB under different levels of chance constraint relaxation for the January Experiment

In March experiments on the other hand, the rule-based controller is not capable of reaching the lowest comfort criterion in all three offices, as shown in Figure 3-41, thus the control design process generates controllers that consume more energy to ensure comfortable interior in all building spaces, as shown in Figures 3-39(b) and 3-41.

Note here that a formulation of the comfort constraint as in Algorithm 2.2.1, that is requiring the *average* constraint of all spaces to be satisfied could have led to high discomfort for some of the offices. This is obvious in the case of the rule-based controller, where the average probability of comfort is close to the lower bound (see Figure 3-39(b)), but offices 007 and 207 have high discomfort, as shown in Figure 3-41(a) for example.

The in-room conditions for the two test cases and for different constraint relaxation levels are shown in the remaining of the Section. Starting with January, the RB controller of the building ensures comfortable interiors for 90% of the occupied time, while leading to discomfort during the morning hours of the first and third controller days in all three offices, as shown in Figures 3-43, 3-44 and

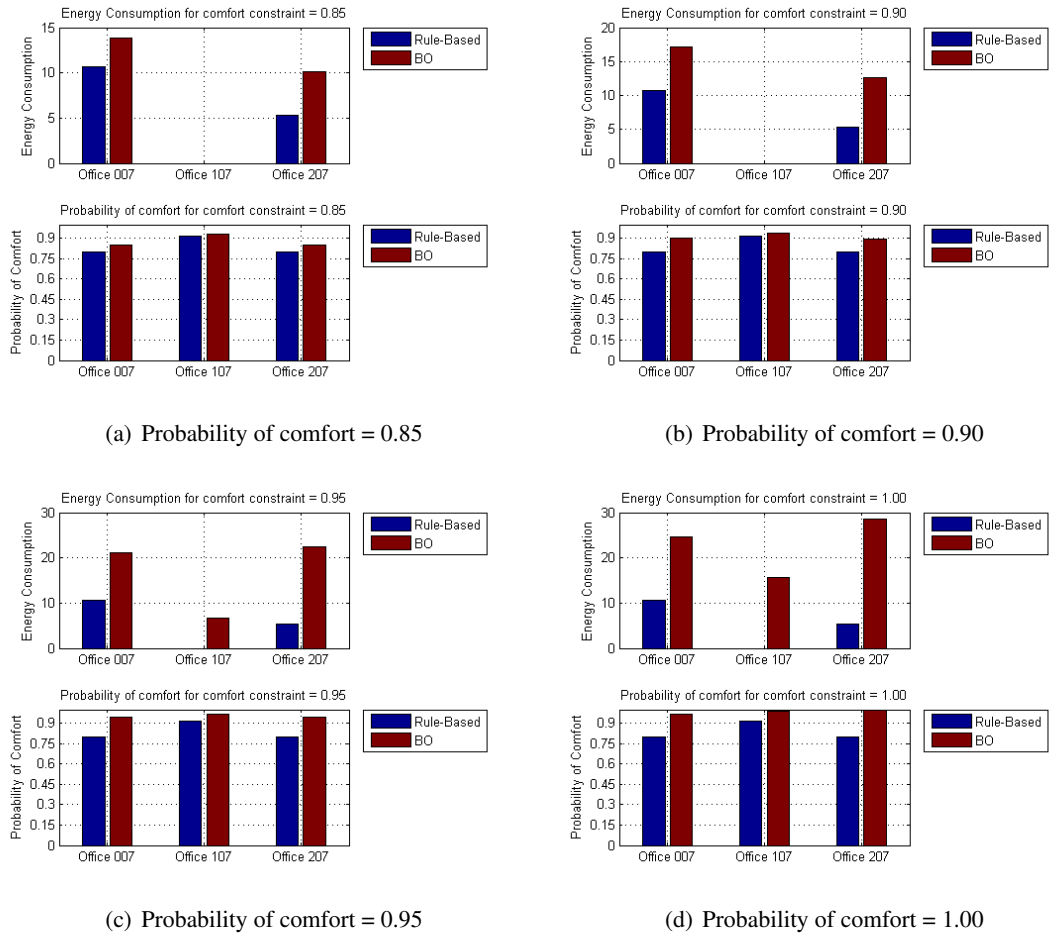


Figure 3-41: Performance of each office of ZUB under different levels of chance constraint relaxation for the March Experiment

3-45.

This means, that setting $\alpha = 0.85$ for the first Control Design task, we allow more discomfort compared to the RB controller (15% of the occupied time), leading to a control strategy with high energy savings. Here, the water temperature is set to the minimum allowed temperature for the entire control period (23°C as shown in Figure 3-42), but in all offices the setpoint during the Setback Mode is higher compared to the Occupancy Mode setpoint. This allows maintaining the offices heated during the night with less energy, while exploiting the internal and solar gains during the day for heating.

Setting $\alpha = 0.90$ means we allow the same amount of violations to the RB controller of the building (see Figure 3-40(b)). On the other hand, the Control Design process designs controllers that lead to a control strategy that saves 22.8% energy compared to the default building strategy, by lowering the hot water temperature after the first day (Figure 3-42) and discovering optimized schedules for the setpoints of the offices, as shown in Figures 3-43, 3-44 and 3-45.

In the case of $\alpha = 0.95$, an interesting property of the stochastic formulation of the constraint emerges. Here, the Control Design process generates controllers that lead to comfortable interiors for all offices on the first day (Figures 3-43, 3-44 and 3-45), by setting high water temperatures (Figure 3-42) and high setpoints during the morning hours of that day. On the other hand, the discomfort levels during the third day are similar as before. This is due to the formulation of the constraint, which requires a certain level of probability of comfort *for the entire occupied period*

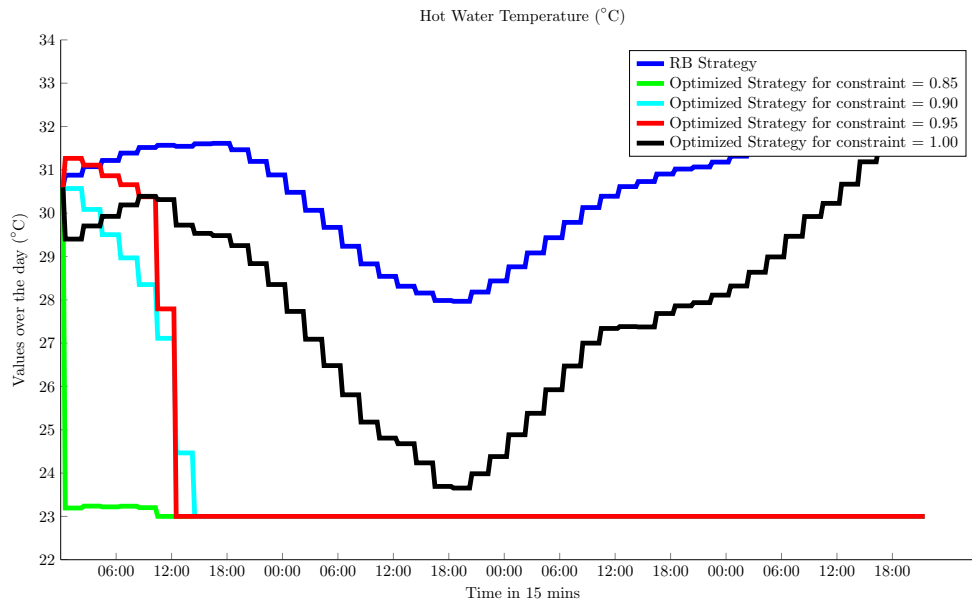


Figure 3-42: Hot water temperature under different levels of chance constraint relaxation, for the January Experiment

(four days in our case), thus not forcing “even” comfort levels in all days.

Finally, for $\alpha = 1.00$, the water temperature follows similar trend with the temperature profile generated by the RB controller (Figure 3-42) and we have higher setpoints in all offices, as shown in Figures 3-43, 3-44 and 3-45. Of course this strategy corresponds to significantly higher energy consumption.

A close look in the operation of the blinds in all offices and for all comfort relaxation levels reveals that the blinds become active (i.e. close) around noon for most days and for all offices to prevent overheating.

For the March case, the RB controller manages to maintain comfort in office 107, but leads to high discomfort in offices 207 and 107, as shown in Figures 3-47, 3-48 and 3-49.

Here, for $\alpha = 0.85$, the Control Design process generates controllers that set the water temperature in the lowest allowed level as for the Winter case (see Figure 3-46). Office 107 (as with the RB case) requires no heating, but for offices 207 and 007 higher setpoints during the night are required to achieve comfortable interiors (Figures 3-47, 3-48 and 3-49) — a strategy that leads to higher energy consumption in these two offices compared to the default controller of the building (Figure 3-41(a)).

For $\alpha = 0.90$, office 107 still requires no heating. Here, as with the Winter case, the water temperature is high during the morning hours of the first day (Figure 3-46) and, combined with the setpoint levels of offices 207 and 007 the strategy leads to less comfort violations, especially for the first day.

For $\alpha = 0.95$, the schedule of the water temperature follows the same pattern to the previous case (Figure 3-46), but the setpoints of all offices are significantly higher, as shown in Figures 3-47, 3-48 and 3-49. For $\alpha = 1.00$, the resulting control strategy is quite similar, since the water temperature drops to the lowest limit after the second day, while offices have high setpoints to ensure comfortable interiors, especially during mornings.

Finally, note that in this case the blinds are activated less times compared to the Winter experiment. Here, the blinds are closed around noon for all offices during the last two days to prevent overheating, since these days are characterized by high solar gains (see Figure 3-38(b)). In contrast, during

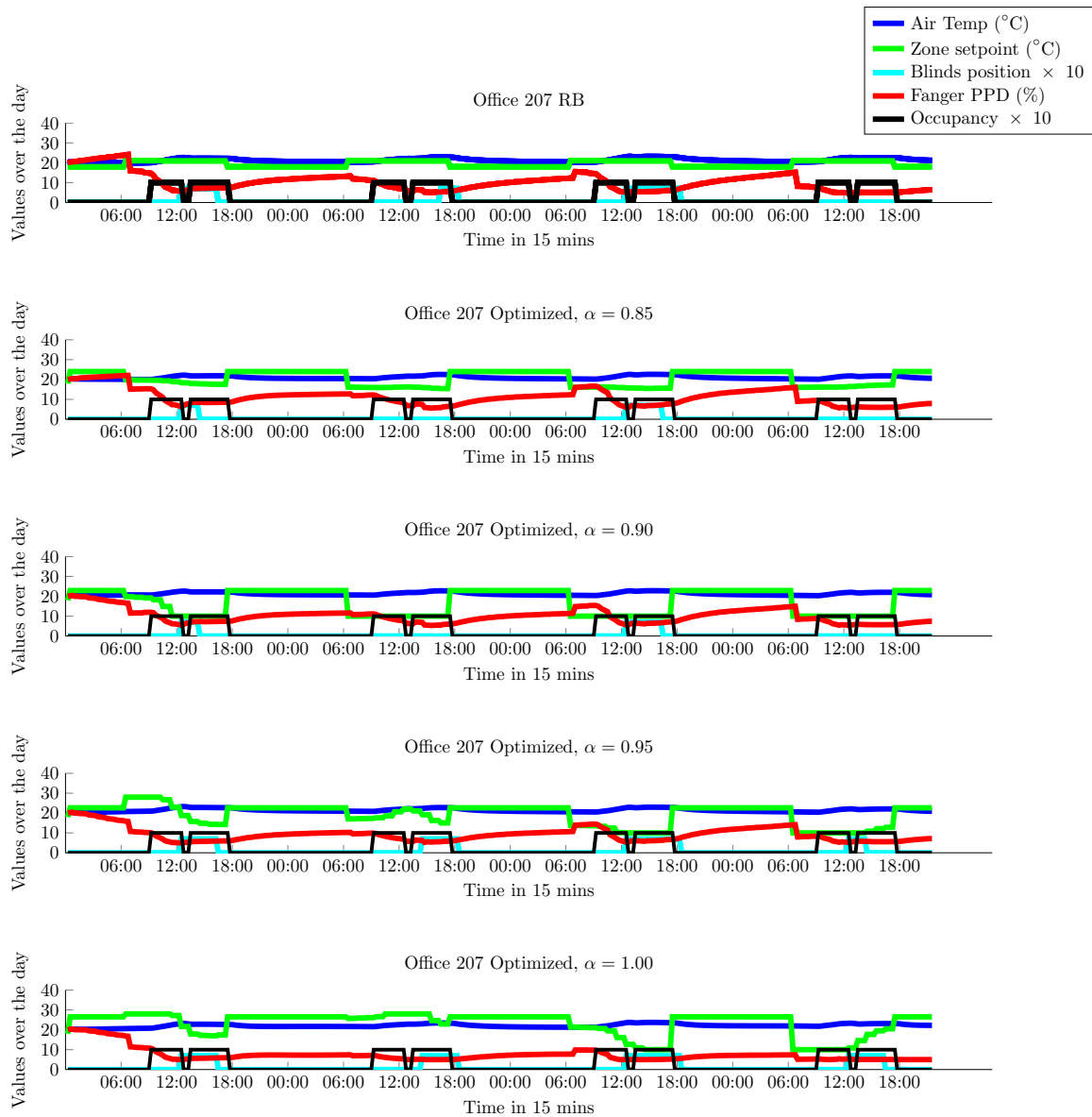


Figure 3-43: Indoor climate conditions for Office 207, under different levels of chance constraint relaxation, for the January Experiment

the first two days the blinds remain mostly inactive to allow exploitation of the heat gains from the sun.

3.4.1.4 Conclusions

In this set of experiments, the control design process has managed to effectively regulate the trade-off between energy consumption and user comfort – compared to static rule-based controllers that have limited flexibility – by exploiting information on the *future* thermal state of the building from the high-fidelity simulation model of the building, using occupancy and weather forecasts. This is achieved by *controlling both distribution and emission systems of the building, as well as the blinds in each office, in a holistic and synergistic manner.*

On the other hand, the effect of the complexity of the control functions becomes apparent. Here, more complex control functions (e.g. using a linear controller function during the Setback Mode

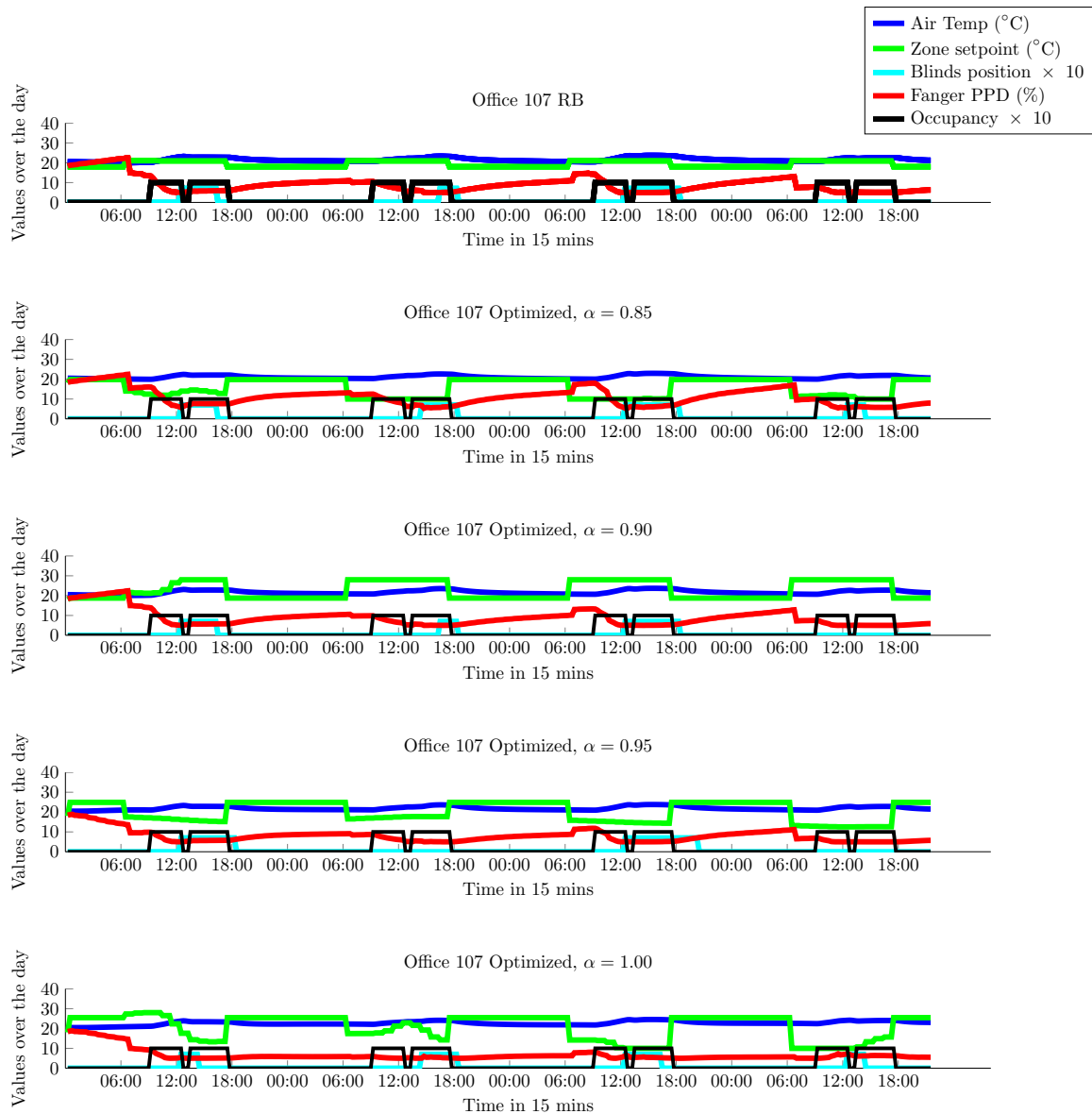


Figure 3-44: Indoor climate conditions for Office 107, under different levels of chance constraint relaxation, for the January Experiment

too in the ZUB building experiment) that provide higher flexibility could have led to more energy savings, but come with higher computational load, since they require more iterations of the simulation-based control design algorithm.

Finally, the slow dynamics of the building are revealed, which are typical for heavy buildings equipped with TABS (Gwerder et al., 2008, 2009). In such buildings if during pre-heating (i.e. during the Setback Mode) less or more heating is applied to the room, this systematically leads to either comfort problems in the morning due to under-heating either to over-heating around noon (especially for sunny days) respectively, since it is very difficult to compensate for the faulty control strategy during the day. This means that in such buildings frequent re-design of the controller is not crucial; instead what is important is to correctly account for the effect of the *predicted* solar and internal gains in the future thermal state of the building.

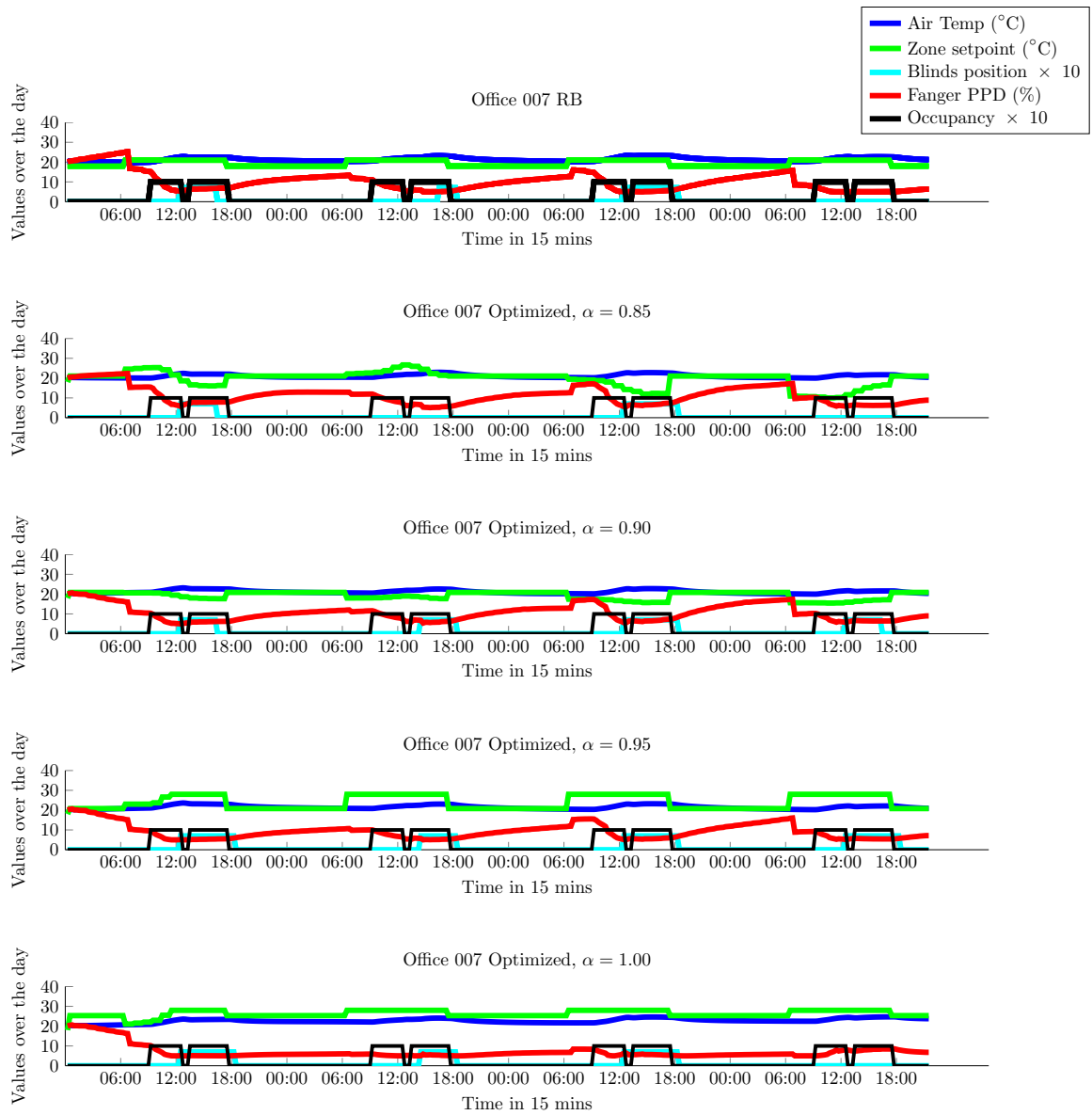


Figure 3-45: Indoor climate conditions for Office 007, under different levels of chance constraint relaxation, for the January Experiment

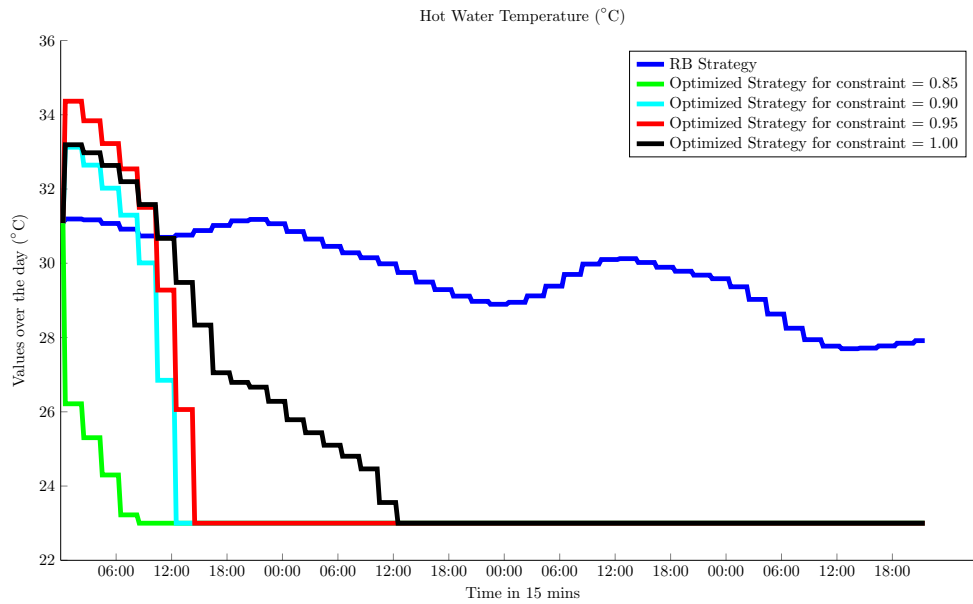


Figure 3-46: Hot water temperature under different levels of constraint relaxation, for the March Experiment

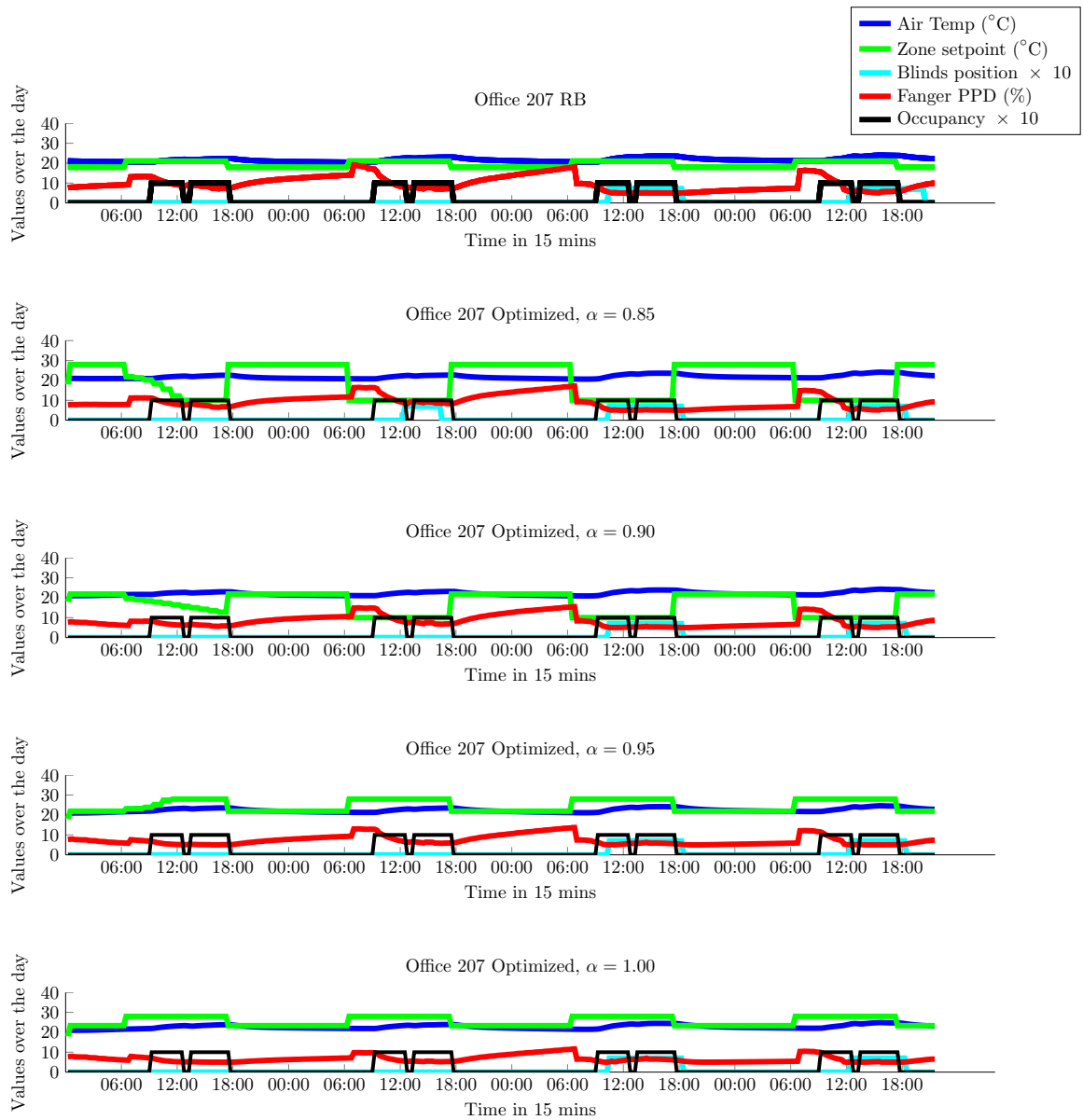


Figure 3-47: Indoor climate conditions for Office 207, under different levels of chance constraint relaxation, for the March Experiment

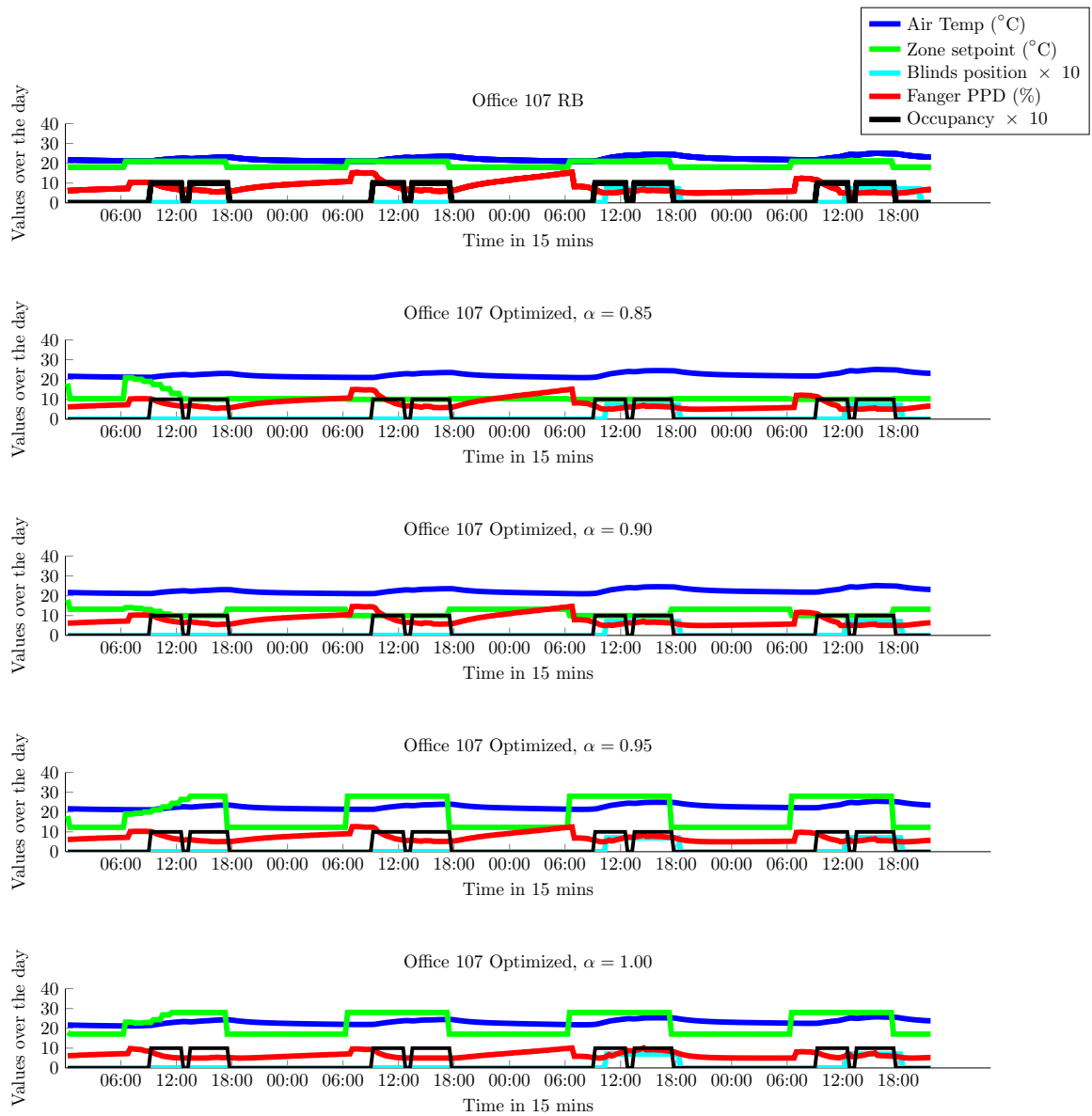


Figure 3-48: Indoor climate conditions for Office 107, under different levels of chance constraint relaxation, for the March Experiment

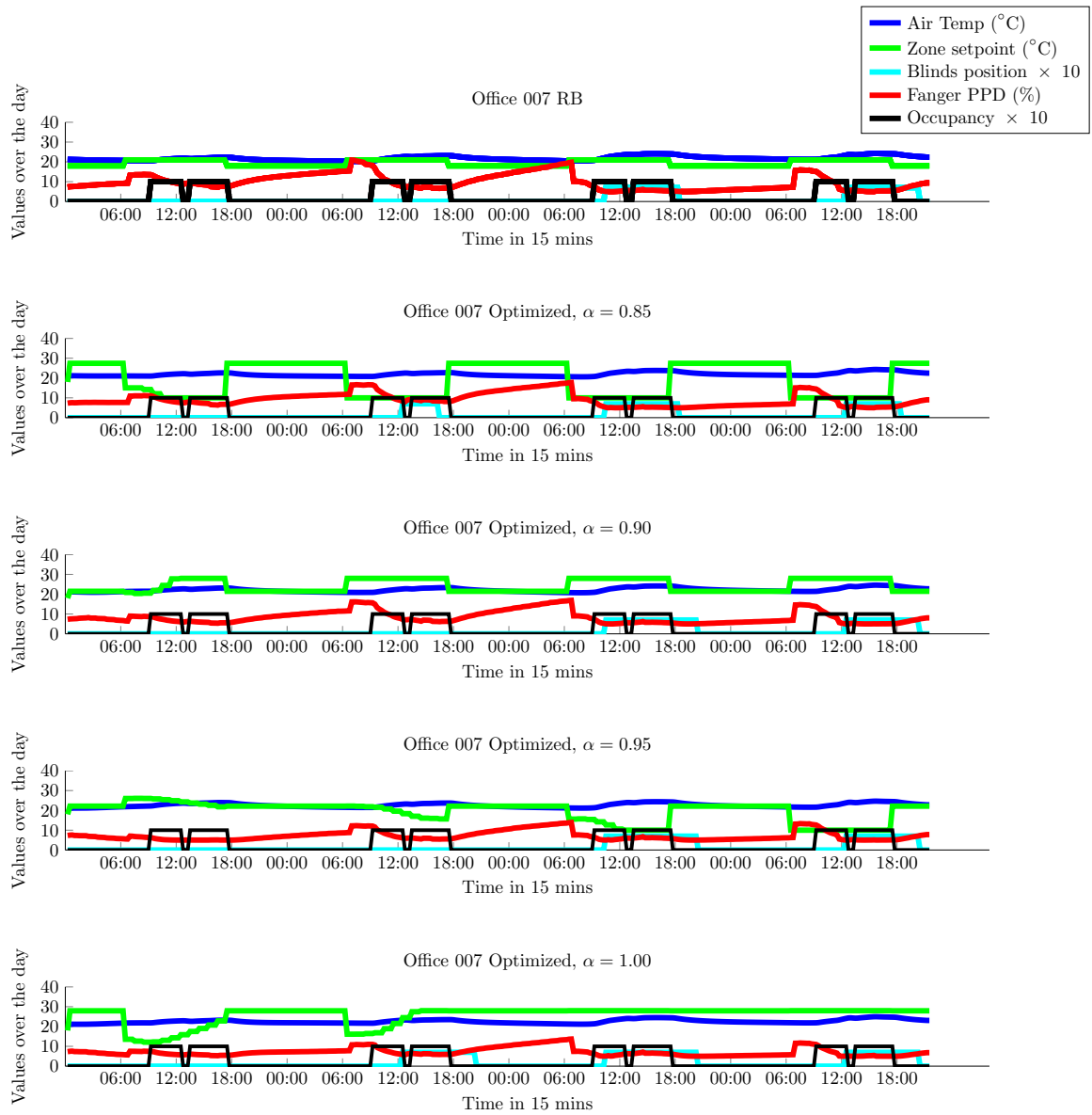


Figure 3-49: Indoor climate conditions for Office 007, under different levels of chance constraint relaxation, for the March Experiment

3.4.2 Real Experiments in ZUB Building

After completing the simulation-based evaluations for ZUB building and getting an understanding of the building and HVAC dynamics, a set of real heating experiments is performed in ZUB during the winter of 2015 – 2016. Here, two types of controllers are deployed: i) a knowledge-based controller and a model-based controller.

The knowledge-based controller follows the same logic as the baseline control strategy, i.e. a heating curve is calculated based on the external temperature and a building setpoint remains constant throughout the experiment. The difference is that the building setpoint and the heating curve are adjusted to save energy compared to the baseline strategy. The model-based controller is designed using the Bayesian Optimization algorithm (Algorithm 2.3.1) and following the MPC paradigm.

The comparison between the two control approaches will indicate whether there are tangible benefits from applying a model-based control design solution over hand-tuned rule-based controllers, designed using not only expert knowledge but also knowledge about the dynamic behavior of the building.

The experiments presented here were performed within the BaaS FP7 project and the communication with the building was achieved through ICT infrastructure developed within BaaS, thus we use specific naming convention (BaaS knowledge-based and BaaS model-based controllers) in the illustration of the results. An overview of the ICT platform architecture is shown in Figure 3-50.

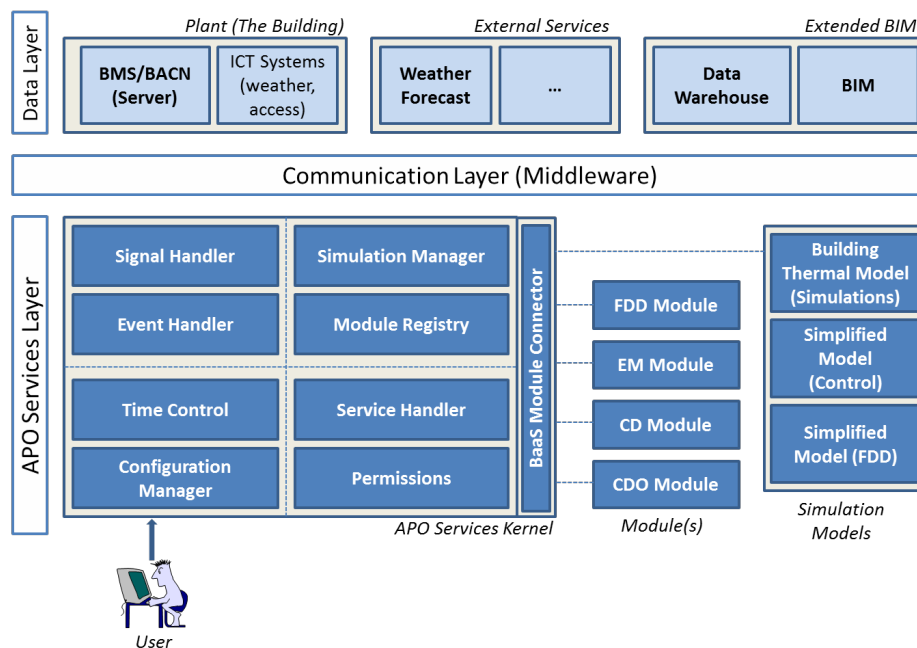


Figure 3-50: BaaS Platform – Core Components (Rovas et al., 2014b)

3.4.2.1 Experimental Setup

For designing the knowledge-based controller, we build upon the baseline strategy. Here, the baseline controller uses a heating curve to generate a new water temperature setpoint every one hour, and maintains the building setpoint at 21 °C constantly. The input of the heating curve is the 24-h running average of the outside air temperature. By reviewing the building inefficiencies using historical data we know that this strategy can lead to overheating of the first floor, especially for cold, sunny winter days. Thus, we have designed a different heating curve that generates lower water

temperatures for higher outside air temperatures, compared to the baseline strategy. In addition, we set the building setpoint to a lower value (19.8 °C) compared to the baseline strategy.

For the model-based control design on the other hand, the sending water temperature is controlled by the following heating curve:

$$u_{CD,k}^{HW} = \theta_1^{HW} T_k^{amb} + \theta_2^{HW} S_k + \theta_3^{HW} \frac{1}{N} \sum_{i=1}^N T_k^i + \theta_4^{HW}, \quad (3.21)$$

with T_k^{amb} the 24-hour running average outside air temperature, S_k the 2-hour running average of the global horizontal radiation and T_k^i the 24-hour running average of the zone air temperature of zone i , all calculated at time k . The water temperature setpoint is limited in the interval $u_{CD,k}^{HW} \in [23, 38]^\circ\text{C}$.

In contrast to the simulation-based evaluations of the previous Section, in the real building it is not possible to control the setpoint of each office individually. Instead, the base setpoint for the whole building, is calculated as:

$$u_{CD,k}^{s,i} = \theta_1^{s,i} T_k^{amb} + \theta_2^{s,i} S_k + \theta_3^{s,i}, \quad (3.22)$$

with T_k^{amb} the 24-hour running average outside air temperature and S_k the 2-hour running average of the global horizontal radiation, all calculated at time k . During Occupancy Mode the setpoint is limited in the interval $[19, 25]^\circ\text{C}$. The final setpoint in each office is calculated by adding the setpoint offset set by the users in each room to the base setpoint of the whole building.

Note here that for the winter experiments we do not control the blinds of the building, a decision made due to the lack of occupancy sensors in the offices. Since there is no way of knowing when an office is occupied, we would be forced to utilize the building occupancy schedule (8:00 – 17:00) for the blinds control configuration. This implies that even if an office is empty, the blinds will be operated in a proper manner to preserve visual comfort, i.e. blocking the solar radiation when required. On the other hand, if an office is empty, we would like to harvest as much solar radiation as possible for two reasons: i) use less energy to heat it up, assuming that occupants will arrive later on the day (e.g. after a lunch break); and ii) to aid heating the neighbouring offices using less energy.

3.4.2.2 Formulation of the Control Design Problem

The task for the control design process is to minimize the total energy consumption of the building, while maintaining comfortable interiors according to Fanger index, by discovering optimized parameters for the controllers of the building (i.e. $\theta \in \mathbb{R}^7$). Note here that since the ground floor hosts conference rooms and a small kitchen, our task is to maintain comfort on the office located on the first and second floors. Following the ISO recommendations for existing buildings of energy class B – like ZUB – an acceptable limit for the Fanger PPD is 10%. In the experiment presented here, we formulate the thermal comfort constraints as stochastic constraints, as before. First, we define the probability of discomfort P_d^i for each office i as follows:

$$P_d^i = \frac{\# \text{ of occupied timesteps with } F_k^i \geq F^l}{\# \text{ of occupied timesteps}}, \quad (3.23)$$

where F_k^i is the Fanger PPD value in office i at time k and F^l is the Fanger PPD value. Next, we define the comfort constraint C^i for each office i as:

$$C^i = 1 - P_d^i < \alpha. \quad (3.24)$$

Due to the inability to control the setpoint of each floor individually, it is impossible to achieve

similar comfort conditions on the first and second floor, since the top floor is exposed to the external weather conditions, while the middle floor is surrounded by heated offices. Thus, the comfort-related requirements from an optimized controller would be to maintain comfortable interiors on the offices of the second floor, while avoiding overheating in the offices of the first floor. In order to assist towards this direction, and in cooperation with the maintenance team of the building, we set $F^l = 10\%$ for the constraints of the first floor and $F^l = 15\%$ for the constraints of the second floor. Finally, we set $\alpha = 0.1$ for both constraints.

3.4.2.3 Results

The knowledge-based controller is applied from 10/12/2015 to 21/02/2016, while the model-based controller from 22/02/2016 to 15/03/2016. For both strategies, a new value for the inlet water temperature is calculated every one hour. For the model-based control design approach, a new set of optimized control parameters (θ^*) is designed and communicated to the building every 2.5 hours, while the prediction horizon is set at three days and the warming-up period at 20 days, due to the high thermal mass of the building.

The behavior of the baseline controller is shown in Figure 3-51. It is characterized by a smooth control strategy, due to the 24-hour averaging of the external temperature and from constant building setpoint. The peak on Monday morning is due to the high-water temperature entering from the district network on the beginning of the week, which causes a spike on the inlet water temperature sensor.

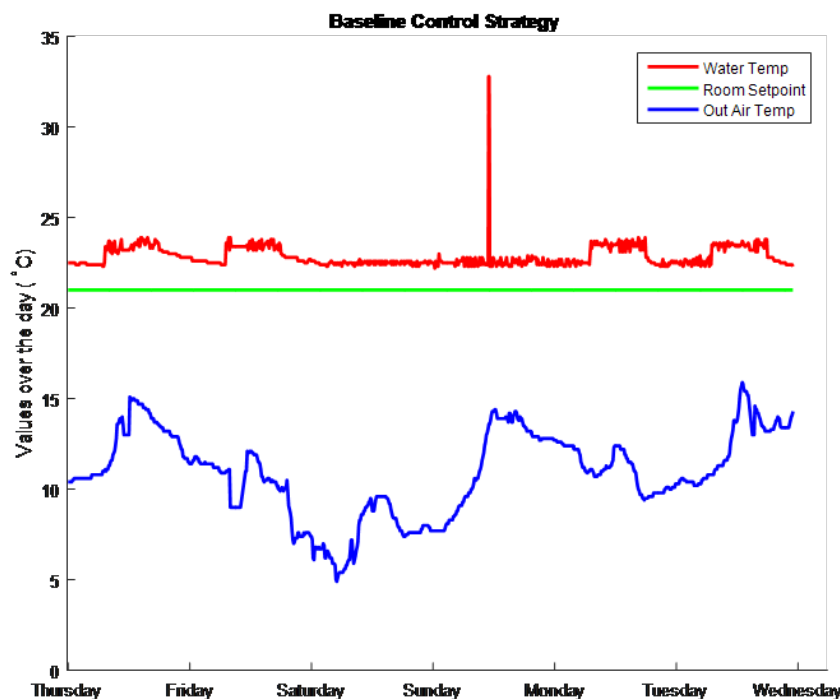


Figure 3-51: Baseline control of ZUB heating distribution system (12/11/2015 – 17/11/2015)

Figure 3-52 shows similar behavior for the knowledge-based controller too. Here, the heating curve generates lower supply temperature values for the TABS compared to the baseline controller, while the baseline setpoint for the building is reduced by 1.2°C.

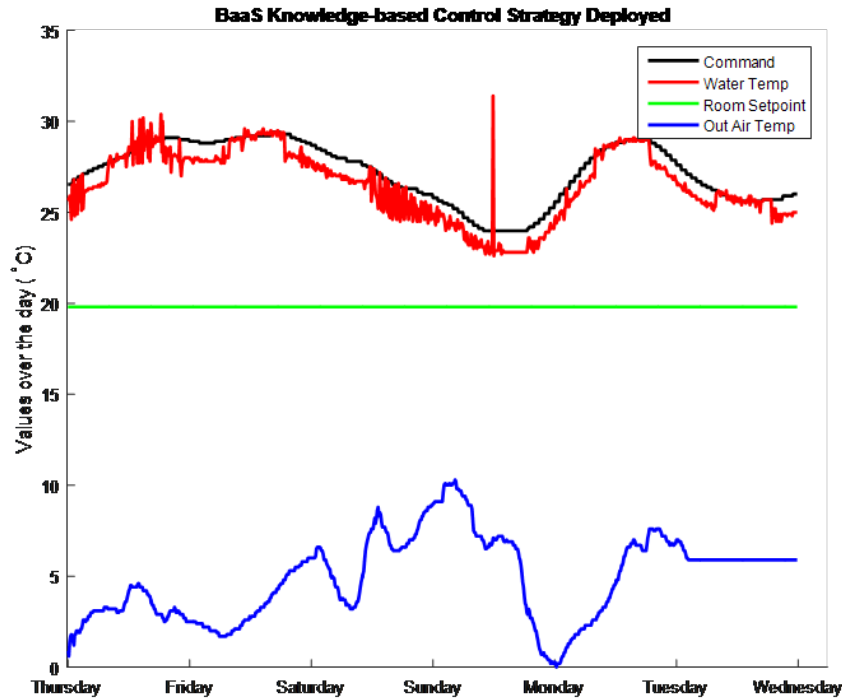


Figure 3-52: Knowledge-based control of ZUB heating distribution system (10/12/2015 – 15/12/2015)

The controller generated by the model-based control design process on the other hand, exhibits radically different behavior, as shown in Figure 3-53. The building is systematically pre-heated on Sunday evening up until Monday morning and then it free-floats for the rest of the week (or some small amount of heating is provided if needed), utilizing the internal gains from the equipment and the occupants, as well as solar gains, for preserving comfortable interiors. This strategy exploits the high thermal mass and air tightness of the building and was discovered automatically by the control design algorithm.

The energy savings compared to the baseline controller for the period of the experiments are evaluated within BaaS project following the IPMVP protocol (Efficiency Evaluation Organization, 2010) and are calculated at (Martin et al., 2016): 11% savings for the knowledge-based controller and 33% savings for the model-based controller for the entire building. Regarding the comfort-related efficiency of the two controllers, Figure 3-54 illustrates the percentage of occupied time a space was in a certain comfort class in offices 106 and 206 of ZUB, for the baseline, the knowledge-based and model-based control strategies, taking into account all occupied periods and the comfort class classification of ISO 7730, using Fanger PMV index. We have to clarify here that the evaluation of thermal comfort is performed only in these two offices, since they are equipped with the proper sensing infrastructure that allows calculation of the actual values of Fanger during the experiment, as well as in the baseline period. Complementing this representation, Figure 3-55 illustrates the same information, but not as time-fractions in a comfort class, but using the Fanger PMV values throughout the days of the experiments. Here, every line is a daily “trajectory” of Fanger PMV values, PMV values greater than zero implying users feeling warm, while PMV values lower than zero that users feel cold.

Both Figures 3-54 and 3-55 lead to the same results. Here, in the baseline strategy the facility management team decides to allow systematic overheating on the first floor of the building (as rep-

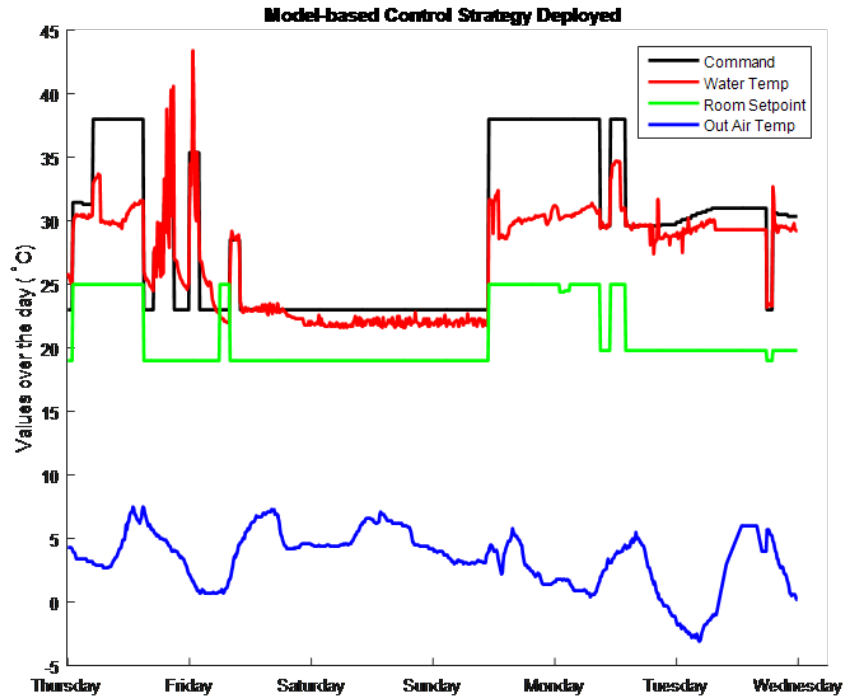


Figure 3-53: Model-based control of ZUB heating distribution system (03/03/2016 – 08/03/2016)

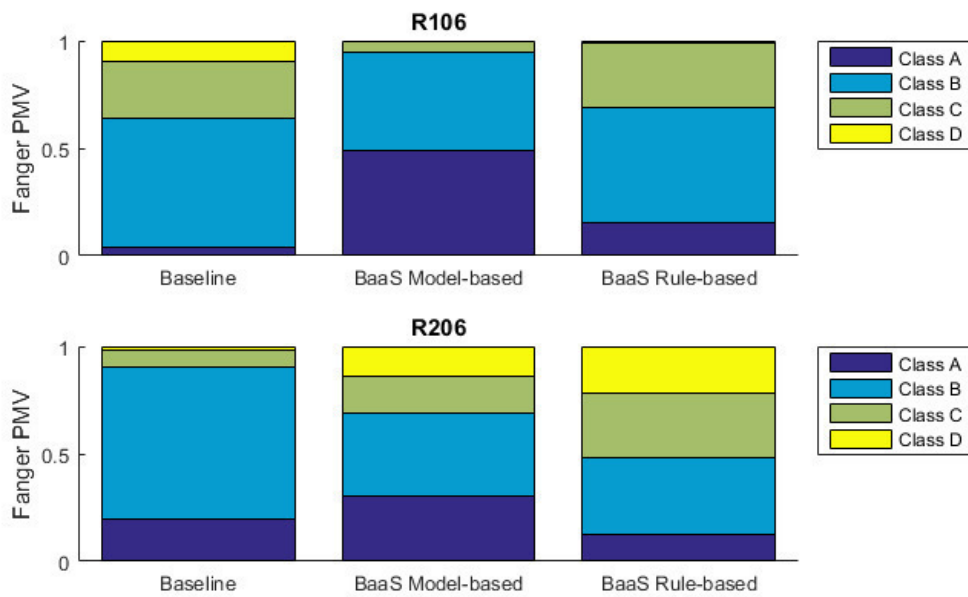


Figure 3-54: Thermal Comfort sensation according to ISO 7730 comfort classes for ZUB building during winter — cumulative evaluation

resented by Office 106), in order to maintain acceptable comfort conditions on the second floor (represented by Office 206). This is illustrated more clearly on Figure 3-54: here the baseline strategy causes Room 106 to be in comfort class C for a significant fraction of time, due to overheating, while Room 206 has good comfort properties. For the knowledge-based controller, even though the designed controllers exhibit good behavior and lead to energy savings, their inability to properly

account for all the predicted and un-predicted disturbances (e.g. weather conditions, occupancy, setpoint tracking errors, etc.) leads to higher discomfort levels compared to the baseline control strategy.

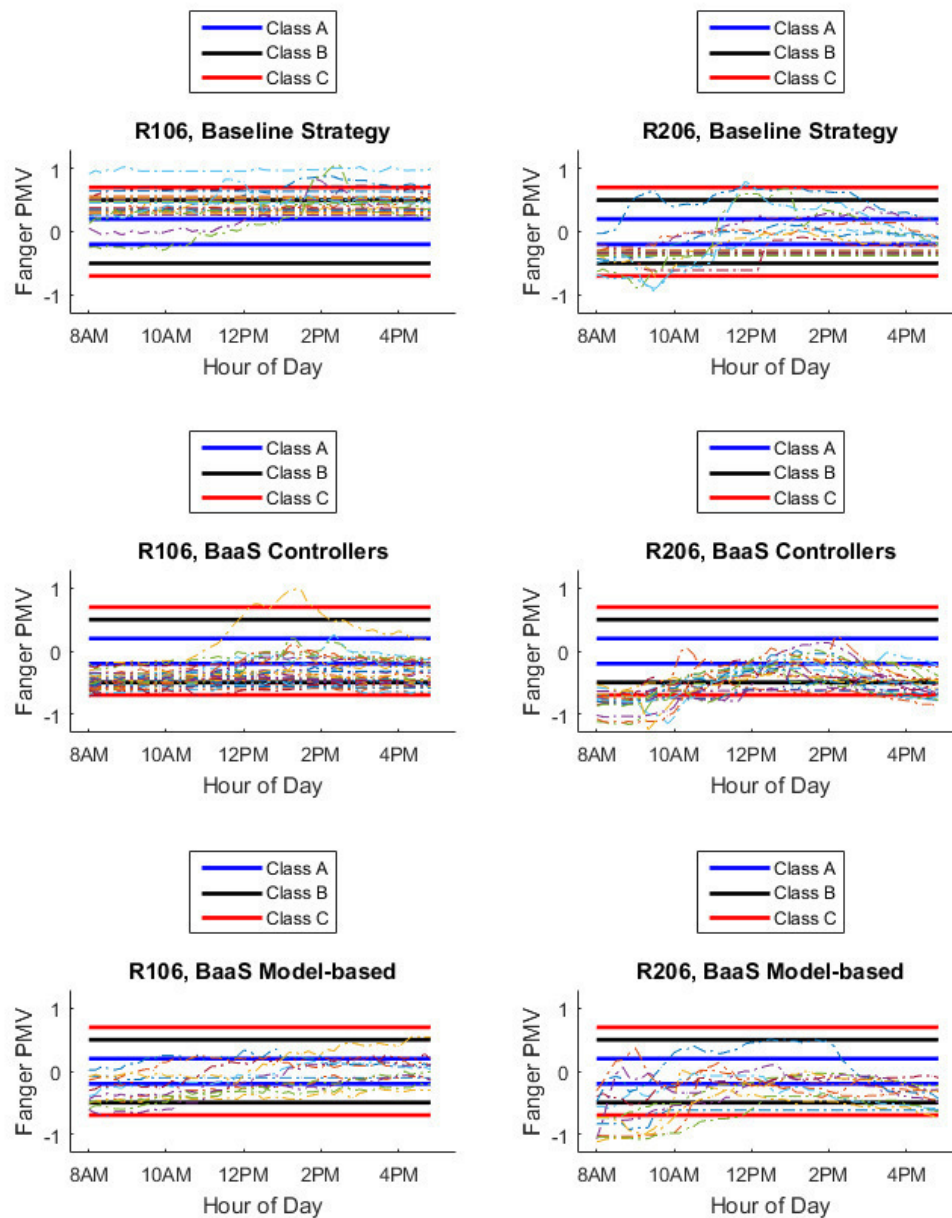


Figure 3-55: Thermal Comfort sensation according to ISO 7730 comfort classes for ZUB building during winter — daily illustration. The solid lines indicate the Fanger PMV limits for comfort classes A, B and C and each dashed line represents the *measured* PMV values for one day of the experiment.

For the model-based control design strategy, as discussed in the previous Section, we set the PMV limit in the ± 0.5 region (comfort class B) for the first floor offices and the PMV limit to the ± 0.75 region (comfort class C), while also allowing some discomfort for a small fraction of time. The

resulting control strategy, leads to Class C comfort levels for some amount of time in Room 206, due to under-heating, and Room 106 has satisfactory comfort conditions. The discovered solution yields significant energy savings.

Even though the model-based control design strategy managed to discover an energy-efficient and comfort-preserving strategy, some stability problems have been noticed throughout the experiment. First of all, the ICT infrastructure was not robust for the entire duration of the experiment, since in several occasions the values for the sensor measurements were not logged. As a result, the controllers were receiving false 24-hour measurements (usually lower if the platform was down during the night without the facility management team noticing), leading to some mild overheating for few days during the model-based control experiment (see the final row of Figure 3-55).

In addition, as shown in Figure 3-54), there is some heating in Friday night, when it is not required. This is caused by the limited expressiveness of the linear controllers, along with the three-day prediction horizon. Here, the algorithm generates a strategy that will be able to cover the heating demands on Monday morning, but due to the linear nature of the controllers, the designed control parameters result in heating the building on Friday night too. This effect was addressed by manually setting the heating curve and the building in the lowest allowed values (23 °C and 19 °C respectively) from Friday afternoon to Saturday noon and then the model-based control strategy would take over again.

3.4.2.4 Conclusions

A real experiment is performed in ZUB building using: i) a knowledge-based controller designed taking into account the dynamics of the building and the HVAC system; and ii) a model-based controller designed using Bayesian Optimization and following the MPC paradigm. Both controllers achieved significant energy savings compared to the baseline controller of the building, but the knowledge-based controller compromised comfort in several days. This is because a static, rule-based controller is unable to properly account for all the predicted and un-predicted disturbances (e.g. weather conditions, occupancy, setpoint tracking errors, etc.), where as the model-based control design approach, utilizing the thermal simulation model of the building and the automated control design setup, was able to make informative decisions and control the building in an efficient manner.

THIS PAGE INTENTIONALLY LEFT BLANK

Chapter 4

Conclusions and Future Work

In the present thesis, we have developed a framework to deliver optimized and integrated operation of all energy-influencing components of a building that include generation, distribution and emission elements. First, a set of parametric control functions (controllers) are identified for each emission/distribution/generation system, following guidelines available in international standards. Next, given (weather, occupancy, etc.) forecasts for a predefined time window, say three days, a surrogate-based stochastic optimization algorithm is used to create candidate controller parameters to be applied to the building, and a detailed thermal simulation model is used to evaluate these candidate solutions. The evaluation is performed on the basis of a defined cost function and a set of (visual, thermal, air-quality, etc.) comfort constraints. The final, improved controllers are communicated to the building-side and are applied to the building.

An important aspect investigated in this thesis, which is also evident on the experimental results, is the topic of (thermal) comfort-based control. A discussion on energy efficiency seems untimely when discussed without any reference to comfort as there is a clear trade-off between comfort and energy. Having methods that allow the automated selection of building operation to desired levels of comfort is both desirable and can have significant implications. On the other hand, in existing state of the art, comfort is often synonymous to the temperature in the building zones being maintained within certain (prescribed) limits. As we investigate in the thesis this assumption while true in certain cases, in many cases is not sufficient to ensure actual comfort for the building occupants, with detrimental effects to health and productivity (when office buildings are considered). In the proposed approach, we define comfort based on ISO 7730, which supports the definition and use of the Fanger index which captures, among other parameters, the influence of air and radiant temperatures along with humidity.

The developed framework has been evaluated on a set of experiments conducted under both simulated and real conditions. These experiments indicate that the designed controllers can lead to improved building operation, with the efficiency of the methodology depending on the accuracy of the simulation model, the complexity of the controller functions and the quality of the initial controller to be optimized.

Apart from results illustrating the performance of the proposed methodology, the real-building experiments conducted helped to shape a clear view on the properties and best application practices of model-based control algorithms in buildings. The main conclusion is that there has to be a clear separation between low-level and supervisory-level control. The best strategy is to determine the supervisory control strategy to be applied in the building and then re-visit the low-level controllers and perform targeted adjustments in order to support the higher-level logic. Attempting to optimize all low-level (e.g. PID gains of valves) and supervisory-level (e.g. operation schedules) control parameters at the same time, can lead to sub-optimal control strategies or even to safety problems

of the building sub-systems.

Regarding supervisory-level control, open-loop controllers (e.g. controllers that generate actions based on the time of day) often fail to capture the effect of very important features (like the solar radiation in a specific day or the actual in-building thermal conditions) and thus can lead to energy- or comfort-related problems, such as overheating. Closed-loop control schemes on the other hand, that utilize sensor feedback, can account for most of the influencing factors/disturbances affecting the building (like weather conditions) and adjust the operation of the controllable elements of the building in order to compensate for their effect.

A counter-intuitive conclusion from the model-based control design process applied in ZUB building is that frequent dynamic updating of the control strategies may not be a critical aspect of an efficient BMS. Especially for buildings with slow dynamics, what is important for the control algorithm is to identify a set of dominant features (such as the solar radiation in the case of ZUB) and adjust the parameters of all building controllers properly. This can lead to a scheme where a specific controller selected from a set of pre-defined control parameters is loaded to the BMS every day. The selection can be based on measured exogenous (e.g. daily weather predictions) and in-building (e.g. estimation of the thermal loading of the building) features. This claim is also supported by the resulting control strategy generated by the model-based control design process in ZUB (and can also be generalized for most buildings with good construction and equipped with HVAC systems with high time-constant). This strategy, in essence, attempts to discover an optimal pre-heating schedule for the entire building. This makes sense, since any change in the control actions (e.g. changing the heating setpoint of an office) has no effect in the indoor climate conditions of the offices in real time, due to the time-delay of the actuating system (TABS). Thus, the best strategy is to pre-heat the building to ensure comfortable interiors early in the morning, but stop heating in time to avoid over-heating in the afternoon.

The analysis on the control properties of the previous paragraph is also a valid argument on why we did not utilize weather predictions as inputs to the controllers designed in our experiments, but used historical data instead. First of all, the use of accurate weather predictions is critical only in the control of slow-reacting buildings (like ZUB), where accurate predictions on e.g. solar radiation can help to determine the optimal pre-heating schedule of the building. In addition, we have verified during the deployment that the quality of the weather predictions can be very low, thus the estimation of the micro-climate in the area of each study building is a strong pre-requisite towards utilizing weather predictions in the control strategy. Finally, another reason is the desire to have future collaboration with building automation solutions providers and encapsulate the designed control parameters in embedded hardware controllers. In this case, there are only few product lines by specific companies with the ability to provide access to external weather forecast services.

Another important aspect of the deployment analysis, is that we have verified the suggestions provided in EN 15232 and ISO 16484 regarding BAC functionalities. Here, indeed controlling all layers of the building systems (generation/distribution/emission) in a coordinated manner can lead to improved building performance compared to control solutions restricted to specific building sub-systems. In addition, higher flexibility and richer collection of controllable elements can lead to more efficient control strategies. The latter has been evident in the case of ZUB, where there was only one setpoint applied to the entire building, preventing us from controlling the offices of the first and second floors independently.

Due to the trade-off between energy consumption and thermal comfort, it is crucial to be able to represent (or predict) thermal sensation of the building's occupants under different HVAC operation strategies — from all available comfort preserving strategies the one that requires the least amount of energy should be preferred. This suggests that the ability to calculate comfort indices such as Fanger, or even the ability to build personalized comfort models for the building occupants (Baker and Hoyt, 2016; Daum et al., 2011; Ghahramani et al., 2014, 2015; Lee et al., 2017; Malavazos

et al., 2014; Romero et al., 2016) should be features of an intelligent BACS.

In addition, the entire deployment and assessment phases of the BAC functionalities have highlighted the significance of TBM functionalities. Fault Detection analytics are crucial for the proper operation of the building, as well as for exploiting the full potential of any advanced control algorithms, since there is no benefit from controlling in an intelligent manner a malfunctioning system.

Finally, an important outcome of this thesis was the realization that an MPC-like controller is not the most viable option for all types of building. A clear example here is the TUC building, heated or cooled by the AC units in each office. In this case, the dynamics of the system are fast, while the construction properties of the building (lightweight building with small insulation and high infiltration) do not allow for intelligent demand-shaping strategies, such as pre-cooling. To add to this, the nature of the HVAC system (AC units) allows the users to override the designed control strategy easily, making the actions of the occupants a critical factor affecting the successful application of an intelligent BACS. In such cases, the cost of developing a simulation model and applying a sophisticated model-based solution cannot be justified. Instead, a collection of TBM functionalities preventing energy-prone user actions (e.g. like switching off the AC unit in an office if a door or a window of the respective office is open) can provide tangible benefits in the energy consumption, with much less development and deployment costs.

In terms of future plans, potential simplifications of the proposed methodology can be investigated. Here, one approach is to initiate a control design process in larger time intervals (e.g. once per day or per week), especially for buildings with high thermal mass and for periods with similar weather conditions for several days (e.g. summers in Crete). Moreover, the outcome of simulation-based control design evaluations (e.g. designing one controller for each day of the year using a meteorological weather file) could be utilized to avoid designing the controllers online.

Finally, in cases where a simulation model does not exist, it might still be possible to derive empirical approaches that can lead to improved operational efficiencies. These data-driven approaches have weaker requirements in terms of data and preparatory work, but can not achieve the full performance potential.

THIS PAGE INTENTIONALLY LEFT BLANK

Bibliography

- Afram, A. and Janabi-Sharifi, F. (2014). Theory and applications of HVAC control systems – a review of model predictive control (MPC). *Building and Environment*, 72:343 – 355.
- Åkesson, J., Årzén, K.-E., Gäfvert, M., Bergdahl, T., and Tummescheit, H. (2010). Modeling and optimization with optimica and jmodelica.org—languages and tools for solving large-scale dynamic optimization problems. *Computers & Chemical Engineering*, 34(11):1737–1749.
- Akimoto, T., Tanabe, S.-i., Yanai, T., and Sasaki, M. (2010). Thermal comfort and productivity-evaluation of workplace environment in a task conditioned office. *Building and Environment*, 45(1):45–50.
- Arango, C., Cortes, P., Onieva, L., and Escudero, A. (2013). Simulation-optimization models for the dynamic berth allocation problem. *Computer-Aided Civil and Infrastructure Engineering*, 28(10):769–779.
- Arteconi, A., Costola, D., Hoes, P., and Hensen, J. (2014). Analysis of control strategies for thermally activated building systems under demand side management mechanisms. *Energy and Buildings*, 80:384–393.
- ASHRAE (2010). ANSI/ASHRAE Standard 55-2010: thermal environmental conditions for human occupancy.
- Atam, E. and Helsen, L. (2016). Control-oriented thermal modeling of multizone buildings: Methods and issues: Intelligent control of a building system. *IEEE Control Systems*, 36(3):86–111.
- Azar, E. and Menassa, C. C. (2015). Evaluating the impact of extreme energy use behavior on occupancy interventions in commercial buildings. *Energy and Buildings*, 97:205–218.
- Azer, N. and Hsu, S. (1977). The prediction of thermal sensation from simple model of human physiological regulatory response. *ASHRAE Trans*, 83(Pt 1).
- Baker, L. and Hoyt, T. (2016). Control for the people: How machine learning enables efficient hvac use across diverse thermal preferences. In *ACEEE Summer Study on Energy Efficiency in Buildings, Pacific Grove, CA, USA*.
- Baldi, S., Michailidis, I., Kosmatopoulos, E. B., and Ioannou, P. A. (2014). A” plug and play” computationally efficient approach for control design of large-scale nonlinear systems using cosimulation: a combination of two” ingredients”. *IEEE Control Systems*, 34(5):56–71.
- Baldi, S., Michailidis, I., Ravanis, C., and Kosmatopoulos, E. B. (2015). Model-based and model-free “plug-and-play” building energy efficient control. *Applied Energy*, 154:829–841.
- Bazjanac, V., Maile, T., O’Donnell, J., Rose, C., and Mrazovic, N. (2011). Data environments and processing in sem-automated simulation with energyplus. In *CIB W078-W102: 28th International Conference. CIB, Sophia Antipolis, France*.

- Bertsekas, D., Hager, W., and Mangasarian, O. (1999). *Nonlinear programming*. Athena Scientific Belmont, MA.
- Brochu, E., Cora, V. M., and De Freitas, N. (2010). A tutorial on bayesian optimization of expensive cost functions, with application to active user modeling and hierarchical reinforcement learning. *arXiv preprint arXiv:1012.2599*.
- Brooks, C., Lee, E. A., Liu, X., Neuendorffer, S., Zhao, Y., and Zheng, H. (2005). Heterogeneous Concurrent Modeling and Design in Java (Volume 1: Introduction to Ptolemy II). Technical Report UCB/ERL M05/21, EECS Department, University of California, Berkeley.
- CEN (2007). *EN15251: Indoor environmental input parameters for design and assessment of energy performance of buildings - addressing indoor air quality, thermal environment, lighting and acoustics*. Brussels.
- Cigler, J. and Privara, S. (2010). Subspace identification and model predictive control for buildings. In *Proceedings of the 11th International Conference on Control Automation Robotics & Vision (ICARCV)*, pages 750–755.
- Cigler, J., Privara, S., Váňa, Z., Žáčková, E., and Ferkl, L. (2012). Optimization of predicted mean vote index within model predictive control framework: Computationally tractable solution. *Energy and Buildings*, 52:39–49.
- Coffey, B., Haghghat, F., Morofsky, E., and Kutrowski, E. (2010). A software framework for model predictive control with genopt. *Energy and Buildings*, 42(7):1084–1092.
- Comite Europeen de Normalization (CEN) (2010). 15232–Energy Performance of Buildings–Impact of Building Automation. *European Standard*.
- Crawley, D., Lawrie, L., Winkelmann, F., Buhl, W., Huang, Y., Pedersen, C., Strand, R., Liesen, R., Fisher, D., Witte, M., et al. (2001). EnergyPlus: creating a new-generation building energy simulation program. *Energy and Buildings*, 33(4):319–331.
- Daum, D., Haldi, F., and Morel, N. (2011). A personalized measure of thermal comfort for building controls. *Building and Environment*, 46(1):3–11.
- D’Oca, S., Fabi, V., Corgnati, S. P., and Andersen, R. K. (2014). Effect of thermostat and window opening occupant behavior models on energy use in homes. In *Building Simulation*, volume 7, pages 683–694. Springer.
- Donaisky, E., Oliveira, G. H., Freire, R. Z., and Mendes, N. (2007). Pmv-based predictive algorithms for controlling thermal comfort in building plants. In *Control Applications, 2007. CCA 2007. IEEE International Conference on*, pages 182–187. IEEE.
- Drgona, J., Kvasnica, M., Klauco, M., and Fikar, M. (2013). Explicit stochastic MPC approach to building temperature control. In *52nd IEEE Conference on Decision and Control (CDC)*, pages 6440–6445. IEEE.
- Duvenaud, D. (2014). *Automatic Model Construction with Gaussian Processes*. PhD thesis, Computational and Biological Learning Laboratory, University of Cambridge.
- Duvenaud, D., Lloyd, J. R., Grosse, R., Tenenbaum, J. B., and Ghahramani, Z. (2013). Structure discovery in nonparametric regression through compositional kernel search. In *Proceedings of the 30th International Conference on Machine Learning*, pages 1166–1174.
- Efficiency Evaluation Organization (2010). International Performance Measurement and Verification Protocol: Concepts and Options for Determining Energy and Water Savings, Volume I. *Efficiency Evaluation Organization (EVO)*.

- Eisenhower, B., O'Neill, Z., Narayanan, S., Fonoberov, V. A., and Mezić, I. (2012). A methodology for meta-model based optimization in building energy models. *Energy and Buildings*, 47:292–301.
- Fanger, P. O. et al. (1970). Thermal comfort. analysis and applications in environmental engineering. *Thermal comfort. Analysis and applications in environmental engineering*.
- Feng, J. D., Chuang, F., Borrelli, F., and Bauman, F. (2015). Model predictive control of radiant slab systems with evaporative cooling sources. *Energy and Buildings*, 87:199–210.
- Fisk, W. J. (2000). Health and productivity gains from better indoor environments and their relationship with building energy efficiency. *Annual Review of Energy and the Environment*, 25(1):537–566.
- Frean, M. and Boyle, P. (2008). Using gaussian processes to optimize expensive functions. In *AI 2008: Advances in Artificial Intelligence*, pages 258–267. Springer.
- Freire, R. Z., Oliveira, G. H., and Mendes, N. (2008). Predictive controllers for thermal comfort optimization and energy savings. *Energy and buildings*, 40(7):1353–1365.
- Gagge, A. (1971). An effective temperature scale based on a simple model of human physiological regulatory response. *Ashrae Trans.*, 77:247–262.
- Garnier, A., Eynard, J., Caussanel, M., and Grieu, S. (2013). Low computational cost technique for predictive management of thermal comfort in non-residential buildings. *Journal of Process Control (In press)*.
- Ghahramani, A., Jazizadeh, F., and Becerik-Gerber, B. (2014). A knowledge based approach for selecting energy-aware and comfort-driven hvac temperature set points. *Energy and Buildings*, 85:536–548.
- Ghahramani, A., Tang, C., and Becerik-Gerber, B. (2015). An online learning approach for quantifying personalized thermal comfort via adaptive stochastic modeling. *Building and Environment*, 92:86–96.
- Ghahramani, A., Zhang, K., Dutta, K., Yang, Z., and Becerik-Gerber, B. (2016). Energy savings from temperature setpoints and deadband: Quantifying the influence of building and system properties on savings. *Applied Energy*, 165:930–942.
- Giannakis, G., Kontes, G., Kosmatopoulos, E., and Rovas, D. (2011). A model-assisted adaptive controller fine-tuning methodology for efficient energy use in buildings. In *Control & Automation (MED), 2011 19th Mediterranean Conference on*, pages 49–54. IEEE.
- Giannakis, G., Pichler, M., Kontes, G., Schranzhofer, H., and Rovas, D. (2013). Simulation speedup techniques for computationally demanding tasks. *Proceedings of BS 2013: 13th Conference of the International Building Performance Simulation Association*, pages 3761–3768.
- Gwerder, M., Lehmann, B., Tödli, J., Dorer, V., and Renggli, F. (2008). Control of thermally-activated building systems (TABS). *Applied energy*, 85(7):565–581.
- Gwerder, M., Tödli, J., Lehmann, B., Dorer, V., Güntensperger, W., and Renggli, F. (2009). Control of thermally activated building systems (TABS) in intermittent operation with pulse width modulation. *Applied Energy*, 86(9):1606–1616.
- Henze, G. P., Kalz, D. E., Liu, S., and Felsmann, C. (2005). Experimental analysis of model-based predictive optimal control for active and passive building thermal storage inventory. *HVAC&R Research*, 11(2):189–213.

- Hoyt, T., Arens, E., and Zhang, H. (2015). Extending air temperature setpoints: Simulated energy savings and design considerations for new and retrofit buildings. *Building and Environment*, 88:89–96.
- IEA Annex 66 (2013). Definition and simulation of occupant behavior in buildings. www.annex66.org.
- International Organization for Standardization (1989). *ISO8996:1989: Ergonomics of thermal environments — determination of metabolic heat production*. Geneva, Switzerland: International Organization for Standardization.
- International Organization for Standardization (2005). *ISO7730:2005: Ergonomics of the thermal environment - Analytical determination and interpretation of thermal comfort using calculation of the PMV and PPD indices and local thermal comfort criteria*. Geneva, Switzerland: International Organization for Standardization.
- ISO, E. (2008). 13790: 2008. *Energy performance of buildings—Calculation of energy use for space heating and cooling*.
- Jones, D. R. (2001). A taxonomy of global optimization methods based on response surfaces. *Journal of Global Optimization*, 21(4):345–383.
- Jones, D. R., Schonlau, M., and Welch, W. J. (1998). Efficient global optimization of expensive black-box functions. *Journal of Global Optimization*, 13(4):455–492.
- Kang, D. H., Mo, P. H., Choi, D. H., Song, S. Y., Yeo, M. S., and Kim, K. W. (2010). Effect of MRT variation on the energy consumption in a PMV-controlled office. *Building and Environment*, 45(9):1914–1922.
- Karagevrekis, A., Baldi, S., Michailidis, I., and Kosmatopoulos, E. (2014). Interconnected micro-grids: An energyplus simulation test case. *Machines Review*, 1:7–13.
- Katsigarakis, K., Kontes, G., Giannakis, G., and Rovas, D. (2016). Sense-think-act framework for intelligent building energy management. *Computer-Aided Civil and Infrastructure Engineering*, 31(1):50–64.
- Khuri, A. I. and Mukhopadhyay, S. (2010). Response surface methodology. *Wiley Interdisciplinary Reviews: Computational Statistics*, 2(2):128–149.
- Kiefer, J. and Wolfowitz, J. (1952). Stochastic estimation of the maximum of a regression function. *The Annals of Mathematical Statistics*, 23(3):462–466.
- Klauco, M. and Kvasnica, M. (2014). Explicit MPC Approach to PMV-Based Thermal Comfort Control. In *53rd IEEE Conference on Decision and Control (CDC)*.
- Klein, S., Beckman, W., and Duffie, J. (1976). TRNSYS - A transient simulation program. *ASHRAE Transactions*, 82(1):623–633.
- Kohavi, R. (1995). A study of cross-validation and bootstrap for accuracy estimation and model selection. In *International Joint Conference on Artificial Intelligence*, volume 14, pages 1137–1145.
- Kolokotsa, D., Pouliezios, A., Stavrakakis, G., and Lazos, C. (2009). Predictive control techniques for energy and indoor environmental quality management in buildings. *Building and Environment*, 44(9):1850–1863.

- Kontes, G., Giannakis, G., Kosmatopoulos, E., and Rovas, D. (2012). Adaptive Fine-Tuning of Building Energy Management Systems Using Co-Simulation. In *IEEE Multi-Conference on Systems and Control*.
- Kontes, G., Valmaseda, C., Giannakis, G., Katsigarakis, K., and Rovas, D. (2014). Intelligent BEMS design using detailed thermal simulation models and surrogate-based stochastic optimization. *Journal of Process Control*, 24(6):846 – 855.
- Kontes, G. D., Giannakis, G. I., and Rovas, D. V. (2013). Demand shifting using model-assisted control. *International Journal of Energy for a Clean Environment*, 14(1).
- Kontogianni, E., Giannakis, G., Kontes, G., and Rovas, D. (2013). Comparing the impact of different thermal comfort constraints on a model-assisted control design process. In *CLIMA 2013, 11th REHVA World Congress, Prague, Czech Republic*.
- Korkas, C. D., Baldi, S., Michailidis, I., and Kosmatopoulos, E. B. (2015). Intelligent energy and thermal comfort management in grid-connected microgrids with heterogeneous occupancy schedule. *Applied Energy*, 149:194–203.
- Kosmatopoulos, E. (2009). Adaptive control design based on adaptive optimization principles. *IEEE Transactions on Automatic Control*, 53(11):2680–2685.
- Kosmatopoulos, E. B., Polycarpou, M. M., Christodoulou, M. A., and Ioannou, P. A. (1995). High-order neural network structures for identification of dynamical systems. *IEEE transactions on Neural Networks*, 6(2):422–431.
- Kouvelas, A., Aboudolas, K., Kosmatopoulos, E. B., and Papageorgiou, M. (2011). Adaptive performance optimization for large-scale traffic control systems. *IEEE Transactions on Intelligent Transportation Systems*, 12(4):1434–1445.
- Lee, S., Bilonis, I., Karava, P., and Tzempelikos, A. (2017). A bayesian approach for probabilistic classification and inference of occupant thermal preferences in office buildings. *Building and Environment*, 118:323–343.
- Lehmann, B., Dorer, V., and Koschenz, M. (2007). Application range of thermally activated building systems TABS. *Energy and buildings*, 39(5):593–598.
- Li, C., Hong, T., and Yan, D. (2014). An insight into actual energy use and its drivers in high-performance buildings. *Applied Energy*, 131:394–410.
- Lilis, G., Giannakis, G., Kontes, G., and Rovas, D. (2015). Semi-automatic thermal simulation model generation from ifc data. In *eWork and eBusiness in Architecture, Engineering and Construction - Proceedings of the 10th European Conference on Product and Process Modelling, ECPPM 2014*, pages 503–510.
- Lin, C., Chang, C., and Hsu, C. (2001). A practical guide to support vector classification. *Technical Report, Department of Computer Science and Information Engineering, National Taiwan University*.
- Lizotte, D. J. (2008). *Practical bayesian optimization*. University of Alberta.
- Luenberger, D. G. and Ye, Y. (2008). *Linear and nonlinear programming*, volume 116. Springer.
- Ma, Y., Anderson, G., and Borrelli, F. (2011). A distributed predictive control approach to building temperature regulation. In *American Control Conference (ACC)*, pages 2089–2094.

- Ma, Y., Borrelli, F., Hancey, B., Coffey, B., Bengea, S., and Haves, P. (2012a). Model predictive control for the operation of building cooling systems. *IEEE Transactions on Control Systems Technology*, 20(3):796–803.
- Ma, Y., Kelman, A., Daly, A., and Borrelli, F. (2012b). Predictive control for energy efficient buildings with thermal storage: Modeling, stimulation, and experiments. *IEEE Control Systems Magazine*, 32(1):44–64.
- Maasoumy, M. and Vincentelli, A. S. (2014). Comparison of control strategies for energy efficient building hvac systems. In *Proceedings of the Symposium on Simulation for Architecture & Urban Design*, page 11. Society for Computer Simulation International.
- Malavazos, C., Tsatsakis, K., and Tsitsanis, A. (2014). Towards a “context aware” flexibility profiling mechanism for the energy management environment. In *MedPower CONFERENCE, Athens, Greece*.
- Maldonado, E., Wouters, P., and Papaglastra, M. (2011). Implementing the energy performance of buildings directive (epbd). In *Featuring Country reports 2010*, page 342. European Union.
- Mařík, K., Rojíček, J., Stluka, P., and Vass, J. (2011). Advanced hvac control: Theory vs. reality. In *Preprints of the 18th IVAC World Congress, Milano, Italy*, pages 3108–3113.
- Marino, C., Nucara, A., and Pietrafesa, M. (2015). Mapping of the indoor comfort conditions considering the effect of solar radiation. *Solar Energy*, 113:63–77.
- Martin, J., Hidalgo, O., Gordaliza, A., Hernandez, J., Macia, A., Kontes, G., and Rodriguez, J. (2016). Reporting period in pilot buildings. BAAS Deliverable 6.3.3.
- Michailidis, I. T., Korkas, C., Kosmatopoulos, E. B., and Nassie, E. (2016). Automated control calibration exploiting exogenous environment energy: An israeli commercial building case study. *Energy and Buildings*, 128:473–483.
- Mockus, J., Tiesis, V., and Zilinskas, A. (1978). Toward global optimization, volume 2, chapter bayesian methods for seeking the extremum.
- Moon, J. W. and Han, S.-H. (2011). Thermostat strategies impact on energy consumption in residential buildings. *Energy and Buildings*, 43(2):338–346.
- Morales-Valdés, P., Flores-Tlacuahuac, A., and Zavala, V. M. (2014). Analyzing the effects of comfort relaxation on energy demand flexibility of buildings: A multiobjective optimization approach. *Energy and Buildings*, 85:416–426.
- Morosan, P., Bourdais, R., Dumur, D., and Buisson, J. (2010). Building temperature regulation using a distributed model predictive control. *Energy and Buildings*, 42(9):1445–1452.
- Moss, K. J. (2015). *Heat and mass transfer in buildings*. Routledge.
- Mosteller, F. (2006). A k-sample slippage test for an extreme population. In *Selected Papers of Frederick Mosteller*, pages 101–109. Springer.
- Nghiem, T. and Pappas, G. (2011). Receding-horizon supervisory control of green buildings. In *American Control Conference (ACC)*, pages 4416–4421.
- Oldewurtel, F., Parisio, A., Jones, C., Gyalistras, D., Gwerder, M., Stauch, V., Lehmann, B., and Morari, M. (2012). Use of model predictive control and weather forecasts for energy efficient building climate control. *Energy and Buildings*, 45:15–27.

- Olesen, B. W. et al. (2002). Radiant floor heating in theory and practice. *ASHRAE journal*, 44(7):19–26.
- Pérez-Lombard, L., Ortiz, J., and Pout, C. (2008). A review on buildings energy consumption information. *Energy and buildings*, 40(3):394–398.
- Pichler, M., Droscher, A., Schranzhofer, H., Kontes, G., Giannakis, G., Kosmatopoulos, E., and Rovas, D. (2011). Simulation-assisted building energy performance improvement using sensible control decisions. In *Proceedings of the 3rd ACM Workshop on Embedded Sensing Systems for Energy-Efficiency in Buildings (Buildsys 2011)*. ACM.
- Privara, S., Vana, Z., Gyalistras, D., Cigler, J., Sagerschnig, C., Morari, M., and Ferkl, L. (2011). Modeling and identification of a large multi-zone office building. In *Proceedings of the IEEE International Conference on Control Applications (CCA)*, pages 55–60.
- Raphael, B. (2011). Active control of daylighting features in buildings. *Computer-Aided Civil and Infrastructure Engineering*, 26(5):393–405.
- Rasmussen, C. E. and Williams, C. K. I. (2006). *Gaussian processes for machine learning*. MIT Press, Cambridge, Mass.
- Regis, R. G. and Shoemaker, C. A. (2005). Constrained global optimization of expensive black box functions using radial basis functions. *Journal of Global Optimization*, 31(1):153–171.
- Remund, J., Kunz, S., and Lang, R. (1999). Meteorom-global meteorological database for solar energy and applied climatology. *Solar Engineering Handbook, version, 4*.
- Renzaglia, A. (2012). *Adaptive stochastic optimization for cooperative coverage with a swarm of Micro Aerial Vehicles*. PhD thesis, PhD thesis, Université de Grenoble.
- Romero, A., Tellado, B., and Tsitsanis, T. (2016). Moebius energy performance optimization framework in buildings for urban sustainability. In *41st IAHS World Congress, Albufeira, Portugal, 13-16th September*.
- Roth, K. W., Westphalen, D., Feng, M. Y., Llana, P., and Quartararo, L. (2005). Energy impact of commercial building controls and performance diagnostics: market characterization, energy impact of building faults and energy savings potential. *Prepared by TAIX LLC for the US Department of Energy*.
- Rovas, D., Kontes, G., Valmaseda, C., Giannakis, G., Chacel, O., Macek, K., Fisera, R., Rojicek, J., Hottges, K., Menzel, K., and Floeck, M. (2014a). Baas advanced use cases. BAAS Deliverable 5.1b.
- Rovas, D., Kontes, G., Valmaseda, C., Giannakis, G., Chacel, O., Macek, K., Fisera, R., Rojicek, J., Hottges, K., Menzel, K., and Floeck, M. (2014b). Building services: Functional and interoperability requirements. BAAS Deliverable 5.1a.
- Sadeghi, S. A., Awalgaonkar, N. M., Karava, P., and Billionis, I. (2017). A bayesian modeling approach of human interactions with shading and electric lighting systems in private offices. *Energy and Buildings*, 134:185–201.
- Schiavon, S., Hoyt, T., and Piccioli, A. (2014). Web application for thermal comfort visualization and calculation according to ashrae standard 55. *Building Simulation*, 7(4):321–334.
- Schiavon, S. and Lee, K. H. (2013). Dynamic predictive clothing insulation models based on outdoor air and indoor operative temperatures. *Building and Environment*, 59:250–260.

- Scholkopf, B. and Smola, A. (2002). *Learning with kernels*, volume 64. Citeseer.
- Scholkopf, B., Smola, A., Williamson, R., and Bartlett, P. (2000). New support vector algorithms. *Neural Computation*, 12(5):1207–1245.
- Shahriari, B., Swersky, K., Wang, Z., Adams, R. P., and de Freitas, N. (2016). Taking the human out of the loop: A review of bayesian optimization. *Proceedings of the IEEE*, 104(1):148–175.
- Široký, J., Oldewurtel, F., Cigler, J., and Prívará, S. (2011). Experimental analysis of model predictive control for an energy efficient building heating system. *Applied Energy*, 88(9):3079–3087.
- Spellucci, P. (1998). A new technique for inconsistent QP problems in the SQP method. *Mathematical Methods of Operations Research*, 47(3):355–400.
- Srinivas, N., Krause, A., Kakade, S. M., and Seeger, M. (2009). Gaussian process optimization in the bandit setting: No regret and experimental design. *arXiv preprint arXiv:0912.3995*.
- Sturzenegger, D., Gyalistras, D., Morari, M., and Smith, R. S. (2016). Model predictive climate control of a swiss office building: Implementation, results, and cost-benefit analysis.
- Sturzenegger, D., Gyalistras, D., Semeraro, V., Morari, M., and Smith, R. S. (2014). BRCM Matlab Toolbox: Model generation for model predictive building control. In *American Control Conference (ACC)*, pages 1063–1069.
- Tang, B. (1993). Orthogonal array-based latin hypercubes. *Journal of the American Statistical Association*, 88(424):1392–1397.
- Tone, K. (1983). Revisions of constraint approximations in the successive QP method for nonlinear programming problems. *Mathematical Programming*, 26(2):144–152.
- Vana, Z., Kubecek, J., and Ferkl, L. (2010). Notes on finding black-box model of a large building. In *Proceedings of the IEEE International Conference on Control Applications (CCA)*, pages 1017–1022.
- Vapnik, V. (2000). *The nature of statistical learning theory*. Springer-Verlag.
- Vapnik, V., Golowich, S., and Smola, A. (1997). Support vector method for function approximation, regression estimation, and signal processing. *Advances in neural information processing systems*, pages 281–287.
- Verein Deutscher Ingenieure (1977). Berechnung der kühllast klimatisierter räume (vdi-kühllastregeln).
- Walton, G. (1989). *AIRNET: A Computer Program for Building Airflow Network Modeling*. US Dept. of Commerce, National Institute of Standards and Technology, National Engineering Laboratory, Center for Building Research, Building Environment Division.
- Wetter, M. (2011). Co-simulation of building energy and control systems with the building controls virtual test bed. *Journal of Building Performance Simulation*, 4(3):185–203.
- Wild, S. M. and Shoemaker, C. (2013). Global convergence of radial basis function trust-region algorithms for derivative-free optimization. *SIAM Review*, 55(2):349–371.
- Woods, J., Winkler, J., and Christensen, D. (2013). Evaluation of the effective moisture penetration depth model for estimating moisture buffering in buildings. *Contract*, 303:275–3000.
- Žáčeková, E., Váňa, Z., and Cigler, J. (2014). Towards the real-life implementation of mpc for an office building: Identification issues. *Applied Energy*, 135:53–62.

Zavala, V. M. (2012). Real-time optimization strategies for building systems. *Industrial & Engineering Chemistry Research*, 52(9):3137–3150.